

**Psidin is required for neuron survival and
axon targeting through two distinct
molecular mechanisms in *Drosophila***

Dissertation
Daniel Stephan



**Psidin is required for neuron survival and
axon targeting through two distinct
molecular mechanisms in *Drosophila***

Dissertation

der Fakultät für Biologie
der Ludwig–Maximilians–Universität München
Angefertigt am Max Planck Institut für Neurobiologie,
Arbeitsgruppe Sensorische Neurogenetik

vorgelegt von
Daniel Stephan
München 2012

Die vorliegende Arbeit wurde zwischen Juli 2008 und Juni 2012 unter Anleitung von Dr. Ilona Grunwald-Kadow am Max Planck Institut für Neurobiologie in Martinsried durchgeführt.

Erstgutachter: Prof. Dr. Rüdiger Klein
Zweitgutachter: Prof. Dr. Rainer Uhl

Dissertation eingereicht am: 06. September 2012
Tag der mündlichen Prüfung: 05. Dezember 2012

Hiermit erkläre ich an Eides statt, dass ich die vorliegende Dissertation selbständig und ohne unerlaubte Hilfe angefertigt habe. Ich habe weder anderweitig versucht, eine Dissertation oder Teile einer Dissertation einzureichen beziehungsweise einer Prüfungskommission vorzulegen, noch mich einer Doktorprüfung zu unterziehen.

München, den 06. September 2012

Daniel Stephan

Table of content

Table of content	I
Index of figures	V
Index of tables	VII
Abbreviations	IX
1 Summary	1
2 Zusammenfassung.....	7
3 Introduction	11
3.1 The olfactory system of <i>Drosophila</i>	12
3.1.1 Organization of the olfactory system in <i>Drosophila</i>	12
3.1.2 Targeting of olfactory receptor neurons	15
3.2 The neuronal cytoskeleton.....	23
3.2.1 Actin filaments and microtubules	23
3.2.2 The growth cone.....	27
3.2.3 Axonal growth	32
3.3 The growth cone as a signal integrator	35
3.4 Psidin	37
4 Aims of this thesis	43
5 Materials	45
5.1.1 Common buffers and solutions	45
5.1.2 Consumables	46
5.1.3 Antibodies.....	47
5.1.4 Enzymes.....	47
5.1.5 Plasmids.....	48
5.1.6 Fly stocks	48
5.1.7 Fly genetics	49
6 Methods	51
6.1 Immunohistochemistry	51
6.2 Preparation of genomic DNA.....	51

6.3	Mapping.....	52
6.3.1	Sequence polymorphism mapping.....	53
6.3.2	PLP-Assay.....	55
6.3.3	RFLP-Assay.....	56
6.3.4	SNP Assay.....	57
6.3.5	Deletion Mapping.....	58
6.4	Cell Culture.....	59
6.5	Primary cell culture.....	59
6.6	Transfection.....	60
6.7	In-situ hybridization.....	60
6.8	Mutagenesis.....	62
6.9	Cloning of dNAA20 (CG14222).....	63
6.10	Generation of Psidin deletions.....	64
6.11	Co-immunoprecipitation.....	65
6.12	F-actin binding assay.....	66
6.13	Engineering “fly-like” yeast Psidin.....	67
6.14	Western blot quantification.....	67
6.15	GAL4/UAS system.....	68
6.16	MARCM.....	69
7	Results.....	71
7.1	Mapping of the mutation “IG978” to the gene locus of Psidin.....	71
7.2	<i>Psidin</i> mutants show class specific defects in olfactory neuron targeting.....	74
7.3	Complete loss of Psidin results in loss of specific ORNs.....	78
7.4	Re-expression of wild type Psidin rescues targeting and cell loss phenotype.....	80
7.5	<i>Psidin</i> mutant axons do not follow their normal targeting pattern.....	84
7.6	<i>Psidin</i> is not required for the initial outgrowth of ORNs.....	86
7.7	<i>Psidin</i> is required cell-autonomously.....	87
7.8	<i>Psidin</i> is expressed during the development of the olfactory system.....	89
7.9	<i>Psidin</i> interacts with <i>dNAA20</i> <i>in vivo</i> and <i>in vitro</i>	90
7.10	NatB interaction domain is required for <i>Psidin</i> / <i>dNAA20</i> interaction.....	96
7.11	<i>Psidin</i> / <i>dNAA20</i> interaction is regulated by serine S678.....	98
7.12	<i>Psidin</i> regulates actin dynamics.....	102

7.13	Loss of Psidin decreases the size of lamellipodia in growth cones	107
7.14	Psidin ^{I6978} maintains ability to bind F-actin	109
7.15	Fly-like yeast Mdm20 can rescue Mdm20 function during cell division	110
8	Discussion	113
8.1	Psidin as regulator of actin dynamics	113
8.2	Psidin is required differentially in olfactory neurons	115
8.3	Psidin is expressed in developing olfactory organs	118
8.4	Psidin as non-catalytic part of the NatB-complex	120
8.5	Psidin has a minimal interaction domain with dNAA20	122
8.6	Psidin is regulated by the conserved serine 678	123
8.7	Psidin's function in an evolutionary context	124
8.8	Concluding remarks	126
9	Acknowledgements	129
10	Literature	131
11	Curriculum vitae	147

Index of figures

Figure 3.1	Organization of the olfactory system in <i>Drosophila melanogaster</i>	13
Figure 3.2	Basic wiring diagram of the olfactory system	16
Figure 3.3	Targeting of ORN axons is a multistep process	18
Figure 3.4	Map of different ORN classes and their projections into the antennal lobe ..	20
Figure 3.5	Structural features of actin filaments	24
Figure 3.6	Structural features of microtubules	26
Figure 3.7	Structure of a growth cone.....	28
Figure 3.8	Actin network in filopodia and lamellipodia	30
Figure 3.9	Different stages of axon outgrowth	34
Figure 3.10	The growth cone as an integrator of different guidance cues	35
Figure 3.11	Protein structure of Psidin.....	37
Figure 3.12	Psidin as an actin binding protein	39
Figure 3.13	Psidin in actin dynamics	40
Figure 6.1	Map of polymorphism marker between the FRT82B and EP strain	54
Figure 6.2	Crossing strategy for deletion mapping	58
Figure 6.3	Cloning strategy for <i>dNAA20</i> with N-terminal myc-tag	63
Figure 6.4	The GAL4/UAS system.....	68
Figure 6.5	MARCM technique.....	70
Figure 7.1	Recombinants stocks obtained during “SNP-mapping”	72
Figure 7.2	Complementation assay	73
Figure 7.3	ORN class specific mistargeting phenotype in Psidin mutants	77
Figure 7.4	Reduction of ORN number in Psidin loss of function mutants.....	79
Figure 7.5	Re-expression of wild type Psidin rescue targeting and cell loss phenotype	82
Figure 7.6	Psidin mutant axons do not follow their normal targeting routes.....	85
Figure 7.7	Psidin is not required for initial outgrowth of ORNs	86
Figure 7.8	Psidin is required cell autonomously	88
Figure 7.9	Psidin is expressed in the developing olfactory organs.....	89
Figure 7.10	Psidin and <i>dNAA20</i> interact in Or59c neurons	91
Figure 7.11	Psidin and <i>dNAA20</i> interact in Or42 neurons	93
Figure 7.12	Knock down of <i>dNAA20</i> in S2 cells	94
Figure 7.13	Psidin and <i>dNAA20</i> interact <i>in vitro</i>	95
Figure 7.14	NatB domain is required for Psidin and <i>dNAA20</i> interaction	97
Figure 7.15	Psidin phosphorylation state regulates ORN survival <i>in vivo</i>	98
Figure 7.16	S678 in Psidin is used to regulate Psidin/ <i>dNAA20</i> interaction	100
Figure 7.17	Psidin and Tropomyosin interact during axon targeting	102
Figure 7.18	Psidin genetically interacts with LimK.....	105
Figure 7.19	Psidin genetically interacts with Cofilin (twinstar)	106
Figure 7.20	Reduced Lamellipodia in <i>psidin</i> loss of function neurons.....	108
Figure 7.21	Psidin ^{G978} is able to bind F-actin	109
Figure 7.22	Fly like Mdm20 can rescue Mdm20 mutants during cell division	111
Figure 8.1	Psidin is required differentially in ORN classes	115
Figure 8.2	Psidin’s two independent functions during ORN targeting and survival	120

Index of tables

Table 5.1	Common lab buffer and reagents	45
Table 5.2	Media	46
Table 5.3	List of commercial kits	46
Table 5.4	List of primary and secondary antibodies	47
Table 5.5	List of enzymes and DNA standards	47
Table 5.6	List of plasmids and DNA templates.....	48
Table 5.7	Common fly stocks	48
Table 5.8	Fly genotypes analyzed for the respective experiment	50
Table 6.1	List of primers used for PLP assay	55
Table 6.2	List of primers used for the RFLP assay	56
Table 6.3	List of primers used for the SNP assay	57
Table 6.4	Primer used for mutagenesis.....	63
Table 6.5	Primer used for dNAA20 cloning	64
Table 6.6	Primer used for the generation of Psidin deletions.....	65
Table 7.1	Quantification of Psidin mutant axons in several ORN classes.....	75

Abbreviations

AEL	After egg laying
AL	Antennal lobe
ANT	Antenna
ANT	Antennal nerve
APF	After puparium formation
CDS	Coding sequence
Da	Dalton
DIV	Days in vitro
ECM	Extracellular matrix
EMS	Ethyl methane sulfonate
FRT	Flippase recognition target
GAP	GTPase activating protein
GEF	Guanine nucleotide exchange factor
GPCR	G-protein coupled receptor
InDel	Insertion/Deletion
IR	Ionotropic receptors
Kac	Potassium acetate
LaN	Labial nerve
LH	Lateral horn
LN	Local interneuron
MARCM	Mosaic analysis with a repressible cell marker
MB	Mushroom body
MCS	Multiple cloning site

MP	Maxillary palp
MT	Microtubules
OR	Olfactory receptor
ORN	Olfactory receptor neuron
PLP	Product length polymorphism
PN	Projection neuron
RFLP	Restriction fragment length polymorphism
RNAi	Ribonucleic acid interference
RT	Room temperature
SNP	Single nucleotide polymorphism
SOG	Subesophageal ganglion
UAS	Upstream activating sequence

1 Summary

The formation of neuronal networks depends on the proper development and targeting of the neurons within the network. One key challenge during the development of such networks is the correct cross linking of axons and dendrites. Only correct synapse formation between dendrites and axons will allow neurons to contribute to the entire network. Therefore further insights into axon targeting mechanisms will help to understand the underlying developmental processes and contribute to future cures for a number of related diseases.

Generally, once a neuron forms an axon, it starts growing towards a certain “target zone”. The underlying axon targeting mechanisms are controlled by a large number of extracellular cues provided by the extracellular matrix and neighboring cells. Depending on the neuron type, axons travel different distances towards their future synaptic partner. During that journey the neurons, more specifically the growth cone, constantly comes into contact with guidance cues. The growth cone symbolizes the forefront of an axon and is responsible to integrate different guidance signals. Depending on their nature, they trigger the local assembly or disassembly of the cytoskeleton and ultimately force the axon to turn into a certain direction. Although different guidance cues activate different signaling pathways, all of these cascades will eventually converge down on the cytoskeleton. These cytoskeletal rearrangements and changes in actin dynamics within the growth cone will promote the turning of the entire axon. In a series of events different guidance cues, attractive and repulsive, will guide the growth cone to its respective target.

In this study I used the olfactory system, more specifically the olfactory receptor neurons (ORNs), of *Drosophila melanogaster* to investigate the mechanisms of axon targeting. The olfactory system of the fruit fly proved to be a very powerful model organism for a number of reasons: First, the number of genetic tools available for *Drosophila* allows the manipulation of many cellular aspects. Second, ORNs have an extremely stereotyped targeting pattern that proved to be a good system to investigate axon targeting mechanisms.

The work presented in this thesis studied the role of the highly conserved actin binding protein Psidin during the development and targeting of ORNs. Herein, I was able to demonstrate that Psidin uses two independent molecular mechanisms to control ORN targeting and survival. To elucidate Psidin's role in the aforementioned processes, I analyzed two predicted null alleles *psidin*¹ (Brennan et al., 2007) and *psidin*^{55D4} (Kim et al., 2011), and one hypomorphic allele *psidin*^{IG978} (this study). The new hypomorphic allele *psidin*^{IG978} was mapped during this study and found to have a single point mutation within Psidin's coding region (E320K).

The data shown in this study demonstrate that Psidin is required at two different time points during the development of the olfactory system. During ORN development, Psidin is required as non-catalytic part of the N-acetyltransferase complex (NatB) to ensure ORN survival. At later stages during development, Psidin functions as an actin binding protein to regulate actin dynamics to ultimately ensure proper ORN axon targeting. I was able to show for the first time that Psidin's previously reported function as actin binding protein in oocytes (Kim et al., 2011), is also true for neurons. The loss of Psidin leads to significantly reduced lamellipodia in growth cones of primary neurons *in vitro*. In agreement with Psidin's role in actin dynamics is the finding that the parallel removal of the actin

stabilizer Tropomyosin rescues the lamellipodia defect in *psidin*¹ primary neurons. This strongly argues for Psidin being an actin destabilizing protein and antagonist of Tropomyosin.

In general, *psidin*¹ and *psidin*^{55D4} mutant axons showed severe mistargeting defects *in vivo* – e.g. defasciculation in Or59c and Or42a neurons or ectopic synapse formation in Or47a neurons. However, axons mutant for *psidin*^{IG978} displayed a less severe phenotype compared to the null alleles. In agreement with *in vitro* data, the parallel removal of Tropomyosin rescued the targeting defect in Or59c neurons *in vivo*. The growth cone and the lamellipodia are both important structures that keep axons responsive towards guidance cues. Therefore the lamellipodia reduction in *psidin* mutants is likely the cause for the observed targeting defects. Nevertheless, Psidin is required differentially among the ORN classes – the ones that project to dorsolateral or ventromedial glomeruli within the antennal lobe (AL) are more affected than centrally projecting classes. ORN classes that are more affected in *psidin* mutants have to turn upon entry of the AL. Therefore those classes (dorsolateral and ventromedial) have a higher requirement of Psidin, which has to maintain the lamellipodium, so that the axon can respond to cues in the first place.

In addition, I overexpressed different isoforms of LimK and Cofilin to artificially create conditions that favor actin stabilization or destabilization. More generally, conditions that promoted actin destabilization and actin stabilization were able to rescue and aggravate the *psidin*¹ phenotype, respectively. In addition to the targeting defect, *psidin*¹ and *psidin*^{55D4} mutants showed a strong reduction in ORN cell numbers. In contrast, cell numbers were not affected in *psidin*^{IG978} mutant flies. Again, ORN classes were affected differently – e.g. Or42a neuron number was reduced by 83%, but Or59c number was only reduced by 46%. Indicating Psidin's function in ORN survival, the expression of the anti-apoptotic protein p35

in *psidin* mutant neurons selectively rescued the cell number, but failed to rescue the targeting defects. Interestingly, the Psidin/Tropomyosin double mutant showed the opposite effect; here the targeting was rescued, but not the cell number. These findings gave strong indications that Psidin has two independent functions during ORN targeting and development.

Psidin is predicted to be the non-catalytic part of the N-acteyltransferase complex B (NatB) in *Drosophila* (Brennan et al., 2007). Here, Psidin (non-catalytic) forms the NatB-complex together with dNAA20 (catalytic). This complex is thought to acetylate nascent protein chains N-terminally. In this study I demonstrated for the first time that both proteins interact *in vivo* and *in vitro*. Indicating that the NatB-complex is involved in ORN survival, the knock-down of dNAA20 in *psidin*^{G978} mutants led to a reduction of ORN cell number that is reminiscent of the cell number in *psidin*¹ or *psidin*^{55D4} background. At the same time, the knock-down of dNAA20 had no effect on the targeting of ORNs. Furthermore I was able to show that wild type Psidin and Psidin^{G978} interact with dNAA20 at comparable levels *in vitro*. This is in agreement with the finding that the *psidin*^{G978} allele selectively affects ORN targeting, but not ORN survival.

In addition, I was able to map the interaction domain between Psidin and dNAA20. This revealed that the point mutation found in *psidin*^{G978} is just outside of the minimal interaction domain. Deletion of the entire interaction domain led to a complete abolishment of the Psidin/dNAA20 interaction. Furthermore I was able to demonstrate that the interaction of Psidin and dNAA20 is regulated by the phosphorylation of a highly conserved serine residue (S678). Expression of the non-phosphorylatable Psidin isoform (S678A) rescued the targeting and cell number phenotype *in vivo*. Contrary expression of the phosphomimetic isoform (S678D) only rescued the targeting phenotype, but failed to

restore ORN cell number *in vivo*. In line with this observation is the finding that the S678D isoform is unable to bind dNAA20 *in vitro*. At the same time the S678A isoform binds dNAA20 at normal levels *in vitro*.

Taken together, the data presented in this work demonstrate that Psidin has two functions during the development and targeting of ORNs using two independent molecular mechanisms: First, during axon targeting Psidin is required as an actin destabilizing molecule and antagonist of Tropomyosin. Psidin maintains the lamellipodia size in growth cones and keeps the cytoskeleton in a dynamic and responsive state. This ensures that growing axons can respond properly to various guidance cues. Second, to ensure ORN survival, Psidin is required as non-catalytic part of the NatB-complex. Here, Psidin interacts with the catalytic subunit dNAA20. The formation of the NatB-complex is regulated by phosphorylation of a conserved serine. In its unphosphorylated state Psidin binds dNAA20 and ensures ORN survival, whereas phosphorylation causes the abolishment of this interaction which results in a reduction of ORN cell number.

Concluding, this thesis unambiguously shows that Psidin is required at different time points during the formation of the olfactory system of *Drosophila*. It utilizes two different pathways to ensure (i) ORN survival as part of the NatB-complex and (ii) ORN targeting as actin binding protein. Due to its strong conservation in higher organisms, the here presented data provide important insights into the function of Psidin's mammalian homologues.

This work was incorporated in the paper Stephan et al. ("*Drosophila Psidin regulates olfactory neuron number and axon targeting through two distinct molecular mechanisms. Daniel Stephan, Natalia Sanchez-Soriano, Laura F. Loschek, Ramona Gerhards, Susanne Gutmann, Zuzana Storchova, Andreas Prokop and Ilona C. Grunwald Kadow*") which is currently under review at The Journal of Neuroscience.

2 Zusammenfassung

Das Entstehen und Funktionieren von neuronalen Netzwerken hängt nicht nur von korrekten Entwicklungsschritten, sondern auch von der Verknüpfung der Neurone innerhalb des Netzwerkes ab. Einzelnen Neurone tragen nur dann zum Gesamtnetzwerk bei, wenn sie untereinander richtig verknüpft sind. Zunächst einmal ist es natürlich wichtig die zugrunde liegenden Entwicklungsschritte genau zu verstehen. Im Rahmen dieser Arbeit habe ich Mechanismen untersucht, die Axone in die Lage versetzen über weite Strecken hinweg ihre jeweiligen synaptischen Partner zu finden. Insbesondere die Auswirkungen auf das Aktinnetzwerk innerhalb eines Neurons bzw. Axons während es von einem Ort zu einem anderen migriert, haben mich interessiert.

Zur Beantwortung dieser Fragen eignet sich das olfaktorische System von *Drosophila melanogaster* besonders und stellt somit einen exzellenter Modellorganismus dar. Zum einen steht eine Vielzahl an genetischen Methoden zur Verfügung, die ein gezieltes Manipulieren verschiedener zellulärer Aspekte ermöglichen. Zum anderen sind die olfaktorischen Rezeptorneurone (ORNs) ein etabliertes Modell um Zielfindungsmechanismen von Neuronen zu untersuchen. Diese Mechanismen werden durch eine große Anzahl an extrazellulären Signalen beeinflusst. Diese Signale können sowohl von der extrazellulären Matrix als auch von benachbarten Zellen stammen. Sobald eines dieser Signale mit dem Wachstumskegel von Axonen in Berührung kommt, löst dieses lokal den Auf- oder Abbau des Zytoskelettes aus. Hierbei wird meist eine Kette von molekularen Signalkaskaden aktiviert, an deren Enden eine Veränderung der Aktinstabilität im Wachstumskegel steht. Hierdurch wird der Wachstumskegel des betroffenen Axons gezwungen seine Wachstumsrichtung zu ändern.

Die hier vorgestellte Arbeit beschäftigt sich mit der Funktion des Aktin-bindenden Proteins Psidin während der Entwicklung des olfaktorischen Systems in *Drosophila melanogaster*. Im Rahmen dieser Arbeit konnte ich zeigen, dass Psidin zwei voneinander unabhängige Funktionen hat. Zunächst wird Psidin als aktin-destabilisierendes Molekül während des Wachstums und Findens der synaptischen Partner von ORNs benötigt. Während die Axone unterschiedlicher Neuronenklassen ihre synaptischen Partner suchen, hat Psidin die Aufgabe das Aktinnetzwerk innerhalb der Axone in einem dynamischen Zustand zu halten. *In vivo* und *in vitro* Experimente in meiner Arbeit zeigten, dass Psidin als Gegenspieler zum Aktin-stabilisierenden Tropomyosin agiert. Psidin knock-out Neurone sind nicht mehr in der Lage auf extrazelluläre Signal zu reagieren, da durch den Verlust von Psidin das Aktinnetzwerk zu unflexibel geworden ist. Dies zeigt sich besonders auffällig bei Neuronen, die während der Entwicklung des olfaktorischen Systems an mehreren Stellen gezwungen werden ihre Wachstumsrichtung zu ändern. Solche Neuronen zeigen einen besonders schweren Defekt in *psidin* Mutanten.

Weiterhin ist Psidin als nicht-katalytischer Teil des „N-acetyltransferase complex B“ (NatB) notwendig, um das Überleben der ORNs zu sichern. Dieser Proteinkomplex besteht aus einem nicht-katalytischen Protein (Psidin) und einem katalytischen Protein (dNAA20); beide zusammen bilden den NatB-Komplex. Dieser Komplex hat die Aufgabe Proteine direkt nach der Translation N-terminal mit einer Acetylgruppe zu versehen. In dieser Arbeit konnte ich zeigen, dass Psidin tatsächlich Teil dieses NatB-Komplexes ist. Des Weiteren konnte gezeigt werden, dass eine konservierte Aminosäure (S678) für die Regulation von Psidin als Teil dieses NatB Komplexes verantwortlich ist. Die phosphoablative Psidin-Isoform (S678A) interagiert normal mit dNAA20 und ist ebenfalls in der Lage seine Funktion als Aktin-bindendes Protein wahrzunehmen. Im Gegensatz dazu ist die phosphomimetische

Psidin-Isoform (S678D) nicht mehr in der Lage mit dNAA20 zu interagieren, kann aber gleichzeitig noch als Aktin-bindendes Protein agieren.

Zusammenfassend zeigen die Experimente dieser Arbeit, dass Psidin zwei unabhängige Funktionen während der Entwicklung des olfaktorischen Systems von *Drosophila melanogaster* hat. Zum einen destabilisiert Psidin das Aktinnetzwerk und agiert als Gegenspieler zu Tropomyosin. Zum anderen ist Psidin Teil des NatB-Komplexes und wird in dieser Funktion durch die Phosphorylierung des Serins 678 reguliert. Nur im unphosphorylierten Zustand kann Psidin mit dNAA20 interagieren und den NatB-Komplex bilden.

3 Introduction

A neuronal network relies on the formation of proper interconnections within the network. It is these very connections that allow a neuronal network to function according to its specifications. In general, a network contains three basic elements: input, processing and output. In biological organisms neurons form all three of these components and also establish connections among themselves to eventually form a network. In nature one can find a great number of different networks, all fine-tuned to master individual tasks. For example, sensory networks are fine-tuned towards visual, auditory or olfactory cues. The same sensory network can differ in its size and complexity from organism to organism. For example, the olfactory system of *Drosophila melanogaster* is made up of 100,000 neurons, whereas in humans it consists of more than 100 billion neurons. Despite these and many other differences between them, all these circuits have one absolute requirement – the formation of functional connections within the network. Neurons send out their axons to establish correct connections with dendrites of other neurons to form a network. It is already amazing that in rather small networks (e.g. the olfactory system of *Drosophila*) 100,000 axons are able to find their individual dendritic partners. However, it is even more astonishing, if one takes into account that these axons, on their journey for their synaptic partners, are surrounded by a large number of other cells. For example, in humans the axons of the sciatic nerve travel up to one meter until they find their target.

The field of axon guidance has attracted scientists for many years, all with the same goal – understanding the principles and mechanisms that allow axons to travel long distances with great precision. The first part of this introduction will try to familiarize the reader with the basic properties of the olfactory system of *Drosophila* and explain why I used

it as a tool to investigate axon guidance. The second part will focus more on molecular aspects within the growth cone of a neuron and its significance for axon path finding.

3.1 The olfactory system of *Drosophila*

For survival, *Drosophila* acquires information about its environment from different sensory channels – e.g. smell, taste and vision. To successfully navigate through its surroundings, the fruit fly's brain creates an internal representation of the outside world based on different sensory inputs. During its life, a fruit fly is challenged with various tasks; among them are many that require a functional olfactory system – such as seeking food sources, identifying potential mates, locating good oviposition sites or avoiding possible threats. *Drosophila's* olfactory system is able to detect and discriminate a large number of volatile compounds (Firestein, 2001). The fruit fly utilizes a large repertoire of olfactory receptors (ORs) and ionotropic receptors (IRs), which are selectively tuned (Schlief and Wilson, 2010; Katada et al., 2005; Abuin et al., 2011). A single OR is activated by a mixture of odors, but also at the same time single odors activate more than one OR. This combinatorial coding of ORs allows the detection of odors in numbers that exceed by far the number of available receptors (Malnic et al., 1999).

3.1.1 Organization of the olfactory system in *Drosophila*

Drosophila's olfactory organ consists of two olfactory appendages – the antennae (ANTs) and the maxillary palps (MPs). Each of these sensory organs is covered with specialized hairs – so called sensilla. These sensilla can be subdivided into three classes according to their morphology (basiconic, trichoid and coeloconic) (Figure 3.1), (Vosshall,

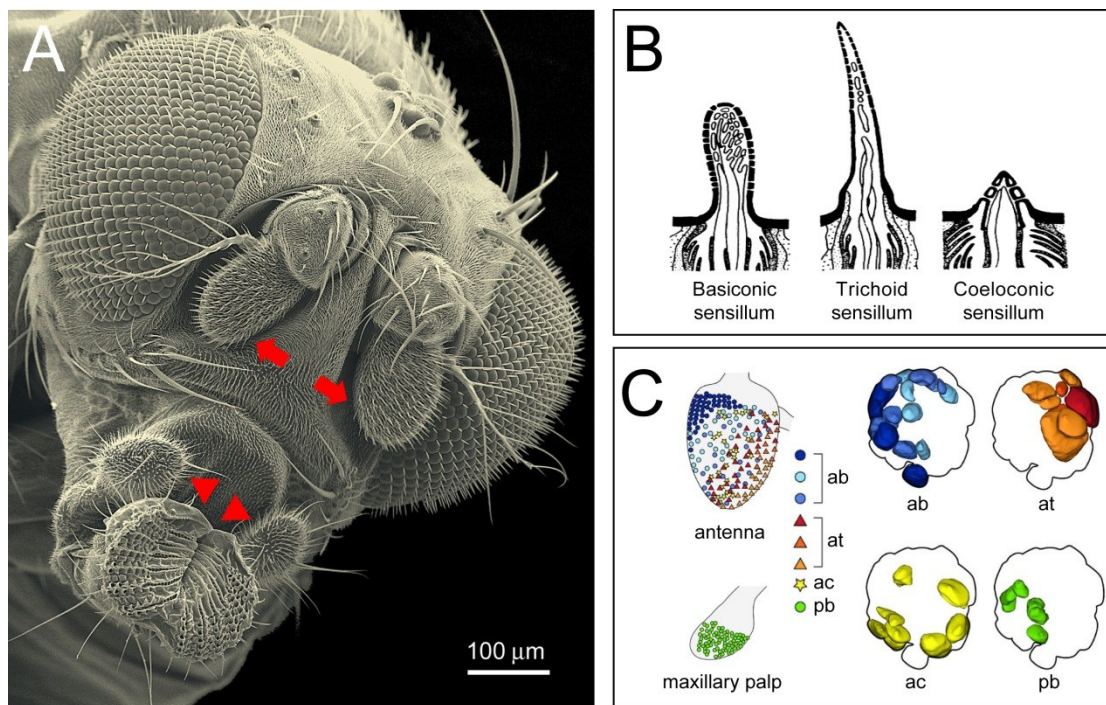


Figure 3.1 | Organization of the olfactory system in *Drosophila melanogaster*

(A) Electron microscope picture of a *Drosophila melanogaster* head with the two olfactory appendages – the two antennae (arrow) and the two maxillary palps (arrowhead). (University of Rochester) (B) The three different sensilla types according to their morphologies. (Vosshall, 2000) (C) Distribution of the different sensilla types across the antenna. (ab, at, ac: antennal basiconic, trichoid or coeloconic; pb: palp basiconic) (Couto et al., 2005).

2000). All three types are found on the third segment of the antenna, whereas basiconic sensilla make up most olfactory sensilla types located on the MP (Stocker et al., 1983; Singh and Nayak, 1985). One individual sensillum is housing a distinct number of olfactory receptor neurons (ORNs) – in the antenna up to four neurons and usually two neurons in the maxillary palp. Sensilla are distributed on their respective organ according to their class (Couto et al., 2005). This special segregation pattern is maintained in part in the antennal lobe (AL), where sensilla of the same OR class send their axons towards the same region of the AL (Couto et al., 2005). ORNs are bipolar neurons that extend their dendrites towards the shaft of their sensillum and make a single axonal projection towards the AL in the central brain. ORNs can express ORs from different types of receptor families. Neurons housed in

trichoid sensilla are mainly expressing ORs, whereas neurons in coeloconic sensilla express the recently discovered IRs (Benton et al., 2009). ORs are members of the G protein-coupled receptor family (GPCRs). Unlike other GPCRs, *Drosophila* ORs were shown to have an inverted membrane topology (Benton et al., 2006). ORNs follow the “one-neuron, one-receptor” rule, so that each ORN expresses a single odor-tuned OR along with a universal co-receptor (Orco, formerly known as Or83b) from a repertoire of 62 different ORs (Hallem et al., 2004; Larsson et al., 2004; Vosshall et al., 1999). In contrast to GPCRs from other organisms, *Drosophila* ORs don't rely on second messengers to activate downstream targets (Wicher et al., 2008). They rather form a complex with the universal co-receptor (Orco) to form a ligand-gated ion-channel (Sato et al., 2008). Another receptor class, the IRs, has recently been discovered in a bioinformatics screen. Similar to ORs, IRs function as heterodimers, together with one of the co-receptors (IR8 and IR25). Neurons expressing IRs are exclusively found in coeloconic sensilla (Benton et al., 2009; Abuin et al., 2011).

There are about 1200 ORNs in one antenna and all of them make axonal projections towards the AL (Stocker, 2001). After the initial outgrowth, all axons fasciculate and together with other neurons form a bundle – the antennal nerve (AN). Within this nerve bundle, they grow towards the AL, where they finally innervate one of the 50 glomeruli. With roughly 120 ORNs, the number of ORNs inside one MP is rather small compared to the ANT. Similarly to the ANT, all MP neurons form the labial nerve (LaN), which also grows towards the AL. Eventually all ORNs converge on the AL, where they segregate and innervate glomeruli in an OR-dependent manner. The insect AL, as many other primary olfactory centers, consists of these so-called glomeruli. The arrangement and number of glomeruli is species specific. The number varies from 43 in *Drosophila* to more than 1000 in locusts (Hansson and Anton, 2000). The individual glomeruli are the part of the AL where ORN axons from a single class

converge and make synaptic contacts with projection neuron (PN) dendrites. PNs relay the olfactory information to higher brain centers (e.g. mushroom body and lateral horn). In addition, LNs form connections between different glomeruli (Figure 3.2), (Chou et al., 2010). Glial cells surrounding the entire AL form a so-called nerve layer around it (Jefferis et al., 2004). In some insects glial cells ensure the proper insulation of the individual glomeruli (Oland et al., 2008). The AL and also the glomeruli as primary olfactory centers share many anatomical and physiological features across the animal kingdom. As mentioned before, it is a common structure in all insect, but can also be found in mammals. In mice, ORNs target towards the olfactory bulb and innervate glomeruli to form synapses with mitral cells, the mouse equivalent of PNs (Komiyama and Luo, 2006). Given the anatomical features of the AL, odorants will activate a certain set ORs, which in turn will activate a specific set of glomeruli. This creates a spatial representation of chemical odors in the brain (Jefferis and Hummel, 2006).

3.1.2 Targeting of olfactory receptor neurons

In order to process olfactory information in the brain properly, it is crucial that the entire network of neurons is connected in a functional way. In the fruit fly's olfactory system one can find multiple levels of wiring specificity. The first level can be found in the ORNs, where the OR choice strictly correlates with the targeting fate of the given neuron. The second level can be found in the PNs, which send axons to one region in the brain (e.g. MB and LH) and dendrites to another region (e.g. the AL). Specifically, PN dendrites have to find ORN axons to form proper synaptic connections. There are three major types of neurons involved in the olfactory circuitry (Ng et al., 2002b). The first order neurons, the ORNs, take up the olfactory information at the receptor level and transmit it to the second order

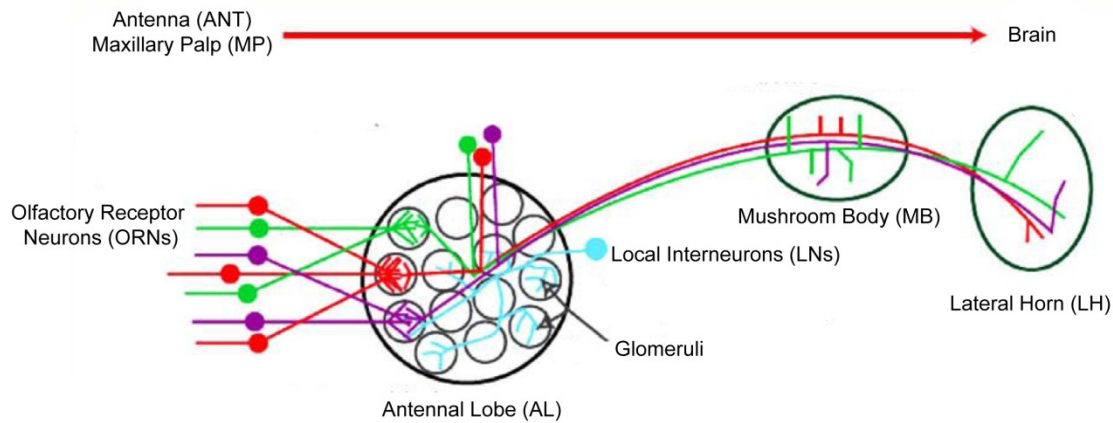


Figure 3.2 | Basic wiring diagram of the olfactory system

The olfactory information is first taken up by certain ORs expressed in ORNs within different sensilla. ORNs send their axons towards the antennal lobe (AL) and target specific glomeruli in a class specific manner. ORNs expressing the same OR always target the same glomerulus. Projection neurons (PNs) send their dendrites to the AL and form the dendritic counterpart for the synapse formation between ORNs and PNs. Intrinsic local interneurons (LN) form an inhibitory network within the AL. The AL serves as a relay station between ORNs and PNs. The olfactory information is relayed to the PNs, which in turn send this input to higher brain center, like the mushroom body (MB) or lateral horn (LH) (Jefferis and Hummel, 2006).

neurons, the PNs. These interneurons relay the olfactory input from the periphery towards higher brain centers. The third major type of neurons is comprised of intrinsic local interneuron (LNs), which mainly form inhibitory but also excitatory connections within the AL (Chou et al., 2010). The cell bodies of PNs and LNs are localized in three distinct clusters surrounding the antennal lobe (Jefferis et al., 2001). One can find around 200 PNs and 200 LNs in the average *Drosophila* brain (Stocker et al., 1990; Chou et al., 2010).

The fruit fly has become an attractive model organism to study the mechanisms of axon guidance over the past years, since it is possible to label individual ORN classes and their synaptic partners in order to dissect the olfactory pathway. Especially the highly specific connections between PNs and ORNs have been studied to understand the underlying mechanism of this complex wiring (Komiya et al., 2004a; Sweeney et al., 2007; Bashaw, 2007). Several important aspects of this complex wiring were addressed by many

researchers during the last years: What mechanisms allow the formation of an olfactory system with this high degree of stereotypy and precision? What mechanisms are required for this high degree of accuracy? Previous studies provide evidence that the entire process of axon guidance is a multi-step process, which requires different molecules at different points during distinct developmental stages (Jefferis et al., 2002). It has been suggested that both neuron populations (PNs and ORNs) are somewhat autonomous with regards to their specification and targeting. Initially, both neuron types form a coarse targeting map, prior to interacting with their future partner, and only at the last steps both “maps” are registered to the respective counterpart (Jefferis et al., 2004). ORNs depend on the map formed by PNs as they will form synapses with respective partner PNs. Mistargeting of PNs results in a corresponding mistargeting of ORNs (Spletter et al., 2007; Tea et al., 2010). Since the spatial organization of ORNs in the maxillary palp and antenna is only partially maintained in the AL (Couto et al., 2005), other mechanisms have to contribute to ensure proper ORN targeting.

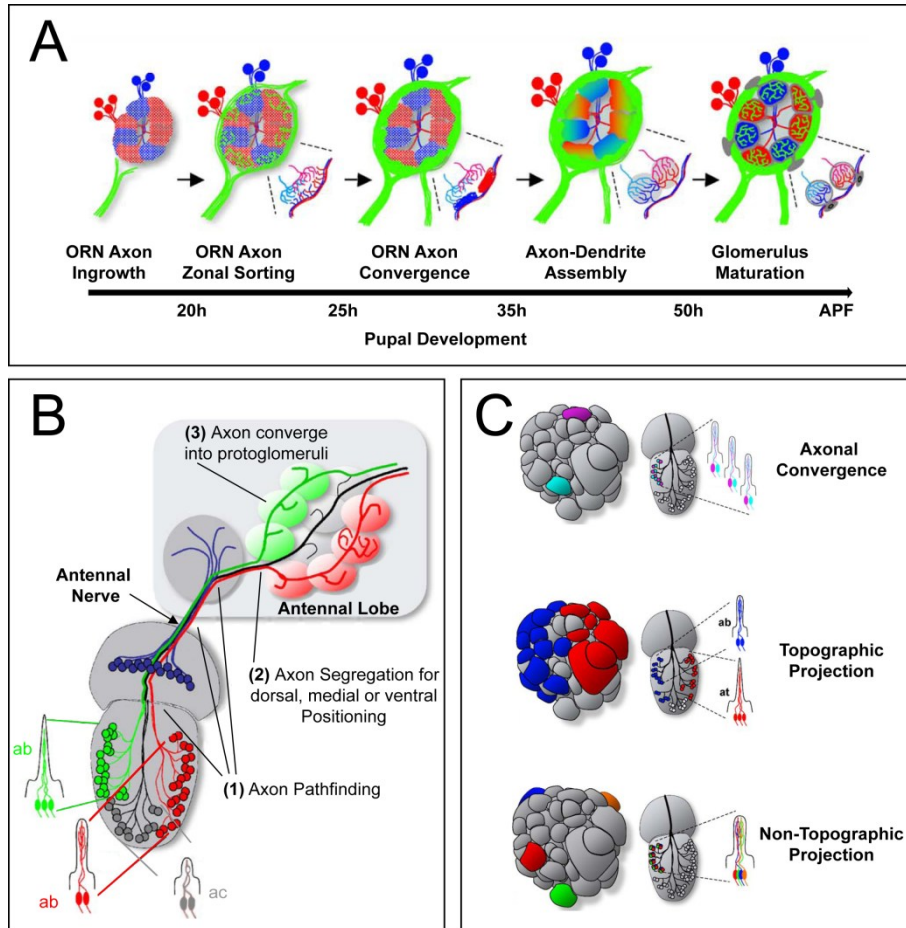


Figure 3.3 | Targeting of ORN axons is a multistep process

(A) Before the ORNs reach the AL, PN dendrites have already formed a protoglomerular map. At around 15h APF ORN axons reach the AL and will project into the periphery (nerve fiber layer) around the AL. They will start innervating their target glomeruli in several discrete steps. From the nerve fiber layer ORN axons will sort out into three different zones. Here axons projecting along the same zone are still bundled. At around 30h APF axons will further sort out. Axons will defasciculate from each other and only axons from the same ORN class will stay together. The assembly of first axonal-dendritic contacts between the PNs and ORNs happens at around 40h APF. Later during pupal development these glomeruli mature further and develop into fully functional units. **(B)** Representation of the different steps of ORN targeting. Scheme is representative for ORNs from the ANT, but the same mechanisms can be found in the MP. ORN axons start to form and grow out of the ANT in three main fascicles formed by the basiconic, trichoid and coeloconic sensilla housed ORNs. Here attractive cues promote the bundling of axons from the same sensilla type. Later all three fascicles merge together with axons from non-olfactory neurons (blue) into the antennal nerve (AN). Again attractive guidance cues promote the formation of the AN. Non-olfactory axons will sort out of the AN early. Once the remaining axons reach the AL, repulsive cues trigger the sorting into three main projection routes (dorsal, medial or ventral). In the last step, axons of the same class sort out and target a specific glomerulus, where they will form connections with the PN dendrites. **(C)** The targeting of ORN axons follows certain rules: (1) Axonal convergence: ORNs expressing the same OR will always target to the same glomerulus. (2) Topographic projection: The sensilla distribution on the ANT is maintained in the brain. ORNs from “ab” and “at” will target to medial and lateral parts of the AL, respectively. (3) Non-topographic projection: Spatial representation in the ANT is not always maintained, so that ORNs from the same sensillum target to entirely different glomeruli. Adapted from (Jefferis and Hummel, 2006).

Neurons housed in neighboring sensilla are more likely to target adjacent glomeruli (Couto et al., 2005). During development ORNs start to form axons and grow out of the third antennal segment in three main fascicles to form the AN (Jhaveri and Rodrigues, 2002). These three main bundles represent three main clusters of ORNs within the antenna. During this initial step intra- and inter-class adhesion factors are required to ensure that the fascicles are formed, which eventually converge into the antennal nerve (Komiya et al., 2004b). Once they leave the third antennal segment, ORNs merge with other sensory neurons (e.g. auditory neurons from the Johnston's organ) and continue to grow within one bundle. It is believed that continued action of inter-class adhesion forces are required to maintain the antennal nerve. This changes as soon as the first neurons segregate from the antennal nerve in order to project towards other brain centers (e.g. antennal mechanosensory and motor center). At this point repulsive inter-class forces are activated to ensure segregation of distinct neuron types. Eventually the antennal nerve will reach the antennal lobe, where all ORNs will spread out over the peripheral nerve fiber layer around the antennal lobe (Oland et al., 2008; Hummel and Zipursky, 2004; Hummel et al., 2003). At this point the ORNs split into three main projection routes – a dorsolateral, central and ventromedial route (Ang et al., 2003). Intra-class adhesion ensures that axons from the same ORN class converge on the same glomerulus, but at the same time inter-class repulsion ensures that neurons from different classes are separated accordingly (Gao et al., 2000). One of the first molecules shown to be involved is the cell surface protein Dscam (Down Synapse Cell Adhesion Molecule) and its downstream effector the serine/threonine kinase Pak and the adaptor Dock. It is believed that Dscam can provide a neuronal identity and is necessary for some ORNs to distinguish between “self” and “non-self” neurons (Hummel et al., 2003). Although *Dscam* mutants show severe targeting defects, most axons are still able to grow towards the

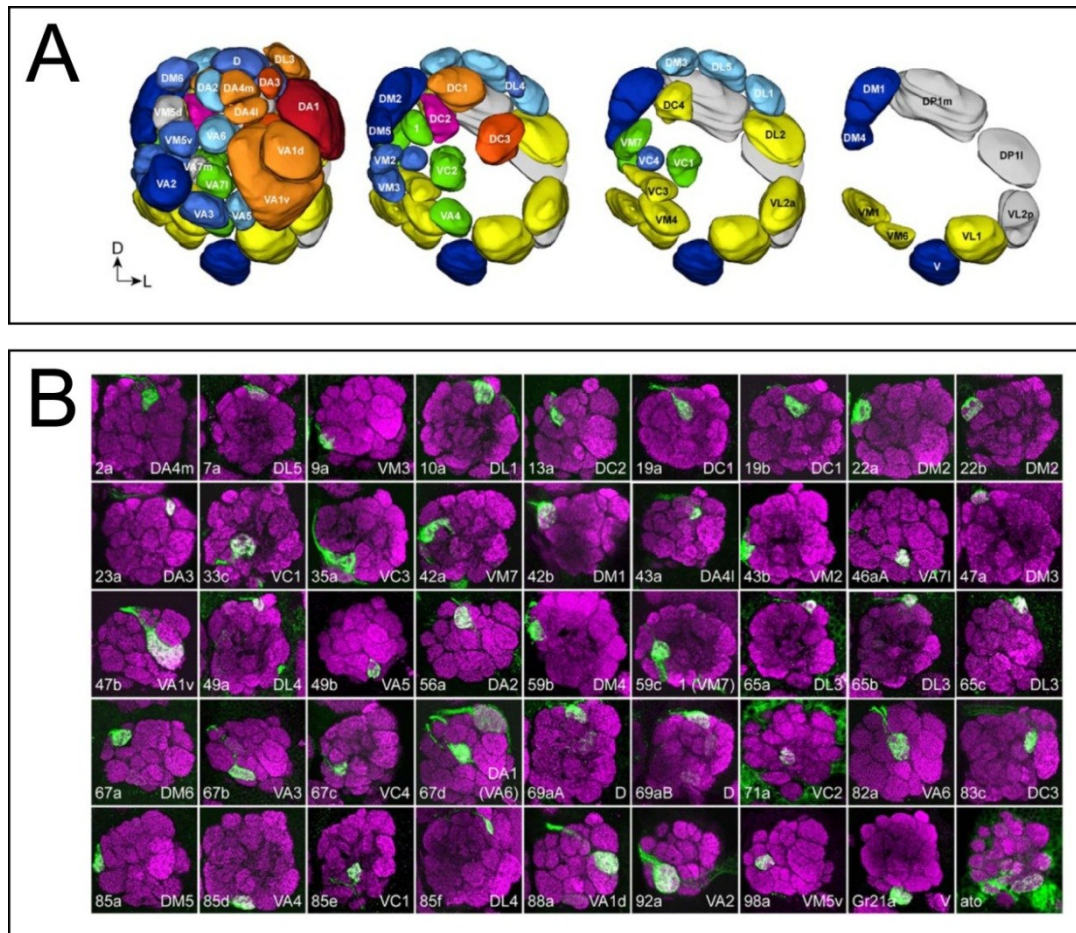


Figure 3.4 | Map of different ORN classes and their projections into the antennal lobe

(A) 3D reconstruction of the antennal lobe showing 49 glomeruli. The view starts anteriorly and stepwise goes posteriorly. Color code represents the sensilla origin of the ORN innervating a particular glomerulus (see Figure 3.1C). **(B)** Antennal lobe showing the innervation patterns of different ORN classes. The different Or-reporter lines are either direct fusion with mCD8-GFP or were crossed to UAS-mCD8-GFP. Brain were stained with anti-GFP to visualize the ORN axons and counterstained with the presynaptic marker NC82. ORNs show a very stereotyped targeting pattern – axons of ORNs expressing the same OR always innervate the same glomerulus. (Couto et al., 2005).

antennal lobe. They often stop prematurely and form ectopic glomeruli (Hummel et al., 2003). Similarly, *dock* and *pak* mutants display a severely disrupted targeting pattern forming ectopic connection across the entire AL (Ang et al., 2003). Interestingly, the class specificity is maintained in *dscam* mutants. Another important class of guidance molecules is the family of Robo (Roundabout) receptors. The different receptors, Robo, Robo2 and Robo3

are expressed across the AL in a complementary pattern. *Robo* mutants show mistargeting defects in the initial positioning of ORN axon terminals shortly after they enter the antennal lobe (Jhaveri et al., 2004). The differential expression of the Robo receptors seems to instruct the axons which one of the three main projection routes they should take (Jhaveri et al., 2004). At later stages, after the axons started to innervate the protoglomeruli formed by the PNs, N-Cadherin, a Ca^{2+} -dependent cell adhesion molecules is required (Hummel and Zipursky, 2004). In this final step local short-range inter- and intra-class interactions lead axons that express the same OR towards a distinct protoglomerulus. N-cadherin is required to promote intra-class adhesion and to stabilize these protoglomeruli (Hummel and Zipursky, 2004). *Ncad* mutants show a severe defect in glomerulus maturation: ORN axons still target to their correct target zone, but fail to form synapses with the PNs and eventually will fail to form mature glomeruli. Additionally, N-cadherin is also required in PNs, where it restricts PN dendrites to a single glomerulus. *Ncad* mutant PNs show a spillover of dendrites into neighboring glomeruli (Zhu and Luo, 2004). It was shown that *Sema-1a* is required to promote inter-class repulsion forces (Lattemann et al., 2007). *Sema-1a* mutant ORNs are unable to sort out and intermingle with other OR-classes at ectopic glomeruli. Another group could show that *Sema-1a* acts together with PlexinA to mediate repulsion to early arriving ORNs in the antennal lobe (Sweeney et al., 2007). In *sema-1a* or *plexA* mutants these early arriving ORNs are no longer restricted in their targeting area and spread out over the antennal lobe. Recently, the transmembrane protein Teneurin was shown to be involved in the final steps of synapse specificity and formation. Teneurins instruct specific ORN-PN matching through homophilic attraction (Hong et al., 2012). Differential expression of Teneurin isoforms could provide a combinatorial code required to instruct the different ORN-PN populations to form synapses. Ectopic expression of Teneurins leads to a

mismatching of ORN-PN pairs. Another molecule, Notch, is involved at several steps of ORN development (Lieber et al., 2011; Lin et al., 2010). Early during development Notch levels regulate, which OR will be expressed in a given neuron. Later, all neurons that were Notch positive at this point collectively target to a specific area of the AL. The antennal lobe can be divided into two complementary regions, a Notch-ON and Notch-OFF region. It was shown that ORNs project to these distinct regions in a Notch-dependent manner (Endo et al., 2007). Another protein that is involved in the receptor choice decision, Acj6 (Abnormal Chemosensory Jump 6), is also involved in the targeting of ORNs (Komiyama et al., 2004a; Bai et al., 2009). Unlike in mouse, the expression of the OR itself doesn't influence the targeting of the ORN. Firstly, the expression of ORs is turned on relatively late in *Drosophila*, at a time point where the ORNs have already reached their target zone. Secondly, it was shown that mis-expression of ORs doesn't alter the targeting pattern of ORNs (Dobritsa et al., 2003). All these different molecules act at different steps during the complex process of axon sorting and synapse formation. Depending on the temporal requirement of a molecule, its malfunction can lead to global or local axon mistargeting.

To conclude with, *Drosophila's* olfactory system is a great tool to investigate axon guidance for a number of reasons. Firstly, the class-specific targeting of ORN axons is highly stereotyped. This allows a thorough analysis in a great number of animals. Secondly, *Drosophila's* olfactory system shares many features with that of mammals. Working with the fruit fly's olfactory system reduces the complexity of the model system (compared to mammals), but at the same time has enough homology to mammalian systems to discover general mechanisms for higher organisms. Lastly, in *Drosophila* the great number of genetic tools allows the manipulation of all components of the olfactory system - even individual ORN classes.

3.2 The neuronal cytoskeleton

If one seeks to understand the mechanisms of axon guidance, one has to look not only at the cellular level (e.g. ORNs), but also at subcellular levels. Here the growth cone of axons is of special interest. As the growth cone is the tip of the growing axon, it is the first part of the neuron that comes into contact with guidance cues. As explained before, axon guidance is believed to be a multi-step process in the olfactory system (Figure 3.3). At every decision point the ORN axon is exposed to different mixtures of guidance cues, which can be repulsive or attractive. Depending on the guidance cues, axons are continuing to grow, stalling growth or changing direction of growth – in all three cases the axon undergoes changes in its actin cytoskeleton. It is the actin cytoskeleton that enables the axon to grow into certain directions in the first place. The following chapter will familiarize the reader with the two major components of the cytoskeleton – actin filaments, microtubules and their different properties. Lastly, I will introduce the structural features of the growth cone and its functions as an integrator of multiple guidance cues during ORN axon guidance.

3.2.1 Actin filaments and microtubules

Actin is an essential cytoskeletal protein and also one of the most abundant cellular proteins (Fine and Bray 1971). Its importance is also reflected in the degree of sequence conservation. *Drosophila* exhibits at least six different actin genes encoding different isoforms (Tobin and Zulauf, 1980). In neurons the predominant isoforms are β -actin and γ -actin, which differ only in a few amino acids. Actin is a globular protein and has a size of 43 kDa (Holmes et al., 1990). Individual actin molecules are referred to as monomeric actin (G-actin), which can under certain conditions polymerize into filamentous actin (F-actin).

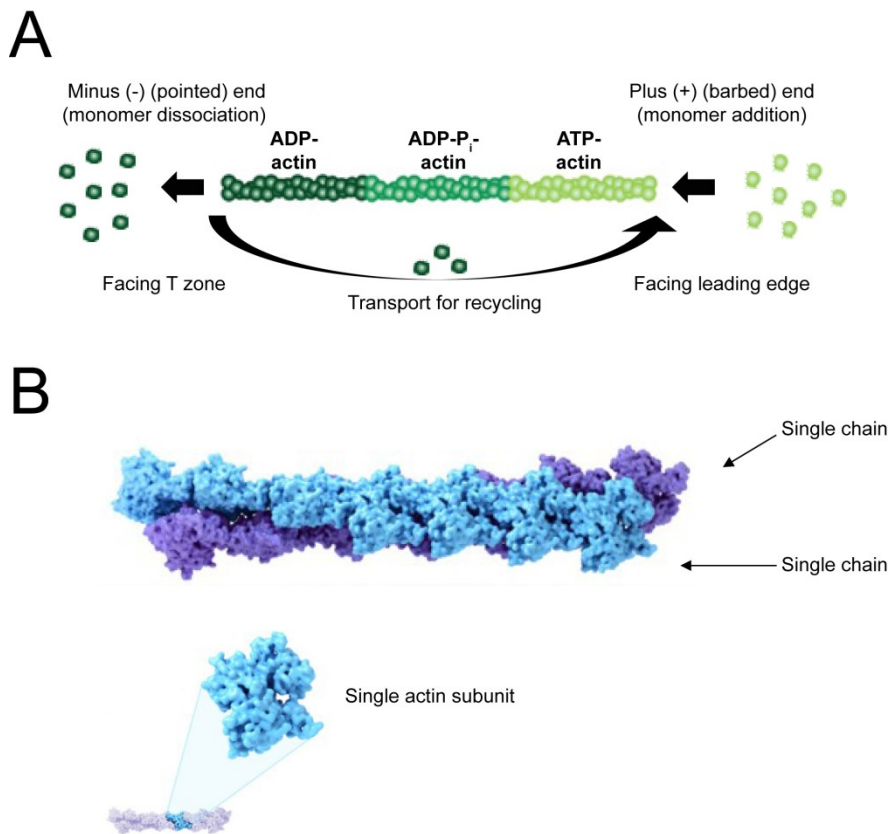


Figure 3.5 | Structural features of actin filaments

(A) F-actin is a polar filament. The majority of actin monomers are added at the plus (barbed) end, whereas most of the dissociation happens at the minus (pointed) end of the filament. The ATP-status of the individual actin monomers in the filaments changes from ATP bound, to ADP- P_i to ADP bound with progressing life time within the filament. Monomers dissociated from the filament are in part recycled and again become part of the G-actin pool. Monomers are recruited from that pool for addition to the plus end of filaments. Within a growth cone, the plus end is facing the leading edge of the cells, whereas the minus end is facing the T zone. Adapted from (Dent et al., 2011). **(B)** 13-mer of an F-actin filament with the two single actin chains colored in light and dark blue. Together the two intertwined chains form a helix with a diameter of 7 nm. Adapted from (Bugyi and Carlier, 2010) and U.S. National Library of Medicine.

Although in the cell both variants are present, F-actin is the major component forming the cytoskeleton. Therefore many studies focus on F-actin. The process of actin polymerization from monomeric G-actin into filamentous F-actin forms the essential basis for all actin dynamics in a cell. The generation of F-actin from a pool of G-actin requires two different steps. The first step requires the initial nucleation of a few actin monomers from the G-actin pool (Tobacman and Korn, 1983). This “seed” will serve as a basic scaffold for a continuous

polymerization to further elongate the filament (Kasai et al., 1962). In the process of polymerization G-actin functions as an ATPase, hydrolyzing ATP to ADP to catalyze actin polymerization (Pollard and Weeds, 1984). Due to the consumption of ATP during this process, F-actin formation is considered to be a major ATP sink in cells. It is known that F-actin can form spontaneously under certain conditions *in vitro* (Cooper et al., 1983; Buzan and Frieden, 1996). However, a minimal concentration of G-actin is required, which allows individual monomers to form seeds (Koestler et al., 2009a). Compared to the *in vitro* situation, a living cell represents a far more complex environment under which actin can polymerize. Actin filaments have a diameter of 7 nm and consist of a two-stranded helix with a right handed twist. F-actin is a polarized filament with the two different ends called “barbed” and “pointed” ends, respectively. Both ends have different polymerization dynamics. The “barbed” end is considered to be the fast growing end, whereas the “pointed” is the slow growing end of the filament (Small et al., 1977). In general, there is an equilibrium between the removal and addition of G-actin to F-actin, which happens at both ends of the filament (Pollard, 1986). However, the concentration of G-actin needed to facilitate its addition to the filament is six times lower at the “barbed” end (0.1 μM) than at the “pointed” end (0.6 μM) (Pollard, 1986). This imbalance eventually leads to one fast growing end and another slow growing end of F-actin. Interestingly, in most living cells the cytoplasmic G-actin concentration (100 μM) is significantly higher than the critical concentration for actin polymerization (0.1 μM). Given that 100 μM pure actin polymerizes *in vitro* in a few seconds, leaving only very little G-actin (Pollard et al., 2000), one could speculate that *in vivo* eventually all G-actin should polymerize into F-actin. It is believed that certain proteins, so called actin binding proteins, not only bind actin, but also strongly influence the availability of actin monomers, the initial nucleation and many other aspects.

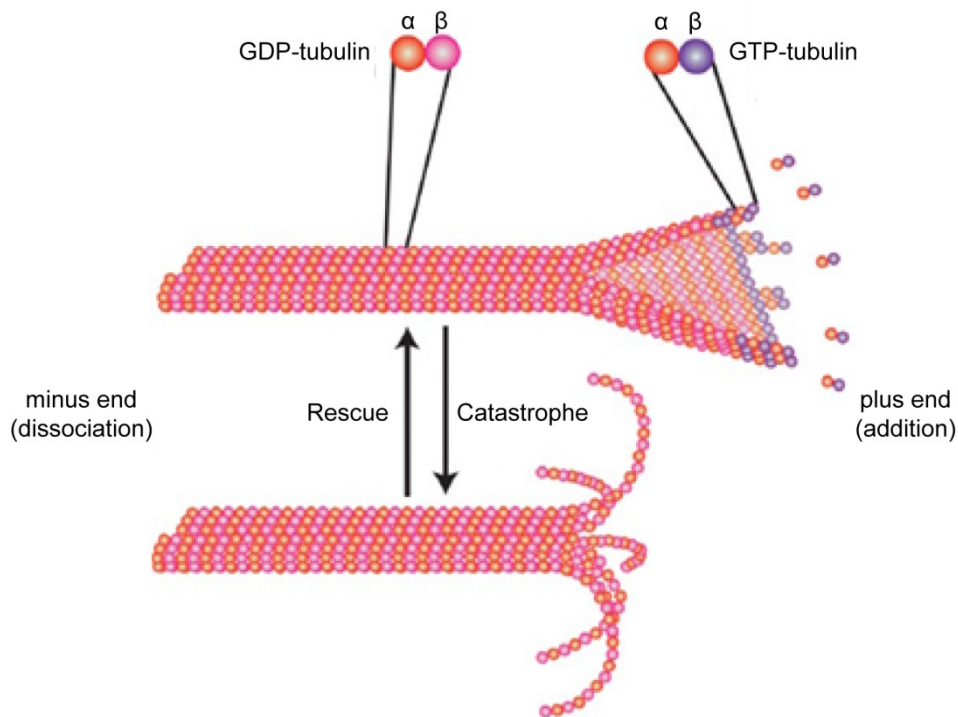


Figure 3.6 | Structural features of microtubules

Microtubules are polar compounds with a plus and a minus end. Tubulin subunits are usually added at the plus end and dissociate from the minus end. Tubulin subunits (α/β) are bound in a GTP state and then rapidly converted to a GDP state. Microtubules form a hollow structure with a diameter of 25 nm. The process of microtubule shrinkage is termed catastrophe, whereas growth is called rescue. Adapted from (Dent et al., 2011).

Using actin binding proteins and influencing the turnover rate of the filament, the cell is able to tightly control its actin cytoskeleton. Actin filaments can be organized in different forms depending on the presence of additional proteins. For example, actin bundling proteins (e.g. Fascin) (Cohan et al., 2001) promote the formation of linear actin bundles, whereas branching proteins (e.g. Arp2/3) (Mullins et al., 1998) promote branched or interconnected actin networks.

The second important component of the cytoskeleton is the microtubules (MT), which consist of α - and β -tubulin subunits and can be up to 100 μm long. Furthermore they are hollow cylinders with a diameter of 25 nm. It is believed that MTs provide the structural support, which is used to transport organelles throughout the cell using motor proteins

(Hirokawa and Takemura, 2004). Structurally MTs are polarized molecules. Tubulin subunits are more rapidly attached at the fast growing plus (+) end, whereas the minus (-) end is the slower growing end (Hirokawa and Takemura, 2004). In neurons MTs are formed in the centrosomal region and extend towards the periphery, where the minus (-) end is facing the centrosome. The plus (+) end exhibits a dynamic instability, where MTs undergo cycles of assembly and disassembly (Tanaka et al., 1995). The organization of MTs is regulated by proteins called microtubule-associated proteins (MAPs). These proteins bind MTs and regulate all kind of aspects, such as the assembly/disassembly rate or the binding to actin filaments.

Together MTs and actin filaments control and maintain the shape of axons. Changes in neuronal morphology are always a result of changes in the cytoskeleton. The motility of neurons and cells in general, strictly depends on actin filaments. MTs have the additional function to serve as a platform for intracellular transport. Actin and MTs also directly interact, when it comes to steering the growth cone into one or the other direction. The following chapter will explain how both structures together form the growth cone and influence actin dynamics.

3.2.2 The growth cone

Neurons require actin filaments to form, extend and guide their axons and dendrites. The cytoskeleton produces the necessary force that allows the neuron to extend forward. The growth cone is composed of two main structures - filopodia and lamellipodia. These are two fundamental cellular structures that provide cell motility. During axon guidance the growth cone as a whole (especially filopodia and lamellipodia) serves as sensor

and integrator of guidance cues (Chacón and Fazzari, 2011; Chauvet and Rougon, 2009; Zheng et al., 1996). An axon receives cues from the extracellular matrix (ECM) or directly from neighboring cells, which can either be attractive or repellent. Usually axons receive more than just one stimulus. At this point the growth cone functions as an integrator of all these different cues (Rose and Chiba, 1999).

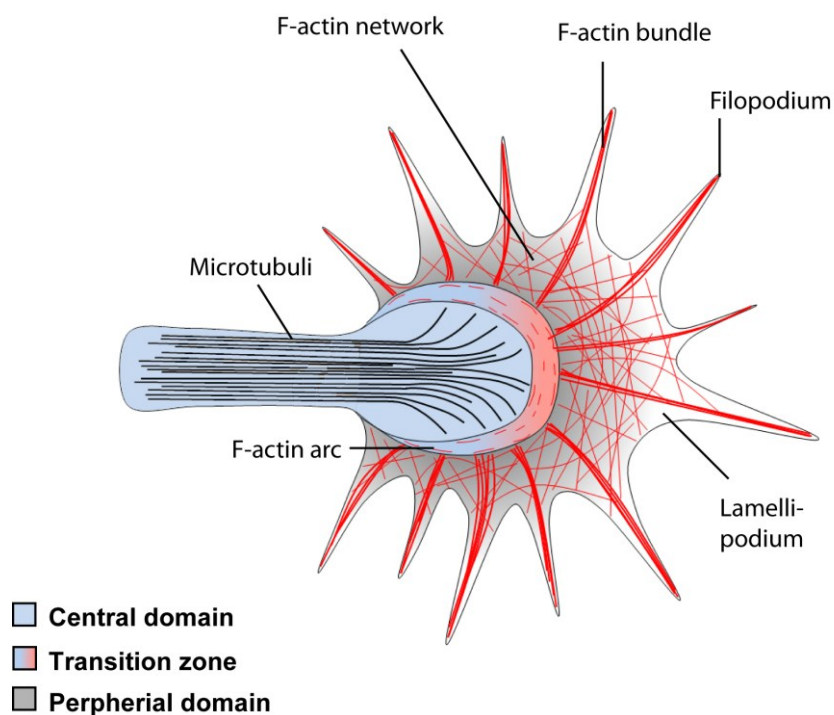


Figure 3.7 | Structure of a growth cone

The structure of a growth cone greatly correlates with its function. The leading edge consists mainly of filopodia, which contains long F-actin fibers. Filopodia serve as “antennae” that explore the surroundings of the growth cone to detect guidance cues. Filopodia are separated by lamellipodia, which contain a “mesh”-like actin network. The growth cone itself consists of three different compartments. The peripheral (P) zone contains the rigid F-actin bundles that form the filopodia and the highly branched actin network of the lamellipodia. The central (C) domain encloses the stable region of the axon shaft, which contains microtubule bundles. Individual pioneering microtubules can grow from the C-domain towards the P-domain to explore new filopodia. The transition (T) zone is separating the C- and P-zone with a ring of perpendicular F-actin. This so called F-actin arc can generate a contractile force using actomyosin motors.

Growth cones can receive repelling cues, which will induce a collapse of MTs and F-actin fibers, or they can receive attractive cues, which induces F-actin polymerization (Fass et al., 2004; Marsick et al., 2010; Gallo and Letourneau, 2004). For example, Robo or Semaphorins are well characterized guidance receptors in the growth cone, both mediating repulsion (Murray and Whittington, 1999; Fujisawa and Kitsukawat, 1998). With this chapter I will first introduce the different structural features of the growth cone, followed by a description regarding its function in axon guidance.

The growth cone consists of three distinct compartments: a central domain (C-domain), a transitional zone (T-zone) and a peripheral zone (P-domain). The C-domain follows the axonal shaft and consists mainly of bundled and stable MT. This part of the growth cone represents a stable basis and least dynamic part. Many organelles and vesicles are localized here using the MTs for transportation (Hirokawa et al., 1998). Single pioneering MTs start to grow further towards the filopodia into the P-domain. These pioneering MTs explore their surroundings for a suitable position to form a new, stable MT bundle (Forscher and Smith, 1988). The edge of the growth cone, the P-domain, is made up of long, rigid F-actin bundles (filopodia) and a mesh-like network of highly branched F-actin (lamellipodia) (Bartles, 2000; Small et al., 1977). Together, these two structures act as sensors for guidance cues in the P-domain. A third compartment, the T-zone, separates the C-domain from the P-domain. An F-actin arc perpendicular to the MTs of C-domain can be found in the T-zone (Schaefer et al., 2002). This arc separates the highly dynamic part (P-domain) from the less dynamic part (C-domain) of the growth cone. It is also believed to restrict pioneering MTs on their way into the P-domain.

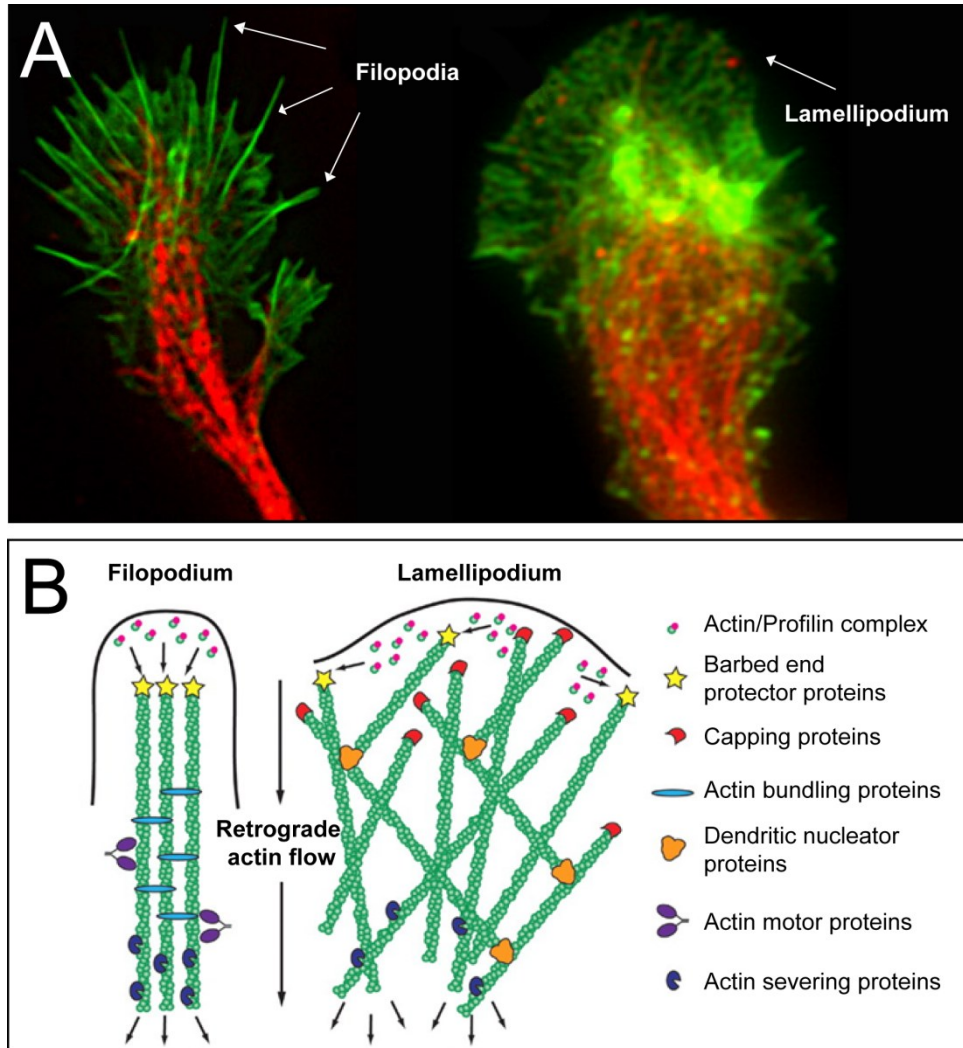


Figure 3.8 | Actin network in filopodia and lamellipodia

(A) Typical growth cone displaying the “antenna”-like structures of the filopodia on the left. F-actin bundles are visible green. Microtubules are visible in red and make up the axonal shaft. Lamellipodia are displayed on the right in green. In contrast to the filopodia, a highly branched actin network is visible. Adapted from the University of Wisconsin-Madison. **(B)** The rigid F-actin bundles in filopodia are formed by F-actin and bundling proteins. Monomeric actin is added to the filament with the help of “barbed”-end binding proteins. Severing happens at the “pointed”-end and is facilitated by actin severing proteins. The constant retrograde flow of actin filaments is depicted by the black arrow. In contrast, the lamellipodium forms a highly branched actin network. The actin mechanics are comparable to filopodia. Adapted from (Dent et al., 2011)

Lamellipodia are flat sheet-like structures, while filopodia are thin spike-like protrusions (Medalia et al., 2007; Small et al., 1977). Both act as sensors of the extracellular environment. Although both structures are formed by actin filaments, the organization of these filaments is fundamentally different. These differences provide different properties to lamellipodia and filopodia. Lamellipodia contribute to the motility machinery of the neuron and have a complicated geometric arrangement of actin filaments, which are organized in highly branched actin networks (Huber et al., 2008). At the periphery of lamellipodia, about 50% of all actin filaments have their fast growing (“barbed” ends) facing the leading edge of the growth cone (Small et al., 1977). It has been shown that Arp2/3 is required to generate this actin meshwork in non-neuronal cells (Mullins et al., 1998; Cooper et al., 2001). However, it is still controversial whether Arp2/3 is also required in neurons. Here, the actin fibers form a dense network of crisscrossing filaments rather than branched filaments (Strasser et al., 2004).

Filopodia extend towards the periphery of the growth cone and act as “antenna” to explore the environment (Gomez et al., 2001). On average, neuronal filopodia are 5-8 μm long. Using their characteristic shape, filopodia greatly increase the extracellular area that can be used to detect guidance signals (Gomez et al., 2001). Due to the circular arrangement of the growth cone and filopodia, even small changes in the filopodia length lead to large changes in the area that the neuron can probe for guidance cues. Within a single filopodium the majority of all actin filaments are arranged as bundles with their fast growing end (“barbed” end) facing the tip of the filopodium. This filament arrangement allows the generation of a protrusive force in the direction of the tip as the “barbed” end continuously polymerizes. This force is eventually driving the membrane outwards. Additionally, filopodia can serve as synaptic precursors (Sekino et al., 2007). Here, filopodia act as dendritic spine

precursors. After the initial encounter with an axon terminal has been made, filopodia undergo a metamorphosis and gradually shift their F-actin network towards a mature synapse (Takahashi et al., 2006).

3.2.3 Axonal growth

Actin filaments are transient structures that undergo cycles of polymerization and depolymerization. Actin filament turnover rates can be increased by positive regulators, such as ADF/cofilin, which is regulated by extracellular signals (Gehler et al., 2004; Sarmiere and Bamberg, 2004). Conversely, inhibition of actin turnover results in the blocking of axon extension, which is followed by a growth cone collapse. Turnover rates differ between lamellipodia and filopodia (Mallavarapu and Mitchison, 1999). It is believed that the lower turnover rate in filopodia is required for the maintenance of its antenna like structure (Sabo and McAllister, 2003). A second mechanism that is important for the regulation of the actin network is the retrograde flow. This term describes the flow of actin monomers from the leading edge of the growth cone towards the central domain (Brown and Bridgman, 2004). The retrograde flow is generated by myosin forces pulling back actin filaments towards the center of the growth cone (Lin et al., 1997). Many different myosin motor proteins seem to play an important role in the generation of the retrograde flow (Diefenbach, 2002). Apart from myosin motor proteins, another factor controlling the retrograde flow rate is the so called “molecular clutch”. This term describes a mechanism, in which a physical link between the actin cytoskeleton and extracellular signal is formed. More specifically, an extracellular signal activates a transmembrane receptor, which in turn mediates the linkage with actin filaments. Recent studies have identified actin binding proteins as mediators of this direct interaction (Hu, 2004). This physical link is able to reduce the retrograde flow of actin

molecules (Suter and Forscher, 2001). Taken together, there are various molecular mechanisms and proteins influencing the two main aspects of actin dynamics: the polymerization rate at the “barbed” end and the retrograde flow rate. Together, both determine the protrusion dynamics within the growth cone.

The process of axonal growth can be divided in four main stages: encounter, protrusion, engorgement and consolidation (Goldberg and Burmeister, 1986) (Figure 3.9). During the protrusion phase the growth cone comes into contact with an attractive cue. A ligand from the ECM binds a guidance receptor of the growth cone, which triggers the formation of the molecular “clutch”. This leads to a reduction of retrograde F-actin flow. Nevertheless, F-actin polymerization continues at the “barbed” end of the filament. Filopodia as well as lamellipodia rapidly extend forward and push the membrane outward (Footer et al., 2007). During engorgement, the actin between the central domain and the attachment site is severed and cleared. As a consequence the F-actin arc realigns towards the new site of growth. This is followed by an invasion of MTs, which are guided by those F-actin arcs. During the consolidation, microtubules are compressed into the newly formed C-domain by myosin generated forces. The motor proteins are located in the F-actin arc and also promote the retraction of filopodia from the area of new growth. This further consolidates the new axon shaft.

In general all three stages of axon outgrowth involve major rearrangements of the neuronal cytoskeleton – starting from the binding of a guidance receptor, which initiates the molecular “clutch”, and ending with the rapid F-actin growth and consolidation. Overall different guidance cues can have different effects, but they all act on the cytoskeleton – activating or deactivating cytoskeleton regulating proteins (actin or

microtubule binding proteins). These proteins shift the balance between F-actin and G-actin in one or the other direction, triggering actin polymerization or depolymerization.

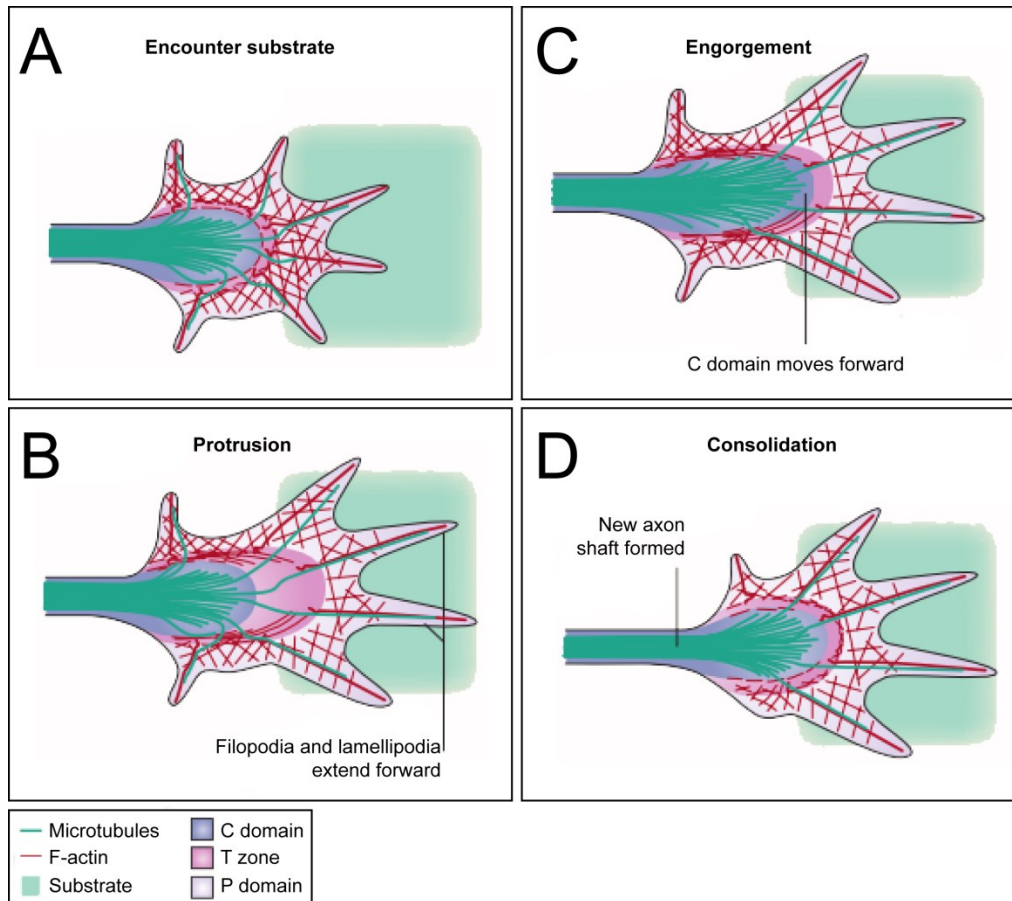


Figure 3.9 | Different stages of axon outgrowth

Drawings represent the four different stages of axon outgrowth. **(A)** The leading edge of the growth cone comes into contact with an attractive cue. This activates guidance receptors and their downstream targets. **(B)** Filopodia and lamellipodia rapidly extend towards the attractive cue. A molecular “clutch” locally links actin fibers at the site of the receptor activation to the membrane. In addition, at the site of activation the retrograde flow of actin is reduced, which further promotes the extension of filopodia and lamellipodia. **(C)** Microtubules from the C-domain push forward to the leading edge. F-actin behind the molecular “clutch” is severed and removed. **(D)** At last, microtubules are compacted along the newly formed axon shaft by actomyosin generated forces. Actin in that area is depolymerized and removed. Adapted from (Lowery and Van Vactor, 2009)

3.3 The growth cone as a signal integrator

The growth cone has to respond to multiple sources of spatial information, which can lead to different reactions of a neuron. If confronted with attractive cues, the growth cone will promote forward movement. If faced with a repellent cue, the growth cone will stall the forward movement until a new attractive cue is recognized. More often the axon will deal with a situation, where the growth cone is confronted with a spatial bias. In this

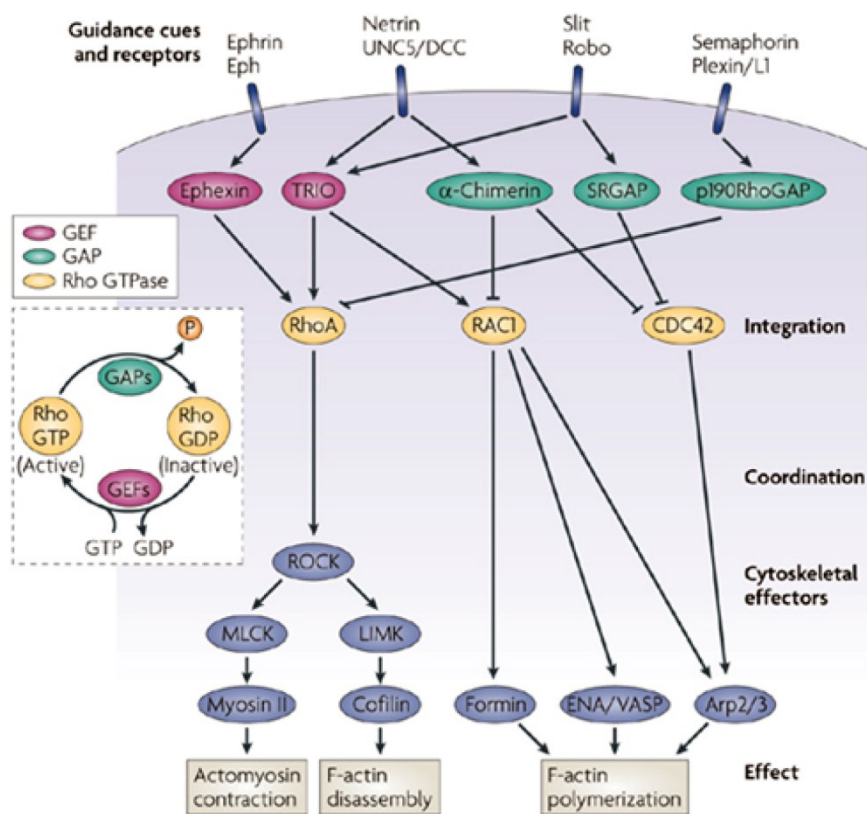


Figure 3.10 | The growth cone as an integrator of different guidance cues

Rho family GTPases act as integrators of different guidance cues. Rho GTPases require GTP for the activation of their downstream targets. They are active in their GTP-bound state and inactive in their GDP-bound state. Many receptor/ligand pairs activate so called GEFs or GAPs. These proteins promote the exchange of GDP for GTP or vice versa, and thereby activating or inhibiting Rho GTPases. Subsequently, they activate downstream actin modifying proteins. Activation or inactivation of these cytoskeletal modifiers can trigger actin polymerization or depolymerization, as well as actomyosin contraction, which ultimately result in a turn of the growth cone. Adapted from (Lowery and Van Vactor, 2009).

case major cytoskeletal rearrangements will lead to a growth cone collapse on one side and a buildup on the opposite side. This will eventually lead to a turning movement of the axon towards the attractive cue. In order to reach its designated target zone, axons have to be able to respond properly to these cues. The growth cone of a neuron therefore acts as an integrator of all these guidance signals. Interestingly the filopodia and lamellipodia are crucial to this process (Gomez et al., 2001). When the formation of both is artificially suppressed, axons are unable to detect local guidance cues (Agarwal et al., 2012). The path of a single axon is usually subdivided into smaller segments, challenging the growth cone with choice points along the way (Wilson, 2010). Guidance cues usually activate Rac1, Cdc42 or other GTPases (Lucanic and Cheng, 2008; Ng et al., 2002a; Hall and Lalli, 2010). These positive cues keep growth cones “on track” during their journey. Negative cues such as Slit, Sema3A or Ephrins stop axons from invading certain areas (Piper et al., 2006; Aizawa et al., 2001; Sahin et al., 2005). Acting as signaling nodes, Rho family GTPases are key proteins in cytoskeletal rearrangements (Ng and Luo, 2004; Hall and Lalli, 2010). Activated by guidance receptors, Rho GTPase regulators are either activating or inhibiting Rho GTPases. This can lead to actomyosin contractions, F-actin disassembly or F-actin polymerization. One recently well described pathway is the interaction between Semaphorin and Mical, which leads to F-actin disassembly (Hung et al., 2010). In another recent publication the same group could show that Mical is physically interacting and modifying actin to promote its depolymerization (Hung et al., 2011). Nevertheless, in a living organism a growth cone will detect multiple positive and negative signals at the same time, which are integrated by Rho GTPases. These proteins function as signaling hubs, since they are the downstream targeting of many guidance receptors (Figure 3.10). Additional levels of control are the so called GEFs (Guanine Nucleotide Exchange Factor) and GAPs (GTPase-Activating Protein), which

inactivate and activate GTPases, respectively (Schmidt and Hall, 2002). Many guidance receptors also have GEFs or GAPs as downstream targets. One can easily imagine that several GAPs and GEFs have the same GTPase as target, so that different guidance signals can converge on a single GTPase. This single GTPase integrates the different inputs and will eventually be activated or inhibited.

3.4 Psidin

ORN axons like other axons use a variety of axon guidance cues to find their target glomerulus as described above. A major aim of this thesis is to understand how downstream signaling pathways including actin binding proteins, such as Psidin, function in the context of ORN axon guidance. Psidin has recently been identified as an APB, but so far nothing is known about its role in neurons and axon guidance. In this last part of the introduction I will give an overview about what is known about Psidin. To this date, only two studies

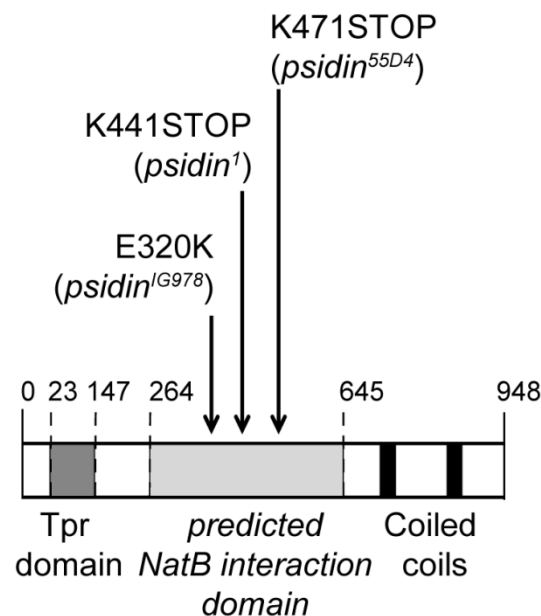


Figure 3.11 | Protein structure of Psidin

Psidin contains three main domains: the tetratricopeptide (TPR) domain at the N-terminus and two coiled coils at the C-terminus and a putative NatB interaction domain in the middle of the protein chain. Three different alleles were used: the two predicted null alleles *psidin*¹, *psidin*^{55D4} and one hypomorphic allele *psidin*^{G978}.

investigated the role of Psidin in *Drosophila*. The following section will present and discuss the findings of both studies and provide a framework about what is known about Psidin.

The 5 kb long *psidin* locus codes for a protein that is 948 amino acids long and has a size of approximately 110 kDa. The only isoform that has been discovered so far is spliced from 7 exons. Psidin contains, at its N-terminus, a tetratricopeptide domain (TPR domain). This domain is known to mediate direct protein-protein interactions (D'Andrea, 2003). In addition, there are two coiled coil domains at the C-terminus of the protein, which usually mediate protein dimerization (Burkhard et al., 2001).

Psidin is highly conserved from yeast to mammals. It is known to be the homologue of the yeast protein Mdm20, which is the non-catalytic part of the N-acetyltransferase B complex (NatB). Psidin is 7% identical and 22% similar with Mdm20 (Brennan et al., 2007). Most of the data about the NatB complex are derived from studies conducted in *Saccharomyces cerevisiae*, which is known to have at least three different characterized Nat complexes (Polevoda and Sherman, 2003b). In general, Nat complexes consist of one catalytic subunit and one auxiliary subunit, which in yeast are Mdm20 and Nat3, respectively. Together they form a complex, which acetylates a large number of proteins at their N-terminus co-translationally. Although a consensus sequence has been identified for the NatB-complex in yeast (Meth-Glu or Met-Asp) (Polevoda and Sherman, 2003b), only few targets are known, such as Tropomyosin in yeast (Singer and Shaw, 2003). Furthermore, in human cell culture the NatB-complex was shown to regulate the cell cycle, possibly via the acetylation of the anti-apoptotic protein p21 (Starheim et al., 2008).

Psidin was first identified in a screen for modifiers of *Drosophila's* immune system. The loss of function phenotype suggested that Psidin is required in larval blood cells to

engulf and degrade bacteria (Brennan et al., 2007). Larval blood cells are part of *Drosophila's* defense against infections. Usually these cells engulf bacteria and digest them in order to clear an infection. However, blood cells mutant for *psidin* are still able to engulf these bacteria, but fail to digest them. In addition, *psidin* mutant larvae fail to activate the entire repertoire of antimicrobial peptides. It was therefore suggested that Psidin is required at crucial stages of phagocytosis and also for the activation of additional downstream molecules (Brennan et al., 2007).

In the second study an additional function of Psidin was discovered. In a screen for modifiers of border cell migration in *Drosophila* oocytes, *psidin* mutant border cells showed severe migration defects. Border cells usually migrate from the tip of the ovary towards the

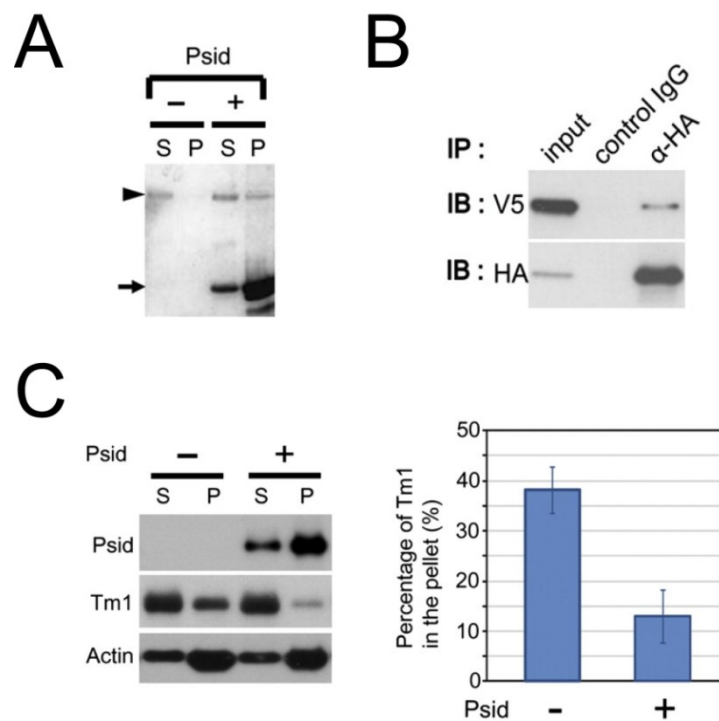


Figure 3.12 | Psidin as an actin binding protein

(A) Psidin (arrowhead) is bound to F-actin (arrow) and can be found in the pellet (P). In the absence of F-actin, Psidin only localizes to the supernatant (S). **(B)** Psidin is able to form homodimers. **(C)** Tropomyosin binds to F-actin. In the presence of Psidin, less Tropomyosin is bound to F-actin. Psidin competes with Tropomyosin for the binding to F-actin. Modified from (Kim et al., 2011).

center in order to separate the nursing cells from the oocyte. They are a popular *in vivo* model to study cell migration mechanisms. *Psidin* mutant border cells, however, failed to migrate this entire distance. Furthermore, it was shown that Psidin is able to directly bind F-actin and compete with Tropomyosin for the binding of F-actin (Kim et al., 2011). The same group also showed that Psidin forms homodimers, possibly via its coiled-coil domain. However, the functional relevance of this dimerization is still unclear.

Both groups show that Psidin is predominantly localized to the cytoplasm *in vivo* and *in vitro* (Kim et al., 2011; Brennan et al., 2007). Nevertheless, Psidin was also found to

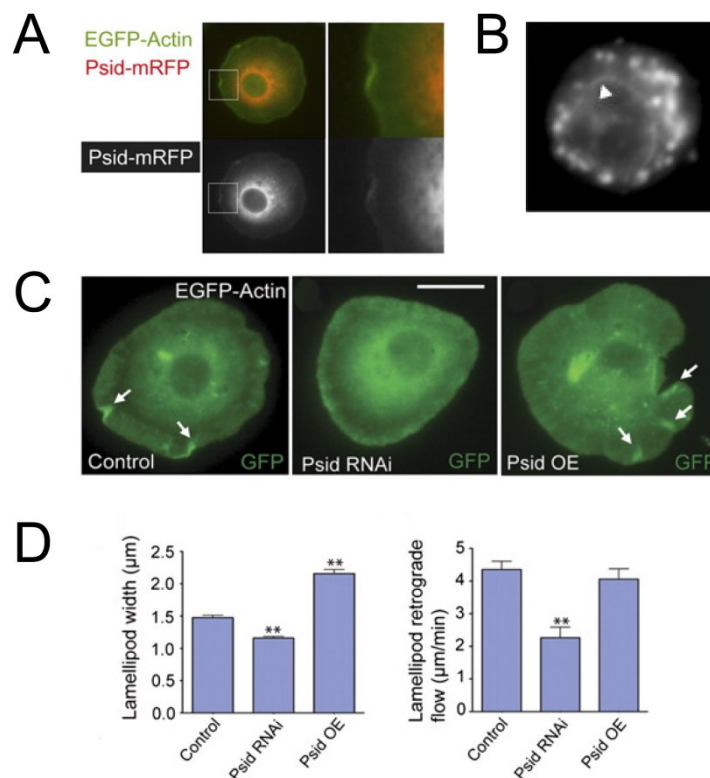


Figure 3.13 | Psidin in actin dynamics

(A) Psidin mainly localizes to the cytoplasm and more specifically the lamellipodium (inset). **(B)** A small fraction of Psidin localizes perinuclear (arrowhead). **(C)** Upon knock-down of Psidin number of membrane ruffles is reduced in S2 cells. Overexpression of Psidin causes increase in ruffle number compared to wild type. **(D)** Quantification of RNAi knock down and overexpression of Psidin. Lamellipodia size is decreased and retrograde flow rate is diminished in cells expressing RNAi, whereas overexpression of Psidin has the opposite effect. Modified from (Kim et al., 2011) and (Brennan et al., 2007).

localize perinuclear (Brennan et al., 2007). It is believed that this localization plays a role in Psidin's function as part of an N-acetyltransferase complex, which will be discussed later. Consistent with its role as actin binding protein, it was shown that Psidin localizes to the lamellipodium in S2 cells. This region greatly contributes to the protrusion dynamics of the cell. *Psidin* mutants show a reduction in actin dynamics, whereas overexpression of Psidin showed increased dynamics. Furthermore, *psidin* mutants exhibited a slower retrograde flow rate of actin, suggesting reduced lamellipodia dynamics (Kim et al., 2011).

4 Aims of this thesis

The goal of this thesis was to investigate mechanisms that control axon targeting in *Drosophila melanogaster*. Many guidance cues have been identified, showing that different repulsive and attractive cues guide ORNs on their way from the sensory organs towards the central brain. However, it remains unclear how these cues affect neurons at subcellular levels. More specifically, how are different signals integrated in the growth cone of a growing axon? Almost every guidance cue affects the cytoskeleton leading to the formation or destruction of actin filaments. Which downstream molecules are important for the restructuring of the growth cone, once a guidance cue activated its downstream signaling pathway?

In this thesis I investigated the role of the actin binding protein Psidin and its putative role as a non-catalytic subunit of the NatB-complex. Psidin has previously been identified as an actin binding protein and shown to be mainly localized in lamellipodia (Kim et al., 2011). It therefore makes an excellent candidate to investigate mechanisms that control actin dynamics. Therefore I examined Psidin's mode of action in neurons. Using fly genetics to manipulate actin dynamics in ORNs, I elucidated Psidin's role in ORN axon targeting *in vivo*.

As mentioned above Psidin is also the homologue of the yeast protein Mdm20, which is part of the NatB-complex in yeast (see introduction page 37). It is known that this complex plays an important role in yeast cell division and it has also been suggested that Psidin is involved in cell cycle regulation in mammals (Trost et al., 2009). Nevertheless, many

recent publications about Mdm20 and hMdm20 (human Mdm20) also speculated about functions independent of the NatB complex (Starheim et al., 2008; Ohyama et al., 2011).

First, I addressed the question whether Psidin is part of this complex in *Drosophila*. I therefore tested for an interaction of Psidin and the predicted catalytic subunit of NatB – dNAA20. Given that Psidin homologues are involved in cell division/cell cycle regulation, it was interesting to investigate for a similar function of Psidin in *Drosophila*.

Second, I examined a predicted interaction domain between Psidin and dNAA20. So far, this interaction domain has only been predicted *in silico* (SMART, EMBL Heidelberg). Third, I analyzed the effect of a potential phosphorylation site in Psidin. This residue has been identified in a previous study (Trost et al., 2009) and was shown to be phosphorylated in hMdm20 *in vivo*.

In general, this work addresses several questions in neuronal network development, with the main goal of characterizing the molecular mechanisms required at different steps during network formation from sensilla differentiation to the targeting of the ORNs:

- (I) What is Psidin's effect on actin dynamics?
- (II) How is actin dynamics influencing ORN axon guidance?
- (III) Is Psidin part of a NatB-complex in *Drosophila*?
- (IV) Is the NatB-complex important for ORN axon targeting?
- (V) How is Psidin regulated?

5 Materials

The following section gives an overview about the materials and methods that were used. For simplicity, reagents used for specific assays can be found in the respective methods section.

5.1.1 Common buffers and solutions

Table 5.1 | Common lab buffer and reagents

Name	Ingredients
Phosphate buffered saline (1L) (1x PBS)	137mM Na ₂ HPO ₄ , pH 7.4 1.5mM KH ₂ PO ₄ 137mM NaCl 2.7 mM KCl
Phosphate buffered saline – 0.5% Triton (1L) (1x PBT)	0.5% Tritin X-100 in 1x PBS
Phosphate buffer lysine (200ml) (1x PBL)	(a) dissolve 3.6g lysine (b) add 0.1M Na ₂ HPO ₄ until pH reaches 7.4 (c) add 0.1M NaH ₂ PO ₄ until volume reaches 200ml (d) filter sterilize (e) store at 4°C for up to 3 months
Periodate-Lysine-Paraformaldehyde (PLP)	add 2ml of 8% PFA in 2ml PBL (4% PFA final)
Blocking Solution	10% donkey serum in PBT (immunohistochemistry) 5% BSA in TBT (Western blot)
Fly water	8ml Propionic acid in 1L ddH ₂ O

Table 5.2 | Media

Name	Ingredients
Luria Bertani medium (1L) (LB)	10g NaCl 10g tryptone 5g yeast extract 20g agar pH 7 <u>for selection the appropriate antibiotics were added:</u> 100 µg/ml Ampicilin, 50 µg/ml Kanamycin
NZY+ (1L)	10g NZ amine 5g yeast extract 5g NaCl pH 7.5 <u>after autoclaving, the following solution were added:</u> 2.5ml of 1M MgCl ₂ 12.5ml of 1M MgSO ₄ 10ml of 2M glucose solution

5.1.2 Consumables

The following commercial kits from the respective manufacturers were used. Unless stated otherwise the kit was used according to the manufacturer's manual.

Table 5.3 | List of commercial kits

Name	Source
QIAprep Spin Miniprep Kit	Quiagen (Germany)
QIAGEN Plasmid Maxi Kit	Quiagen (Germany)
QIAquick PCR Purification Kit	Quiagen (Germany)
QIAquick Gel Extraction Kit	Quiagen (Germany)
QuikChange Lightning Site-Directed Mutagenesis Kit	Agilent (USA)
Actin Binding Protein Kit	Cytoskeleton (USA)
Effectene transfection kit	Quiagen (USA)

5.1.3 Antibodies

Table 5.4 | List of primary and secondary antibodies

Name	Source
<u>primary antibodies:</u>	
anti-GFP (rabbit, 1:1000)	Clontech (USA)
nc82 (mouse, 1:20)	DSHB (USA)
anti-discharge (mouse, 1:200)	DSHB (USA)
anti-HA (rat, 1:1000)	Roche (Switzerland)
anti-myc (rabbit, 1:1000)	Abcam (UK)
<u>secondary antibodies:</u>	
anti-mouse-Cy5 (1:200)	Dianova (Germany)
anti-rabbit-488 (1:200)	Dianova (Germany)
anti-rat-HRP (1:500)	Jackson (USA)
anti-rabbit-HRP (1:500)	Jackson (USA)

5.1.4 Enzymes

Table 5.5 | List of enzymes and DNA standards

Name	Source
Taq Polymerase	NEB (USA)
Takara Taq Polymerase	Takara (Japan)
Restriction endonucleases	NEB (USA)
T4 Ligase	NEB (USA)
1 kb ladder	NEB (USA)
100 bp ladder	NEB (USA)

5.1.5 Plasmids

Table 5.6 | List of plasmids and DNA templates

Name	Source
pP{UAST}-Psidin-HA	Denis Montell (USA)
pP{UAST}-Psidin ^{IG978} -HA	This study
pP{UAST}-dNAA20-myc	This study
pP{GAL4}-Ubiquitous-gal4	Lab collection
pRS405-MDM20	This study
pRS405-MDM20 ^{K304E}	This study
dNAA20 cDNA (LD30731)	Berkeley Drosophila Genome Project (USA)
pP{UAST}-RNAi (dNAA20)	VDRC Stock Center (Austria)

5.1.6 Fly stocks

All flies were raised at 25°C at 70% relative humidity on standard cornmeal medium.

The following table lists important and frequently used stocks. For simplicity, composite stocks of these “parental stocks” are not listed.

Table 5.7 | Common fly stocks

Stock	Source	Stock number
Or-GAL4	Bloomington Stock Center (USA)	various
Actin-GAL4	Bloomington Stock Center (USA)	4414
UAS-mCD8-GFP	Lab stock collection	
UAS-syt-GFP	Lab stock collection	
UAS-Psidin-HA	Denise Montell (USA)	
UAS-Psidin ^{IG978} -HA	This study	
UAS-Psidin ^{S678A} -HA	This study	
UAS-Psidin ^{S678D} -HA	This study	
FRT82,CL,gal80/TM2	Lab stock collection	
eyFlp	Lab stock collection	
Df(3R)DI-BX12, ss ¹ e ⁴ ro1/TM6B, Tb ¹	Bloomington Stock Center (USA)	3012
w ¹¹¹⁸ ; Df(3R)ED6025/TM6C, Sb ¹	Bloomington Stock Center (USA)	8964

Table 5.7 | (continued from previous page)

Stock	Source	Stock number
w ¹¹¹⁸ ; Df(3R)ED5942/TM6C, cu ¹ Sb ¹	Bloomington Stock Center (USA)	8922
w ¹¹¹⁸ ; Df(3R)BSC475/TM6C, Sb ¹ cu ¹	Bloomington Stock Center (USA)	24979
w ¹¹¹⁸ ; Df(3R)BSC636/TM6C, cu ¹ Sb ¹	Bloomington Stock Center (USA)	25726
w ¹¹¹⁸ ; Df(3R)ED6027/TM6C, cu ¹ Sb ¹	Bloomington Stock Center (USA)	9479
Df(3R)H-B79, e*/TM2	Bloomington Stock Center (USA)	4962
w ¹¹¹⁸ ; Df(3R)BSC517/TM2	Bloomington Stock Center (USA)	25021
w ¹¹¹⁸ ; Df(3R)BSC516/TM2	Bloomington Stock Center (USA)	25020
w ¹¹¹⁸ ; Df(3R)Exel6185, P{XP-U}Exel6185/TM6B, Tb ¹	Bloomington Stock Center (USA)	7664
w ¹¹¹⁸ ; Df(3R)BSC518/TM2	Bloomington Stock Center (USA)	25022
w ¹¹¹⁸ ; Df(3R)BSC488/TM2	Bloomington Stock Center (USA)	24992
w ¹¹¹⁸ ; Df(3R)BSC141/TM6B, Tb ⁺	Bloomington Stock Center (USA)	9501
Df(3R)BSC43, st ¹ ca ¹ /TM2, pp	Bloomington Stock Center (USA)	7413
w ¹¹¹⁸ ; Df(3R)BSC124/TM6B, Tb ¹	Bloomington Stock Center (USA)	9289
FRT82B-Psidin ^{55D4}	Denise Montell (USA)	
FRT82B-Psidin ^{55D4} , Tm1 ^{ZCL0722}	Denise Montell (USA)	
FRT82B-Tm1 ^{ZCL0722}	Denise Montell (USA)	
FRT82B-Psidin ¹	Kathryn V. Anderson (USA)	
FRT82B-Psidin ^{IG978}	This study	
Or42a-mCD8-GFP/CyO	Thomas Hummel (Austria)	
Or42a-mCD8-GFP, act-gal4/CyO	This study	
Or59c-mCD8-GFP/CyO	Thomas Hummel (Austria)	
Or59c-mCD8-GFP, act-gal4/CyO	This study	
RNAi (dNAA20)	VDRG Stock Center (Austria)	18213
RNAi (dNAA20)	NIG-Kyoto Stock Center (Japan)	14222R-3
RNAi (dNAA20)	NIG-Kyoto Stock Center (Japan)	14222R-4

5.1.7 Fly genetics

The following table summarizes the fly genotypes of all experiments that were used for the different experiments. Flies of the respective genotypes were used for subsequent analysis – such as dissections, staining, counting etc.

Table 5.8 | Fly genotypes analyzed for the respective experiment

Experiment	Genotype
MARCM analysis	eyFlp/+ ; Or-GAL4 UAS-syt-GFP/+ ; FRT82B,CL,gal80/X eyFlp/+ ; Or-GAL4 UAS-mCD8-GFP/+ ; FRT82B,CL,gal80/X
Rescue experiment	eyFlp/+ ; Or59c-mCD8-GFP,act-gal4/UAS-Psidin-HA ; FRT82B,CL,gal80/X eyFlp/+ ; Or59c-mCD8-GFP,act-gal4/UAS-Psidin ^{IG978} -HA ; FRT82B,CL,gal80/X eyFlp/+ ; Or59c-mCD8-GFP,act-gal4/UAS-p35 ; FRT82B,CL,gal80/X eyFlp/+ ; Or59c-mCD8-GFP,act-gal4/UAS-Psidin ^{S678A} -HA ; FRT82B,CL,gal80/X eyFlp/+ ; Or59c-mCD8-GFP,act-gal4/UAS-Psidin ^{S678D} -HA ; FRT82B,CL,gal80/X
Tracing experiment	eyFlp/+ ; Or47a-mCD8-GFP/+ ; FRT82B,CL,gal80/X eyFlp/+ ; Or42a-mCD8-GFP/+ ; FRT82B,CL,gal80/X
Developmental analysis	eyFlp/+ ; elav-GAL4 UAS-mCD8-GFP/+ ; FRT82B,CL,gal80/X
Genetic interaction with <i>dNAA20</i>	eyFlp/+ ; Or59c-mCD8-GFP,act-gal4/UAS-RNAi (dNAA20) ; FRT82B,CL,gal80/X eyFlp/+ ; Or42a-mCD8-GFP,act-gal4/UAS-RNAi (dNAA20) ; FRT82B,CL,gal80/X
Tropomyosin interaction	eyFlp/+ ; Or59c-mCD8-GFP,act-gal4/+ ; FRT82B,CL,gal80/FRT82B eyFlp/+ ; Or59c-mCD8-GFP,act-gal4/+ ; FRT82B,CL,gal80/FRT82B-Psidin ¹ eyFlp/+ ; Or59c-mCD8-GFP,act-gal4/+ ; FRT82B,CL,gal80/FRT82B-Psidin ^{55D4} eyFlp/+ ; Or59c-mCD8-GFP,act-gal4/+ ; FRT82B,CL,gal80/FRT82B-Tm1 ^{ZCL0722} eyFlp/+ ; Or59c-mCD8-GFP,act-gal4/+ ; FRT82B,CL,gal80/FRT82B-Tm1 ^{ZCL0722} ,Psidin ¹
Cofilin	eyFlp/+ ; Or59c-mCD8-GFP,act-gal4/UAS-Tsr ^{S3A} (const. active) ; FRT82B,CL,gal80/X eyFlp/+ ; Or59c-mCD8-GFP,act-gal4/UAS-Tsr ^{S3E} (inactive) ; FRT82B,CL,gal80/X
LimK	eyFlp/+ ; Or59c-mCD8-GFP,act-gal4/UAS-LimK (wild type) ; FRT82B,CL,gal80/X eyFlp/+ ; Or59c-mCD8-GFP,act-gal4/UAS-RNAi (LimK) ; FRT82B,CL,gal80/X eyFlp/+ ; Or59c-mCD8-GFP,act-gal4/UAS-LimK (kinase inactive) ; FRT82B,CL,gal80/X

"X" stands for three different genetic backgrounds: FRT82B, FRT82B-Psidin¹ and FRT82B-Psidin^{IG978}

6 Methods

6.1 Immunohistochemistry

Adult flies were anesthetized with CO₂ and transferred to ice-cold ethanol (100%). After 30 seconds flies were transferred from ethanol to ice-cold phosphate buffered saline (PBS). Single flies were dissected in room temperature PBS. After dissection, brains were fixed in PLP (4% PFA) for 1 hour at room temperature, followed by three washes in PBT (0.5%) for 15 minutes each. Afterwards brains were incubated in blocking solution (10% donkey serum) for 15 minutes at room temperature. Brains were incubated in blocking solution with primary antibody overnight at 4°C. At the next day brains were washed three times with PBT for 15 minutes and then incubated with secondary antibody in blocking solution for 2-3 hours at room temperature. Finally brains were washed three times for 15 minutes with PBT and mounted in Vectashield (Vectorlabs) and stored at 4°C in the dark. Specimens were analyzed using confocal microscopy (Olympus FV1000, Leica SP2). Images were processed in ImageJ and Adobe Photoshop.

6.2 Preparation of genomic DNA

Flies were collected and anesthetized with CO₂ and put on ice. Solution A was added according to the amount of collected flies (100 µl for 1-5 flies, 200 µl for 6-10 flies and 400 µl for up to 50 flies). Flies were then homogenized in Solution A and incubated for 30 minutes at 70°C. Subsequently 14 µl 0.8M KAc (potassium acetate) was added per 100 µl of Solution A. This mixture was then incubated for 30 minutes on ice. After incubation, the

mixture was centrifuged and the supernatant was transferred to a new tube. The supernatant was mixed with 1 volume of phenol:chloroform (1:1) and again centrifuged. The aqueous phase was transferred to a new tube and mixed with ½ volume of isopropanol. Mixture was again centrifuged and supernatant was removed. Pellet was washed with ethanol (70%) and finally redissolved 100 µl distilled water.

Solution A

0.1M Tris HCl pH9.0

0.1M EDTA

1% (v/v) SDS

1% DEPC

DNase inhibitor

Stock solution was kept at room temperature without DNase inhibitor and 1% DEPC.

These components were added freshly to an aliquot of the stock solution on the day of use.

6.3 Mapping

In order to identify new player involved in axon guidance, a large EMS (ethyl methane sulfonate) screen was conducted as described previously (Cayirlioglu et al., 2008). Potential mutants were screened for targeting defects using eyFLP mediated clonal analysis. The screen was limited to the right arm of the third chromosome. At the beginning of this study the mutation of the new *psidin* allele, *psidin*^{G978}, had to be mapped to the *psidin* locus using two different methods: “Polymorphism-Mapping” (Berger et al., 2001) and “Deletion Mapping”.

6.3.1 Sequence polymorphism mapping

Polymorphism mapping was performed as described earlier (Berger et al., 2001). This technique utilizes polymorphisms – such as single nucleotide polymorphisms (SNPs) or insertion/deletion (InDels), to map mutations. In general, recombination events between a “marker” stock and to “to-be-mapped” stock are utilized to map a mutation. Different assays (PCR-product length polymorphism (PLP), restriction fragment length polymorphism (RFLP) and single nucleotide polymorphisms (SNPs)) were used to determine the exact breakpoint at which the recombination occurred. In addition, flies were dissected and scored for the known targeting phenotype of the *psidin*^{IG978} allele. A major advantage of this mapping method over the traditional “deletion mapping” is that flies are scored for the targeting phenotype rather than for the lethality of *psidin*^{IG978}. Since this allele originates from an EMS screen, which could induce multiple mutations, depending on the conditions, the lethality could be a secondary phenotype that has no connection to the observed axon targeting defect.

Male flies of the *psidin*^{IG978} stock carrying a proximal FRT82B site were crossed to virgins carrying a distal EP insertion. This led to multiple random recombination events in the germ line of female flies between these two chromosomes across 3R. These recombination events occur naturally in *Drosophila*, interestingly only in female flies. The new “recombined” 3R chromosome was a mixture of the original, FRT82B site carrying chromosome, and the new EP (dominant white marker) carrying chromosome. Virgins of the F1 generation were collected and crossed to an additional stock that allows for screening of the F2 generation for eye-color mosaicism, which was used as a read-out for a recombination event. Single males of the F2 generation that scored positive for eye-color

mosaicism were maintained as a stock. The breakpoint of the recombination event in each stock was determined using the PLP-, RFLP-assay and SNP sequencing.

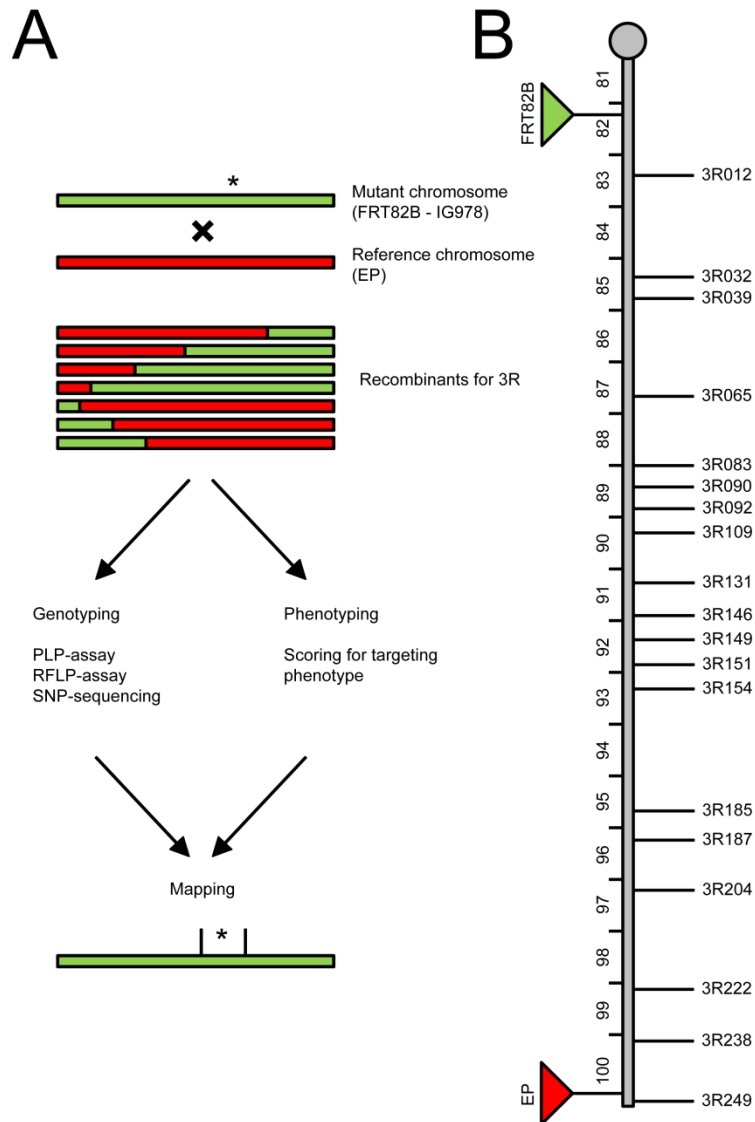


Figure 6.1 | Map of polymorphism marker between the FRT82B and EP strain

(A) Experimental road map to map the mutation in *psidin*^{IG978}. Chromosome carrying the mutation (green) and a reference chromosome (red) are crossed. The individual flies from the F1 generation will have chromosomes with random recombination events. Single males are further crossed and maintained as stock. From these stocks the F2 generation was used for genotyping and phenotyping. The genotype was determined using the PLP, RFLP or SNP assay. Stocks were crossed to Or59c to score for the known targeting phenotype of *psidin*^{IG978}. Using the obtained data, the mutant could be mapped to a small area. **(B)** Map of all polymorphism marker between the FRT82B and EP strain along the 3R chromosome. Green triangle represents the FRT82B insertion site. Red triangle represents EP (*w*⁺) insertion site. Numbers from 81 to 100 represent the cytological areas from the centrosome of the third chromosome (81) towards the distal end (100) of the chromosome. Different numbers represent polymorphism marker across the entire chromosome.

6.3.2 PLP-Assay

The PCR-product length polymorphism (PLP) distinguishes polymorphisms using the length of PCR products. Using a set of primers (Table 6.1), which binds to different regions of 3R, distinct fragments were PCR amplified. Due to insertions or deletions the amplified fragments were of different size, depending on their chromosomal origin (FRT or EP). Fragments were analyzed using 2.5% agarose gels.

PCR-Program

1	5'	94°C	39 cycles
2	30''	94°C	
3	30''	60°C	
4	1'	72°C	
6	5'	72°C	
7	∞	4°C	

Table 6.1 | List of primers used for PLP assay

Marker	Primer		Product size	
	Left	Right	FRT	EP
3R012	AAGGAAACGAATTAAGGCAGACCCA	TGGGAAAAGGGAACGTAAAGAGCA	171	198
3R032	AAGGGCTATGATCCGGTTAATGTCTGG	GCATCGATTGAGGAAGTGTTTGATTCTTTG	186	201
3R039	TGGCAGCTACTGGGATACTGGGTCTCT	CACAGGACGAGAACTGTGCGTTGG	144	153
3R065	GAGACGTGATAGCATTGACCGACAC	TCCGCCACTGAAGACACAATTACAC	228	196
3R083	ATCGCTGGCCTTTGCTGGCTTT	ACGATGCGTTATGCAAATTCTCCTTCATTT	217	207
3R092	GCGACAGCGCAAAAACTCCTGT	AAGATCATTCTCACGTTCTCACGATG	217	252
3R151	CCATGTCGCACTTTCTTTGATATTTGCTTTC	CAAGGCTCACGCACAGGCACTC	211	195
3R204	TGCCCTTATTATGTGACCCCAAAAACT	TCCTTTGATCGTTTATATCAAGCTTTGGGAAAT	178	189
3R222	CGAGATCACAGATATCTTCATAGGGGAACA	AAGTGGGGTTTCAATAACAGCGTGC	162	145
3R238	CCCTCGACCCGATTTTCACATACT	GGACACACCCAGGAGATGTCGTTGT	162	153
3R249	ATGGAATGCAAAAATAACAATCCCGAAACA	CGCACAGGCAGGCTACACAAAA	147	166

6.3.3 RFLP-Assay

The restriction fragment length polymorphism (RFLP) assay utilizes the same mechanism as the PLP assay. The PCR amplified fragments (Table 6.2) are later digested with specific restriction enzymes. The resulting restriction patterns were analyzed using 1% agarose gels. After the digest the pattern differed depending on the origin of the respective chromosomal part.

PCR-Program

1	5'	94°C	39 cycles
2	30"	94°C	
3	30"	60°C	
4	2'	72°C	
6	5'	72°C	
7	∞	4°C	

Table 6.2 | List of primers used for the RFLP assay

Marker	Primer		Enzyme
	Left	Right	
3R090	AAGGAAACGAATTAAGGCAGACCCA	TGGGAAAAGGGAACGTAAAGAGCA	<i>Avi</i> II
3R109	AAGGTGGATGTGGATTGGGAAGTGG	ACGAAAATGTGTGTAGCGAAGCAAAGGA	<i>Bam</i> HI
3R151	CAGCGGCAGGCAAAGTCATAAAAGTC	CAAACGGGACAAAAGTGAGAGCGAAA	<i>Cla</i> I
3R187	GGTGTTTTGATTCCGTTGGGTATGATGT	GGAACAGCAGCCGATGAAAGTAATATGTG	<i>Bgl</i> II

6.3.4 SNP Assay

Regions of chromosome 3R with known SNPs were PCR amplified and sequenced. Sequences were then aligned and compared to a reference in order to determine the chromosomal origin.

Table 6.3 | List of primers used for the SNP assay

Marker	Primer		SNP
	Left	Right	
3R131	GTTGAGCGAAAAGGGCAGCAAG	GGGCAAGGACAAGGACAAGGACAAA	A/G
3R146	GCTTTCGTGCTGTTCCGGCTTGTTTT	TTTTCGCCTCCACCTTCCTGCTC	G/A
3R149	TTGGGGCTTAGTATGGTCAATGGGGGTTACCT	CTGGCCATAAACAAGACATCCCACAAAATG	A/T
3R154	CGGTTGCTGGATTCTTCTCGTCTG	TTTGCTTTCGCCTCTGCGTTTATTTT	C/T
3R185	GCTCCCATTTCCACCCAGACAC	CCTTTTCGCTTCCCGCTCACTT	A/T

6.3.5 Deletion Mapping

As a second approach to map the mutation in *psidin*^{IG978} to a gene, mutant flies were crossed against a defined set of deficiencies (Bloomington Deficiency Kit, Table 5.7), which cover most of the right arm of the third chromosome. Since the mutation in *psidin*^{IG978} causes lethality one can easily utilize the lethality to map the mutation. Each deficiency stock had a defined part of chromosome 3R deleted. For each cross the obtained Mendelian ratio was compared to the theoretical ratio in order to distinguish complementing from non-complementing deficiencies. Non-complementing deficiency indicated that the mutation in question was located within the deleted fragment of the chromosome.

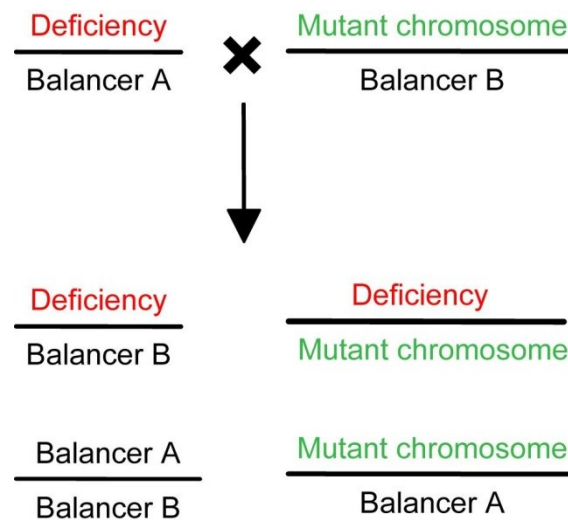


Figure 6.2 | Crossing strategy for deletion mapping

The mutant chromosome carrying the *psidin*^{IG978} mutation was crossed to several deficiencies. For each cross the expected Mendelian ratio was determined and compared to the obtained ratio. Doing this, it was possible to determine whether a deficiency complemented the lethality of *psidin*^{IG978}.

6.4 Cell Culture

The S2 cell line is derived from a primary culture of late stage *Drosophila melanogaster* embryos (20 hours old) (Schneider, 1972).

Cells were cultured in complete Schneider's Medium and passaged weekly using a 1:10 dilution. S2 Cells were kept at 28°C without additional CO₂ as a loose, semi-adherent monolayer in tissue culture flasks

Complete cell culture medium

S2 cell medium (Invitrogen)

50ml FBS (heat-inactivated)

5ml Penicillin/Streptomycin (100x)

6.5 Primary cell culture

Drosophila primary neuron cultures were generated as described previously (Sánchez-Soriano et al., 2010). In brief, cells were removed with micromanipulator-attached capillaries from stage 11 embryos (6-7 hours AEL at 25°C) (Campos-Ortega and Hartenstein, 1997), treated for 5 minutes at 37°C with dispersion medium, washed and dissolved in 30-40 ml of Schneider medium (Schneider, 1964). Then, the aliquots were transferred to coverslips, kept as hanging drop cultures in airtight special culture Chambers (Dübendorfer and Eichenberger-Glinz, 1980) usually for 6 hours at 26°C. Cultured *Drosophila* neurons were analyzed 6 hours after plating. They were fixed (30 minutes in 4% paraformaldehyde-0.05 M phosphate buffer, pH 7.2), then washed in PBS 0.1% Triton X-100 (PBT). Incubation with antibodies was performed in PBT. Microtubules were stained with anti-tubulin (1:1000; Sigma) and FITC or Cy3-conjugated secondary antibodies (1:200; Jackson ImmunoResearch).

Filamentous actin was detected with TRITC-conjugated phalloidin (Sigma). Stained *Drosophila* neurons were mounted in Vectashield (Vector Labs). Primary neuron culture images were taken using an AxioCam camera mounted on an Olympus BX50WI microscope. Lamellipodia area was quantified using ImageJ. Statistical analyses were carried out with Sigma Stat software using a *t*-test or Mann-Whitney rank sum test.

6.6 Transfection

S2 cells were transfected using the Effectene kit according to the manufacturer's manual (Qiagen).

6.7 In-situ hybridization

All solutions used in the dissection or hybridization procedure were RNase free. Pupae of the desired stage were dissected in ice cold PBS and fixed in 4% PFA o/n or longer. Samples were dehydrated through several methanol steps and stored in 100% methanol at -20°C for a minimum of 2 hours.

Day 1: Samples were taken from -20°C and incubated for 1 hour at RT in a solution made of 80% Met-OH and 20% of a 30% H₂O₂ solution. Rehydration was continued in sequential methanol steps and samples were washed 3 x 5 minutes in PBST followed by incubation in prehybridization solution for 1 hour at 55°C with gentle rocking. Dig-labeled RNA probes were diluted in hybridization solution, pre-heated to 55°C and incubated with the samples o/n at 55°C.

Day 2: Blocking reagent was dissolved in MABT at 70°C for several hours. Samples were washed 3 times 1 hour each in solution I, II and II at 55°C. After washing 3 times for 5 minutes in MABT at RT and twice for 30 minutes at 55°C to avoid background staining, samples were incubated with blocking solution for 1.5 hours at RT. To detect dig-labeled RNA, samples were incubated o/n at 4°C with an anti-DIG antibody conjugated with alkaline phosphatase (AP, Roche, 1:1000).

Day 3: Samples were rinsed and washed with MABT at least 8-10 times for 30 minutes at RT before incubation in NTMT. Following equilibration in NTMT for 10-20 minutes developing solution was added. After the staining was developed, samples were rinsed in PBST and post fixed in 4% PFA. Pictures were taken at the Leica MZ500.

Solutions for in situ hybridization

Prehybridization solution

50% Formamide deio
0.2% Tween 20
0.5% Chaps
5mM EDTA pH 8.0
50mg/ml Heparin
50mg/ml t-RNA (SIGMA R-5636; Lot 082K9135)
5x SSC pH4.5
0.2% Blocking Reagent
Distilled water was added to mark 50 ml, dissolved with rocking at 70°C and stored at -20°C.

Solution I

50% Formamide deio
5x SSC pH4.5
0.2% Tween 20
0.5% Chaps
Distilled water was added to mark 50 ml. Always prepared fresh.

Solution II

50% Formamide deio
2x SSC pH4.5
0.2% Tween 20
0.1% Chaps
A final volume of 50 ml was made and always prepared fresh.

Solution III

2x SSC pH4.5

0.2% Tween 20

0.1% Chaps

Distilled water was added to mark 50 ml and always prepared fresh.

5x Maleic acid buffer (MAB)

Maleic acid (58g)

NaCl (44g)

Adjusted pH to 7.5: using 25-30 g NaOH pellets and then 5N NaOH. Made up a final volume of 1L and stored at 4°C.

MAB-Tween

1x MAB

0.1% Tween®20

Stored at RT.

Blocking solution (w/v)

1x MABT

0.2% Blocking Reagent (#1096 176, Roche)

Blocking reagent was dissolved while rocking at 70° and kept on ice. Always prepared fresh.

NTMT (200ml)

5M NaCl (4ml)

1M Tris-HCl (pH 9.5) (20ml)

1M Mg Cl₂ (10ml)

Tween®20 (200µl)

Developing solution (10ml)

BCIP (11µl)

NBT (14µl)

NTMT (10 ml)

6.8 Mutagenesis

Site directed mutagenesis experiments were performed according to the manual (QuikChange Lightning Site-Directed Mutagenesis Kit, Agilent). Briefly, primer designed with a specific point mutation were used to PCR amplify the entire template vector. Afterwards the PCR product was transformed into E. coli. DNA from the obtained colonies was extracted and sequenced to ensure successful mutagenesis.

Table 6.4 | **Primer used for mutagenesis**

Name	Primer	
	5' to 3' sequence	
3'-Psidin ^{S678A}	aggttgagggtgcttcaagtacgtGCGctgatgcttc	
5'-Psidin ^{S678A}	gaagcatcagCGCacgtacttgaagcacctcaacct	
3'-Psidin ^{S678D}	gttgagggtgcttcaagtacgtGATctgatgcttcgactctttgcc	
5'-Psidin ^{S678D}	ggcaaagagtcgaagcatcagATCacgtacttgaagcacctcaac	
3'-Psidin ^{IG978}	atctggcgcggttgAAGctacaccaacgc	
5'-Psidin ^{IG978}	gcgttggtgtagcTTCaaccgcgcaga	

6.9 Cloning of dNAA20 (CG14222)

In order to express the gene *CG14222* (hereafter termed *dNAA20*), I cloned the coding sequence (CDS) into a pUAST vector. The final construct was designed to have an N-terminal myc-tag and to be under the control of an UAS element. The final construct was cloned in two steps into the vector. In the beginning the appropriate restriction site for the endonucleases were selected based on the multiple cloning site (MCS) and the CDS of *dNAA20*. In the first cloning step the CDS was cloned into the vector using *Xba* I and *Not* I restriction sites. This fragment contained a STOP codon, but no start codon. In the second step, I cloned the myc-tagged into the N-terminal region using an adaptor duplex. This

**Figure 6.3** | **Cloning strategy for *dNAA20* with N-terminal myc-tag**

Coding sequence of *dNAA20* was cloned in pUAST vector using *Xba* I and *Not* I. This fragment had no ATG, but a STOP codon. Myc-tag was inserted using an adaptor duplex with an *EcoR* I and *Not* I restriction site. To put the myc-tag in the correct reading frame, an additional glycine was inserted upstream of the *Not* I site. The cDNA clone LD30731 was used as a template.

duplex was designed to have a *Not* I and *EcoR* I restriction site. In order to put the sequence into the correct reading frame an additional glycine was inserted upstream of the *Not* I restriction site. The primers were designed to have the respective restriction sites.

Table 6.5 | Primer used for dNAA20 cloning

Name	Primer
	5' to 3' sequence
5'- <i>Not</i> I	tagcgccgcaccacgttgcgac
3'- <i>Xba</i> I	ggctctagatcaattcatatctatatgttccag
Adaptor duplex 1	aattcatggaacaaaaacttatttctgaagaagatctgggc
Adaptor duplex 2	ggccgccagatcttcttcagaataagttttgttccatg

6.10 Generation of Psidin deletions

Psidin deletions of different sizes were generated in a PCR-mediated approach. The wild type Psidin gene cloned into the pUAST vector was used as a template. Primer pairs were used in a PCR reaction to generate a shortened Psidin vector. In order to digest the remaining wild type template, PCR products were digested with *Dpn* I. Subsequently PCR products were digested with *Pac* I for 1 hour at RT and finally ligated overnight. Ligation mixture was transformed into One Shot Top10 chemical competent cells (Invitrogen). Plasmid was purified and sequenced in order to verify the deletion.

Table 6.6 | Primer used for the generation of Psidin deletions

Name	Primer		Δ size [bp]	Δ position [aa]	Protein size [kDa]
	5' to 3' sequence				
3'- Pacl-Psidin ^{ΔNatBfull}	ttaaattaacgatcacgatctgcgtcc		1146	264-645	74
5'- Pacl-Psidin ^{ΔNatBfull}	ttaaattaacggggccattatccgatgg				
3'- Pacl-Psidin ^{ΔNatB23}	ttaaattaagctctccaacaacaacttgct		786	384-645	88
5'- Pacl-Psidin ^{ΔNatB23}	ttaaattaacggggccattatccgatg				
3'- Pacl-Psidin ^{ΔNatB2}	attaattaagctctccaacaacaacttg		417	384-522	102
5'- Pacl-Psidin ^{ΔNatB2}	ttaaattaaccagattcagctggactccatg				
3'- Pacl-Psidin ^{ΔNatB1}	gtaattaacgatcacgatctgcg		339	264-378	105
5'- Pacl-Psidin ^{ΔNatB1}	gattaattaacagcaagttgttggagag				

6.11 Co-immunoprecipitation

Drosophila S2 cells were used to express Psidin and dNAA20. The GAL4/UAS system was utilized to drive the expression of these proteins. Expression of UAS-Psidin-HA and UAS-dNAA20-myc was driven by ub-GAL4. Briefly, 1×10^6 cells were seeded in 6-well plates the day before transfection. Transfection was done using the Effecten Transfection Kit (Quiagen). Cells were harvested after three days after transfection and lysed in lysis buffer (50 mM Tris, 150 mM NaCl, 2 mM EDTA, 1% Triton, protease inhibitor (Sigma)) and centrifuged at 3300 rpm (1g) for 5 minutes. The supernatant was discarded and cells were resuspended in 300 μ l lysis buffer. Afterwards cells were homogenized and incubated at 4°C for 30 minutes. The homogenate was centrifuged at 3300 rpm (1g) for 5 minutes. Supernatant was transferred to a new tube and diluted in lysis buffer. Solutions were incubated with the respective antibody (anti-HA or anti-myc) for 2 hours at 4°C. Afterwards 40 μ l of beads (slurry 50% (v/v), blocked with 1% BSA) were added. This mixture was incubated for 2 hours at 4°C. Samples were boiled in 6 μ l SDS buffer (6x) for 10 minutes and loaded onto a protein gel.

6.12 F-actin binding assay

To test the ability of wild type Psidin and mutated Psidin^{IG978} for their F-actin binding capabilities, I performed an F-actin binding assay. Both proteins were overexpressed in S2 cells using a general GAL4-driver (ub-GAL4) to drive the expression of the Psidin constructs (UAS-Psidin-HA and UAS-Psidin^{IG978}-HA). Cells were transfected using the Effectene transfection reagent (Quiagen) and harvested after 3 days *in vitro* (DIV). S2 cells were centrifuged down (3300 rpm (1g) for 5 minutes) and the supernatant was removed. Cells were resuspended in lysis buffer (50 mM Tris, 150 mM NaCl, 2 mM EDTA, 1% Triton, protease inhibitor (Sigma)) and homogenized for 1 minute. HA-tagged proteins were purified from the cell lysate using an anti-HA affinity gel (EZview™ Red Anti-HA Affinity Gel, Sigma). Afterwards protein solutions were ultra-centrifuged at 150,000 g for 1 h at 4°C to remove any residual contamination. The F-actin binding assay was performed according to the manufacturer's manual (Actin Binding Protein Kit, Cytoskeleton). Briefly, the test proteins Psidin and Psidin^{IG978} were incubated in the presence and absence of F-actin. BSA and α -actinin served as a negative and positive control, respectively. After the incubation the mixture was again ultra-centrifuged at 150,000 g for 1.5 hours at 24°C. Afterwards the supernatant and pellet was separated. The pellet was resuspended and together with the supernatant shortly incubated with SDS loading buffer and finally loaded in an SDS-gel. If a protein is able to bind F-actin, it should be present in the pellet together with F-actin. Contrary, it should only be visible in the supernatant if it's not able to bind F-actin. BSA as a negative control should only be present in the supernatant, whereas parts of α -actinin (positive control) should be present in the pellet fraction.

6.13 Engineering “fly-like” yeast Psidin

Saccharomyces cerevisiae strain YZ1143 (*mdm20* deletion was kindly provided by Dr. Sherman, University of Rochester Medical Center) carrying a complementing plasmid p[*CEN URA3 MDM20-3HA*] was used for the analysis. Integrative vector pRS405 [*LEU2*] carrying either a wild type *MDM20-myc* or a mutant allele *MDM20*^{K304E}-*myc* was digested by *Xcm* I to facilitate integration into the yeast genome. Selected transformants were grown on 5'FOA plates lacking leucine to remove the complementing plasmid. The presence of the integrated allele was confirmed by PCR and subsequent sequencing. Temperature sensitivity was determined at 30°C and 37°C. For actin staining, exponentially growing cells were fixed with formaldehyde for 10 minutes, washed 3 times in PBS and resuspended in Alexa-fluor-phalloidin (1:1000). After 30 minutes incubation at RT, the cells were washed with PBS, mounted on slides in 70% glycerol/PBS/0.05% para-phenylenediamine and immediately visualized.

6.14 Western blot quantification

Western blots were quantified using ImageJ. The ratio of dNAA20 to Psidin^X was quantified measuring the intensity of the respective bands. I compared the amount of dNAA20 pulled-down with wild type Psidin versus the amount of dNAA20 pulled-down with a Psidin variant. I measured the respective bands of HA-captured Psidin and pulled-down dNAA20. Only the HA-bound fraction of Psidin can effectively pull down dNAA20. The same was done for wild type Psidin and dNAA20, which was used as a reference on each blot. We used the wild type control to normalize the pull-down of dNAA20 with a Psidin variant on each individual blot.

6.15 GAL4/UAS system

The GAL4/UAS system is used to control the expression of proteins spatially and temporarily (Brand and Perrimon, 1993). The GAL4 protein specifically binds to the upstream activating sequence (UAS) and promotes the expression of the downstream protein. The GAL4 protein can be under the control of various promoter elements (e.g. olfactory receptors). I used the GAL4/UAS system to visualize the targeting pattern of ORNs. Here, the promoter region of different ORs was fused to a GAL4 sequence. This allowed the expression of GAL4 in neurons that intrinsically express the respective OR. Furthermore, I combined these GAL4 lines with different UAS lines – such as UAS-syt-GFP or UAS-mCD8-GFP to visualize the presynaptic area or entire cell bodies, respectively. Furthermore I also used the GAL4 system to re-express or overexpress proteins that were under the control of an UAS element.

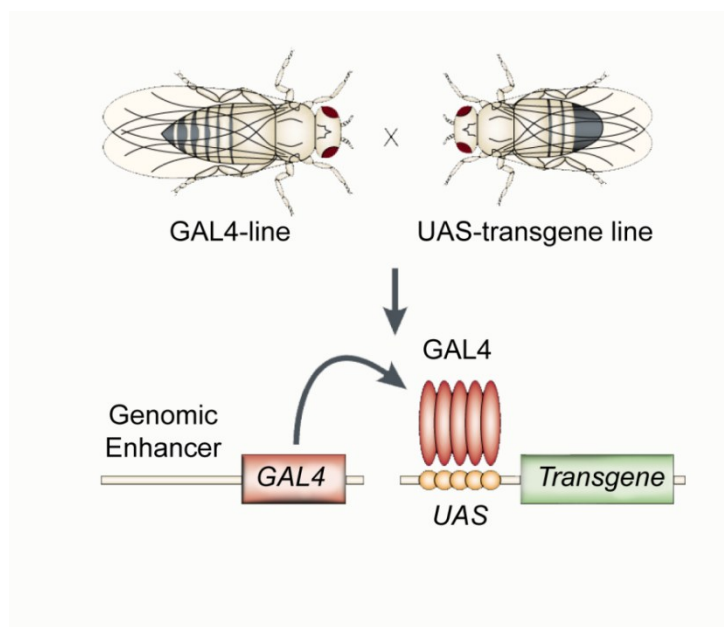


Figure 6.4 | The GAL4/UAS system

Two fly line are crossed – one containing the GAL4 element and one containing a transgene under the control of the UAS element. The offspring will contain both chromosomes so that the transgene is expressed depending on the driver GAL4 line. The expression of the GAL4 protein is control by the genomic enhancer region upstream (e.g. OR enhancer region). The GAL4 protein binds the UAS element upstream of the transgene and promotes it expression. Modified from (Muqit and Feany, 2002).

6.16 MARCM

The mosaic analysis with a repressible cell marker (MARCM) is a common technique in *Drosophila* to label specific cells in a mosaic of many different cell types (Lee and Luo, 1999). Analyzing lethal mutations can be problematic, because it is sometimes not possible to work with homozygous lethal mutations. MARCM is also widely used to generate conditional knock-outs. The GAL4/UAS system is used to label a certain population of cells. In order to generate conditional knock-outs, the chromosome carrying the mutation also carries a Flippase Recognition Target (FRT) site on the same arm of the chromosome. In addition, heterozygous cells carry a *gal80* in *trans* to the mutation of interest. The FRT site will be targeted by a flippase to induce mitotic recombination events between two chromosomes. During cell division the cell will give rise to two daughter cells. These two daughter cells will be homozygous for the mutation and wild type, respectively. In forward MARCM mutant cells will be labeled by the GAL4/UAS system, whereas wild type cells carrying the *gal80* protein are not labeled. Here the *gal80* protein represses the expression of the GAL4 protein. I used a flippase that is fused to the *eyeless* promoter, *eyFlp*. Using this flippase I generated between 60-70% mutant cells in the ANT and MP (Newsome et al., 2000). At the same time the brain will not be affected, so that any observed phenotype is solely due to knock-out in the olfactory organs, rather than changes in the brain.

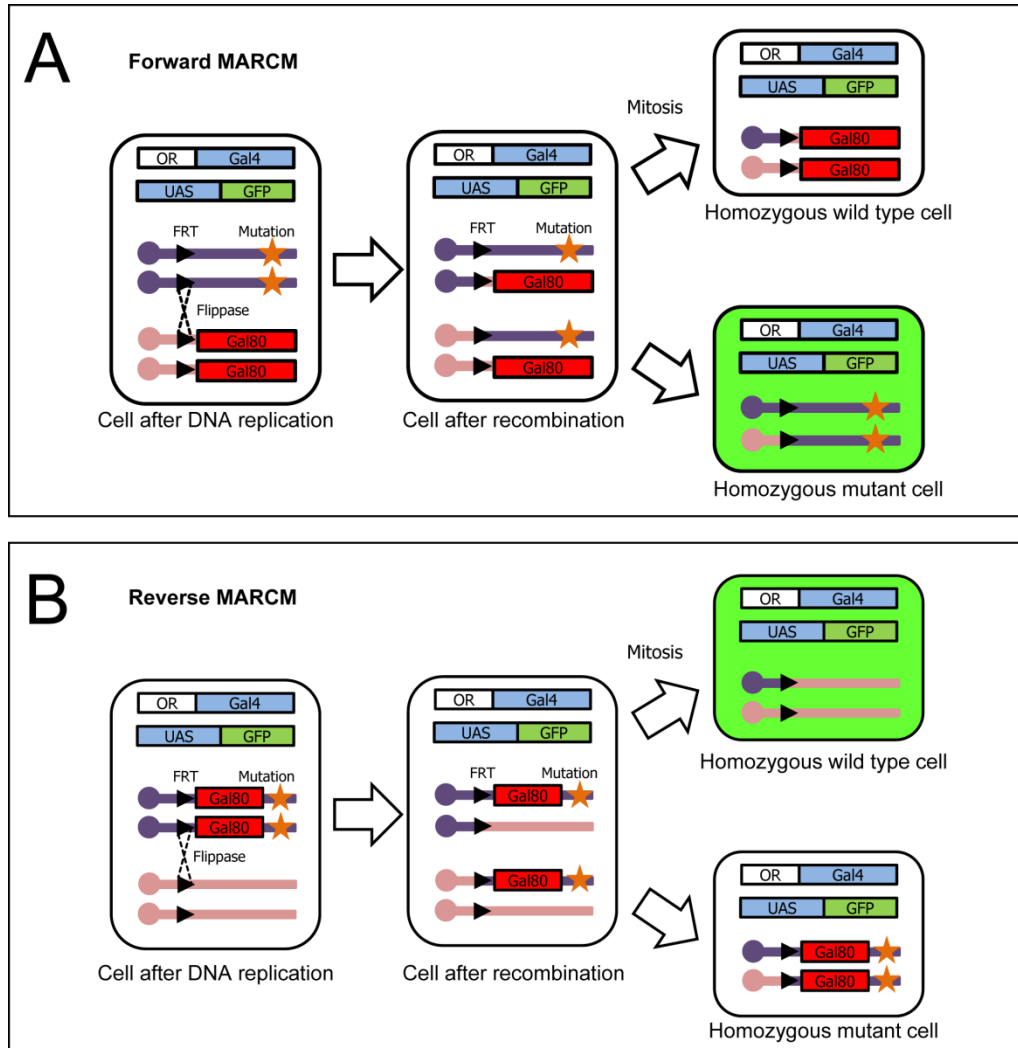


Figure 6.5 | MARCM technique

(A) Forward MARCM specifically labels mutant cells in an otherwise wild type background. It uses the GAL4/UAS system to label a certain population of cells. Furthermore one needs the mutation of interest on the same arm of the chromosome as a FRT site. In addition the *gal80* repressor is required in *trans* to the mutation of interest. After mitotic recombination the cell divides and gives rise to two daughter cells: one homozygous mutant (labeled in green) and the second wild type cell (not labeled). **(B)** Reverse MARCM used the same basic principle, but labels the population reversely. Here, the mutation has to be in *cis* to the *gal80* repressor. The daughter cell will be homozygous mutant (not labeled) and wild type (labeled)

7 Results

The scope of this work was to identify new players involved in axon targeting and elucidate their mode of action. The mutation “IG978” was previously identified in an EMS screen in the laboratory of Laurence Zipursky (University of California, Los Angeles) by my supervisor and colleagues. This mutation showed an interesting mistargeting phenotype of some classes of ORNs to the AL and was selected as a candidate to further investigate the mechanisms of axon targeting. As part of this thesis, the mutation “IG978” was mapped to the gene *Psidin*.

7.1 Mapping of the mutation “IG978” to the gene locus of *Psidin*

As a first experiment I used the “Single-nucleotide-polymorphism-mapping” method as an approach to map the mutation. SNP-mapping utilizes recombination events between a marker stock and the second “to-be-mapped” fly stock (see methods page 53). Males that scored positive for recombination were maintained as a stock. Later each line was then scored for the targeting phenotype. The exact breakpoint of the recombination was determined using the PLP-, RFLP-assay and SNP sequencing (Berger et al., 2001; Figure 6.1). In total sixteen recombinant stocks were obtained during this screening. The phenotype was scored by comparing the targeting phenotype of the recombinant stock with the original “IG978” stock. Out of these sixteen stocks only five showed a normal targeting pattern and therefore scored negative for a phenotype. All the remaining eleven stocks scored positive for the phenotype. Using the above mentioned assays the mutation could be mapped to a region between the marker 3R109 and 3R185 (Figure 7.1). This already narrowed down

potential genes of the mutation, but to ultimately map the mutation of “IG978” I used deletion mapping with the Bloomington deficiency kit (Table 5.7). Deficiency stocks covering regions between the marker 3R109 and 3R185 were crossed to FRT82B-IG978 and each crossed was scored for lethality. In total four deficiency stocks failed to complement the lethality of the “IG978” (Figure 7.2). Using this complementation assay I was able to further pinpoint the mutation to a region between the breakpoints of two deletions, BSC636 and BSC517 (Figure 7.2). Within this area a loss of function mutant of CG4845 (Psidin) failed to complement the lethality of “IG978”. Using these two approaches, the mutation “IG978” was mapped to the gene locus of Psidin.

Stock #	Phenotype	92	109	131	146	149	151	154	185	187	204	222	238	249
59	no	red	red	red	red									
4	no	red	red	red	red									
41	no	red	red	red	red									
57	no	red	red	red	red									
64	no	green	green	red	red	red	red							
109	yes	green	green	green	green	green	green	red	red	red	red	red	red	red
131	yes	green	green	green	green	green	green	red	red	red	red	red	red	red
162	yes	green	green	green	green	green	green	red	red	red	red	red	red	red
164	yes	green	green	green	green	green	green	red	red	red	red	red	red	red
166	yes	green	green	green	green	green	green	red	red	red	red	red	red	red
173	yes	green	green	green	green	green	green	red	red	red	red	red	red	red
65	yes	green	red	red	red	red	red							
69	yes	green	red	red	red	red	red							
63	yes	green	green	green	green	green	green	white	white	red	red	red	red	red
71	yes	green	red	red	red	red	red							
77	yes	green	red	red	red									

Figure 7.1 | Recombinants stocks obtained during “SNP-mapping”

Each recombinant was scored for a mistargeting phenotype. Different polymorphism markers across the chromosome 3R were used to determine the breakpoint of the recombination. Green boxes indicate that the chromosome at this position originates from the original chromosome carrying the mutation (FRT82B-IG978). Red boxes indicate that the chromosome at this position originates from the EP-carrying line, which was used for the recombination. White boxes indicate positions, which were not determined.

Finally, the entire *psidin* locus was sequenced and compared to a reference sequence. A single point mutation exchanging a glutamate for a lysine at position 320 was identified.

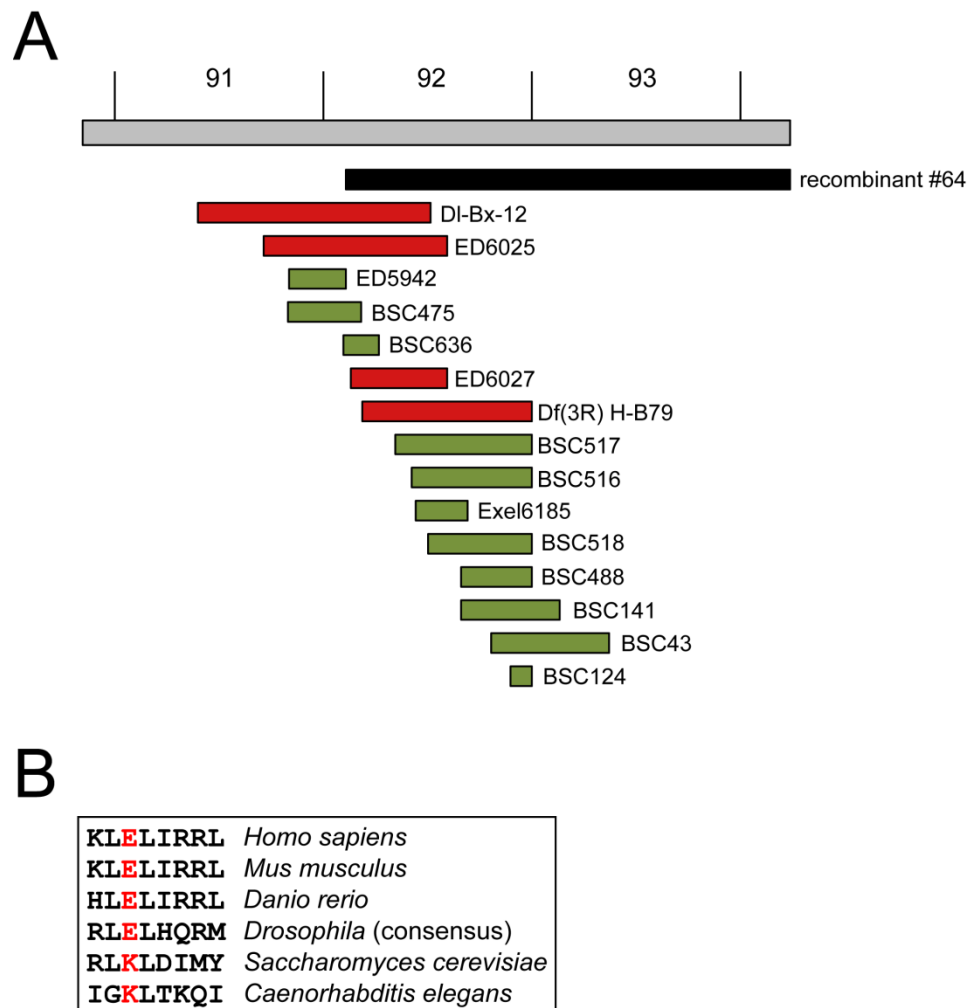


Figure 7.2 | Complementation assay

(A) The stock carrying the mutation “IG978” was crossed to several deficiency stocks covering the cytological region 91-93 on the right arm of the third chromosome. Black rectangle represents recombinant #64, which showed no targeting phenotype and had the most distal recombination breakpoint. Green rectangles symbolize deficiencies that could complement the lethality of “IG978”. Red rectangles represent the four deficiencies that failed to complement the lethality. **(B)** The mutation found in the new allele *psidin*^{IG978} exchanges a glutamate for a lysine at position 320. This residue is highly conserved in *Drosophila* species, but also in other higher organisms. Interestingly, the wild type residue in yeast resembles exactly the mutation found in *psidin*^{IG978}.

7.2 *Psidin* mutants show class specific defects in olfactory neuron targeting

In order to analyze the targeting pattern of neurons homozygous mutant for *psidin*, I used the MARCM technique. Combining this method with eyFlp recombinase allows generating 50-70% mutant clones of olfactory receptor neurons (ORNs) (Newsome et al., 2000). Neurons were mutant either for the putative hypomorphic allele *psidin*^{G978}, harboring the missense mutation E320K, or for two expected null alleles *psidin*¹ (Brennan et al., 2007) and *psidin*^{55D4} (Kim et al., 2011), harboring a STOP codon at K441 and K471, respectively (Figure 3.11). Wild type Or47a-expressing ORNs targeted the dorsomedial glomerulus DM3 (Figure 7.3). In *psidin* mutants, however, they additionally innervated a ventromedial glomerulus (Figure 7.3). Similarly, Or67d wild type axons projected along a dorsolateral route towards its target glomerulus. Mutant Or67d axons displayed a shift in their growth path, making misprojections to a ventromedial area of the antennal lobe (AL). In general the majority of dorsolateral projecting neurons (e.g. Or47a, Or10a, Or67d and Or88a) displayed a mistargeting phenotype (e.g. shift in growth path) and ectopic synapse formation. Similarly ventromedial targeting ORNs (e.g. Or59c, Or42a, Or92a, Gr21a, Or46a and Or33c) displayed strong mistargeting (Figure 7.3, Table 7.1). Mutant Or59c and Or42a axons reach their wild type glomerulus, but then seem to defasciculate and spread out in a dispersed pattern. In addition mutant Or92a and Or46a axons form ectopic synapses along their ventromedial projection route (Figure 7.3). In contrast, centrally projecting ORNs like Or47b, Or71a and Or88a axons, which travel a short distance to their target zone at a straight angle from the AL entry point were hardly affected (0%, 7% and 0%, Table 7.1). In summary, analyzing the frequency of phenotypes of thirteen representative ORN classes, it can be concluded that targeting towards glomeruli is affected in a distance- and projection route-dependent manner, with neurons projecting dorsolateral and ventromedial being the most

affected (Figure 7.3, Table 7.1). In addition to that in *psidin*¹ mutants, glomeruli appeared to be innervated by fewer axons. Again, ORN classes are affected differently, with Or42a, Or88a and Or46a affected strongly, showing no innervation of mutant axons in the AL. Other classes, e.g. Or47a, Or47b and Or22a, showed a milder reduction of innervation in the AL. Interestingly the mistargeting phenotype of Or47a seems to be identical in both *psidin*^{IG978} and *psidin*¹ background.

Table 7.1 | Quantification of Psidin mutant axons in several ORN classes

Targeting phenotype was quantified using MARCM analysis of the respective Or-marker. ORN survival was scored in three categories: (++) no cell loss, (+) mild cell loss, (-) complete loss of cells. Quantification of a targeting phenotype was not applicable (N.A.) in ORN classes that showed a complete loss of neurons (-).

ORN	Wild type		<i>psidin</i> ¹		<i>psidin</i> ^{55D4}		<i>psidin</i> ^{IG978}		
	targeting	ORN survival	targeting	ORN survival	targeting	ORN survival	targeting	ORN survival	
10a	67%	++	100%	+	N.D. ^a		94%	++	dorso-lateral
47a	11%	++	80%	+	N.D.		79%	++	
67d	0%	++	79%	++	53%	+	53%	++	
21a	0%	++	16%	++	14%	++	22%	++	central
22a	0%	++	0%	+	0%	+	0%	++	
47b	0%	++	31%	+	N.D.		7%	++	
71a	0%	++	N.A. ^b	-	N.D.		0%	++	
88a	0%	++	N.A.	-	N.D.		0%	++	
33c	0%	++	100%	+	N.A.	-	63%	++	ventromedial
42a	0%	++	N.A.	-	N.A.		100%	++	
46a	0%	++	N.A.	-	N.D.		88%	++	
59c	0%	++	90%	+	93%	+	92%	++	
92a	0%	++	83%	++	N.D.		53%	++	

^a not determined

^b not applicable (due to 100% cell loss)

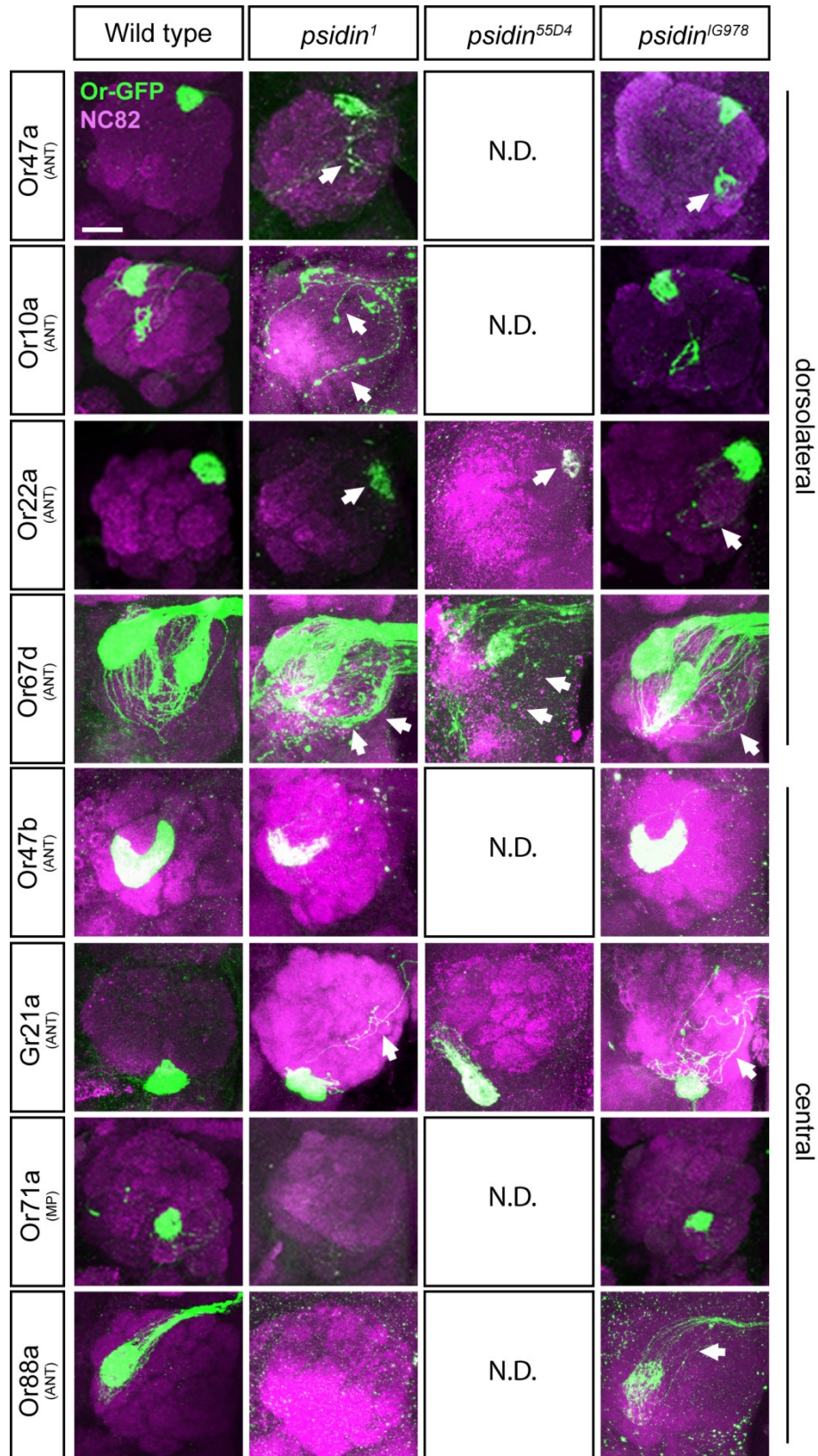


Figure 7.3 | ORN class specific mistargeting phenotype in *Psidin* mutants

(Figure legend see next page)

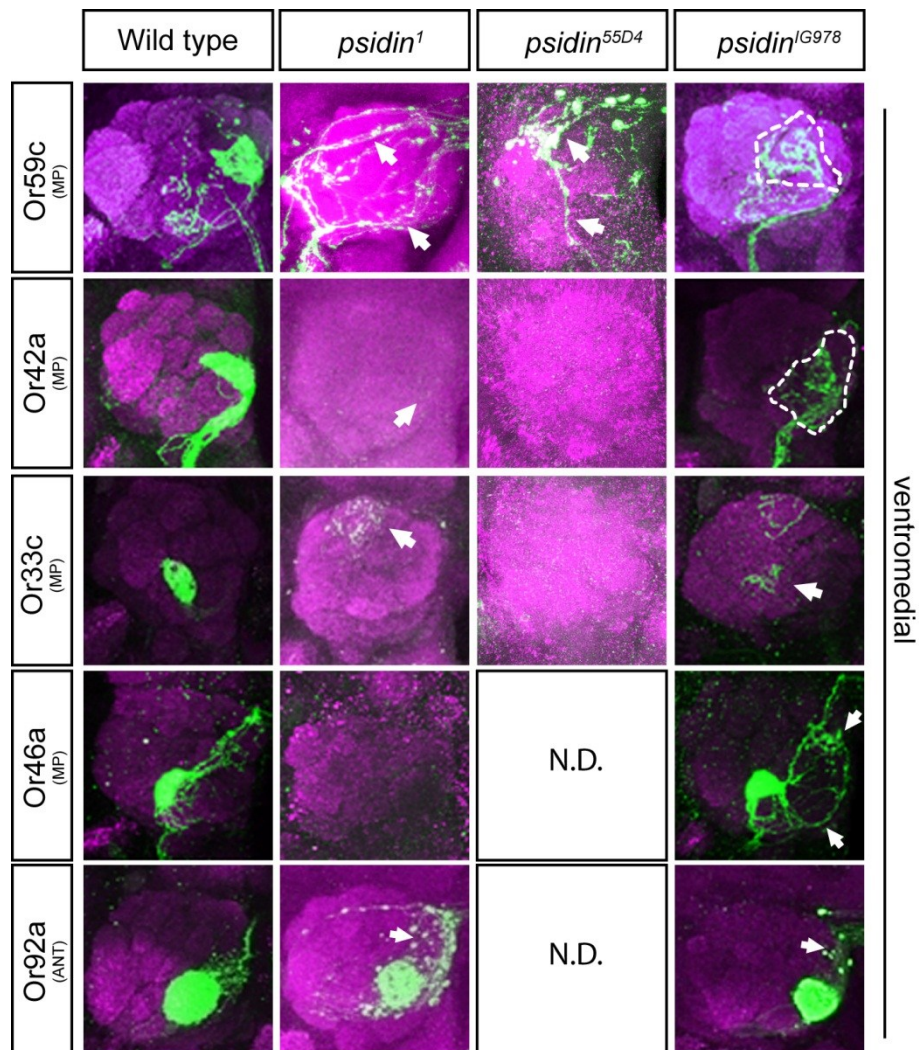


Figure 7.3 | ORN class specific mistargeting phenotype in Psidin mutants

MARCM analysis of different ORN classes, which are grouped according to their projection route. Axons were visualized using Or-GAL4 and UAS-syt-GFP or UAS-mCD8-GFP. Adult fly brains were dissected and stained with anti-GFP and NC82. ORN classes are affected differently. Axons growing along the dorsolateral (e.g. Or47a and Or67d) and ventromedial (e.g. Or59c and Or92a) are strongly affected, whereas axons using a central route (e.g. Or47b and Or71a) are less affected. Several classes show a strong (Or88a, Or46a and Or33c) or milder (Or22a and Gr21a) cell loss phenotype, which is visible in the adult brain due to lower innervation of the glomerulus. Scale bar is 20 μ m.

7.3 Complete loss of Psidin results in loss of specific ORNs

The analysis of the targeting pattern of several ORN classes revealed that in *psidin*¹ mutants, several glomeruli frequently appeared to be less innervated by ORN axons (Figure 7.3). In cell culture, Psidin homologues of yeast and human were shown to be required for cell growth, survival and division (Polevoda and Sherman, 2003b; Starheim et al., 2008). Therefore this reduced innervation might be caused by a reduction in ORN cell number. To test this possibility, I analyzed the total neuron number of several subsets of ORNs using eyFlp mediated mosaic analysis: ORNs located in the maxillary palp and Or42a, Or59c (both maxillary palp) and Or47a (antenna) classes of ORNs. The general co-receptor, Or83b/Orco, is co-expressed in every ORN. I counted the number of Or83b positive neurons in the MP to estimate the overall ORN number. The analysis of Or83b positive neurons revealed that this cell number is significantly reduced by 34% comparing wild type (n=35) and *psidin*¹ mutants (n=23). In contrast, the cell number is not significantly changed in the hypomorphic background *psidin*^{G978} (n=31) compared to wild type. I obtained similar results for the individual ORN classes, with no significant change in the hypomorphic *psidin*^{G978} background (Or59c: -20%, Or42a: -8%, Or47a: +16%), but a strong reduction in the *psidin*¹ background (Or59c: -48%, Or42a: -83%, Or47a: -55%). Overall the cell number did not change significantly in the hypomorphic *psidin*^{G978} background, but was markedly reduced in *psidin*¹ background. Furthermore ORN classes seemed to be affected differently by the cell loss with some classes nearly absent and others hardly changed.

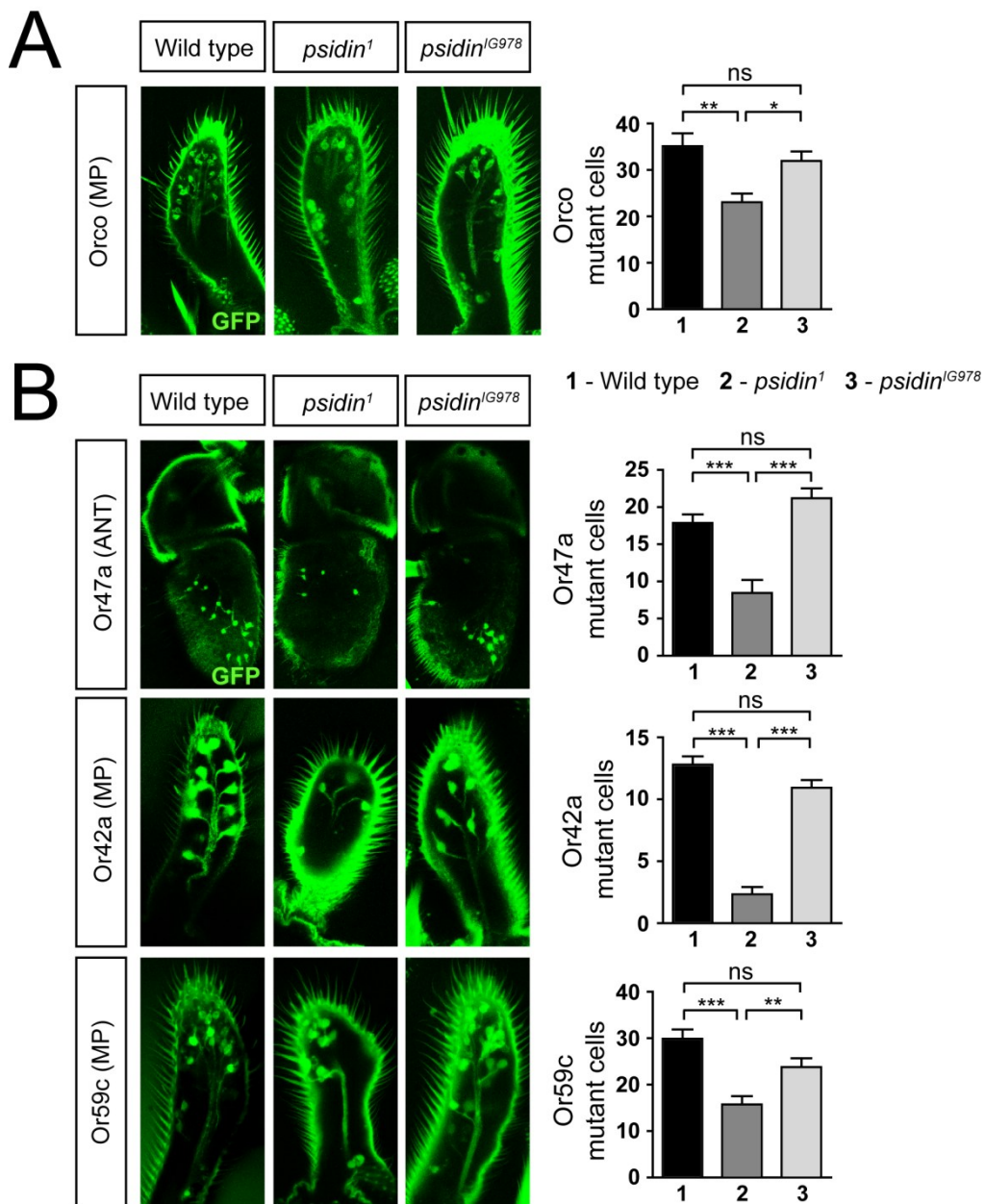


Figure 7.4 | Reduction of ORN number in Psidin loss of function mutants

Homozygous mutant clones were generated using eyFlp MARCM. Cells were visualized using Or-gal4, UAS-mCD8-GFP. **(A)** The number of mutant Or83b/Orco positive neurons in *psidin*¹ and *psidin*^{G978} background. Cell number is reduced in the *psidin*¹ background, whereas *psidin*^{G978} mutants are not significantly affected. **(B)** The number of *psidin*¹ and *psidin*^{G978} mutant cells in one antennal marker (Or47a) and two maxillary palp marker (Or42a and Or59c). Reduction of cell number is visible in *psidin*¹, but not in *psidin*^{G978} background. Bar graphs: One-way ANOVA, Bonferroni post-test for normally distributed values (* $p < 0.05$, ** $p < 0.01$, *** $p < 0.001$). Error bars \pm SEM.

7.4 Re-expression of wild type Psidin rescues targeting and cell loss phenotype

In order to verify that the targeting and cell loss phenotypes are caused by the loss of Psidin, I used the GAL4/UAS system to re-express wild type Psidin in the background of the *psidin* mutants. Wild type Psidin was selectively re-expressed in mutant eyFlp clones in the antenna and maxillary palp (Table 7.1). Re-expression of Psidin sufficiently rescued the targeting phenotype in *psidin*^{IG978} background (54% vs. 0%) and *psidin*¹ background (72% vs. 0%) (Figure 7.5A,C). Overexpression of Psidin had no effect in wild type neurons (0% vs. 0%) (Figure 7.5A,C). In addition, expression of Psidin completely restored the cell number in *psidin*¹ background (n=23 vs. n=33), but it had no effect on the cell number in *psidin*^{IG978} background (n=32 vs. n=28) and wild type neurons (n=36 vs. n=33) (Figure 7.4B). To elucidate Psidin's role in the cell loss phenotype I overexpressed the anti-apoptotic protein p35 and the mutated Psidin^{IG978} in both mutant backgrounds. This completely rescued the cell number in *psidin*¹ mutant background (n=23 vs. n=33) (Figure 7.4B). Again there was no significant change in cell number in wild type and *psidin*^{IG978} background (n=32 vs. n=29). Interestingly, expression of p35 did not completely rescue the targeting defect of *psidin*¹ mutant axons. There was only an improvement of the mistargeting to 53%, which exactly resembled the targeting phenotype of *psidin*^{IG978} mutants (54%), (Figure 7.5). No further improvement in the targeting phenotype was observed upon p35 expression in *psidin*^{IG978} mutants (53% vs. 50%) (Figure 7.5A,C). Similar the expression of Psidin^{IG978} could rescue the cell number of *psidin*¹ (n=23 vs. n=32). At the same time the targeting phenotype in *psidin*¹ was rescued to levels of *psidin*^{IG978} (55% vs. 73%) mutants, with almost no strong targeting phenotype left (9%). Overexpression of Psidin^{IG978} in *psidin*^{IG978} mutants had no effect on the cell number (n=32 vs. n=29). Although the targeting defect was increased in *psidin*^{IG978}

mutants overexpressing Psidin^{IG978} (55% vs. 71%), the quality of the targeting did not change.

I could not observe any strong targeting defects in those neurons.

Taken together, targeting and cell loss phenotype were rescued by re-expression of wild type Psidin. In contrast, overexpression of the anti-apoptotic protein p35 selectively rescued the cell loss phenotype, but not the targeting defects. This suggests that Psidin prevents apoptosis of ORN precursors during development. Interestingly the expression of Psidin^{IG978} could also selectively rescue the cell number in *psidin*¹ mutant clones. In addition Psidin^{IG978} can partially rescue the targeting defects. Thus, Psidin clearly shows independent requirements for ORN survival and axon targeting.

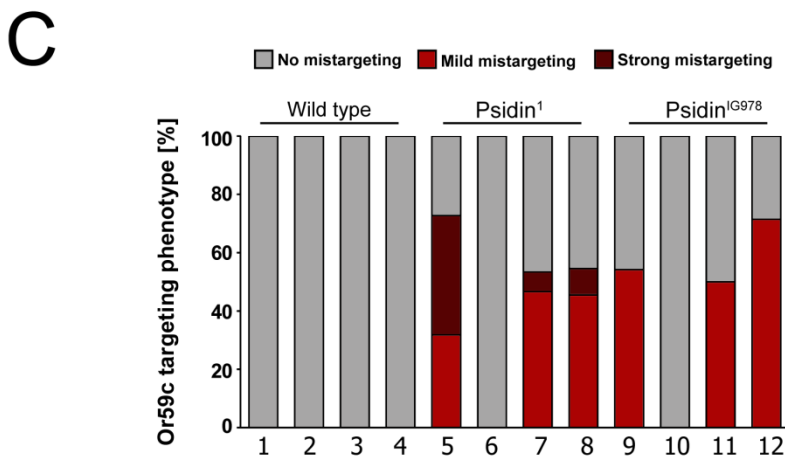
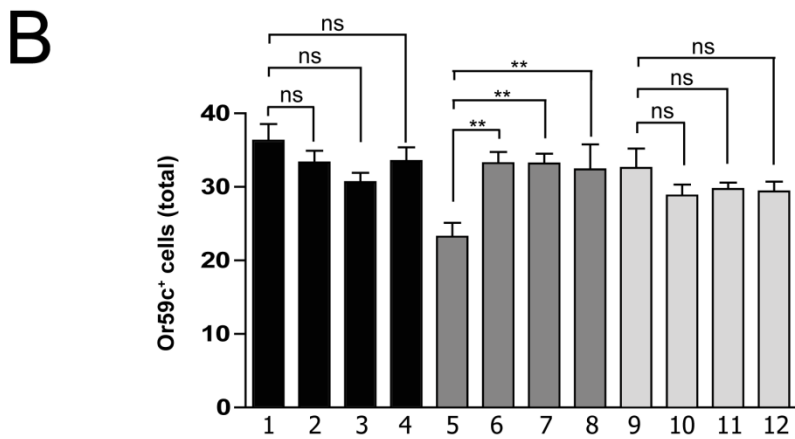
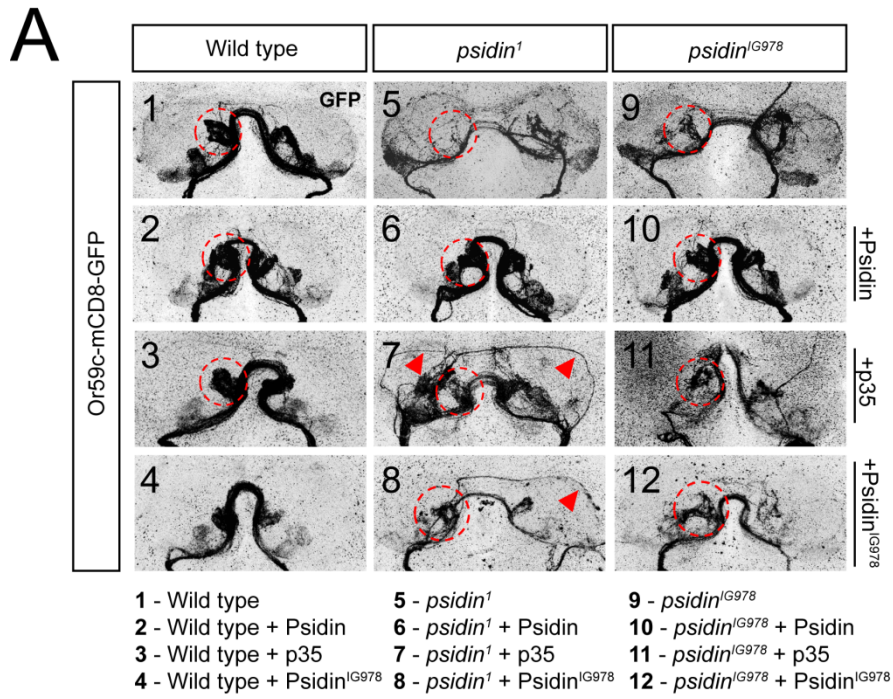


Figure 7.5 | Re-expression of wild type Psidin rescue targeting and cell loss phenotype

(Figure legend see next page)

Figure 7.5 | Re-expression of wild type Psidin rescue targeting and cell loss phenotype

Wild type Psidin, Psidin^{IG978} and p35 was expressed under the control of act-GAL4 in eyFlp clones. Axons were visualized using a Or59c::mCD8-GFP direct fusion construct. **(A)** Targeting pattern of Or59c neurons in wild type, *psidin*^{IG978} and *psidin*¹ background, in the presence and absence of Psidin, Psidin^{IG978} and p35 expression. Expression of wild type Psidin rescued the targeting phenotype of *psidin*¹ and *psidin*^{IG978}. Expression of Psidin^{IG978} and p35 rescues the targeting up to the level of *psidin*^{IG978} mutants. The strong targeting phenotype is almost completely rescued upon expression Psidin^{IG978} and p35. **(B)** Total cell number of Or59c positive neurons in wild type, *psidin*¹ and *psidin*^{IG978} background, in the presence and absence of Psidin, Psidin^{IG978} and p35 expression. Cell number is rescued upon expression of wild type Psidin, Psidin^{IG978} and p35 in any background. **(C)** Quantification of the mistargeting phenotype in wild type, *psidin*¹ and *psidin*^{IG978} background, in the presence and absence of Psidin and p35 expression. Bar graphs: One-way ANOVA, Bonferroni post-test for normally distributed values (* p<0.05, ** p<0.01, *** p<0.001). Error bars ± SEM.

7.5 *Psidin* mutant axons do not follow their normal targeting pattern

To further understand the nature of the observed mistargeting phenotype I analyzed the projection routes of one antennal and one maxillary palp ORN class that were strongly affected by the mutation in *psidin*^{IG978}, *psidin*¹ and compared it to the wild type background. Wild type Or47a axons normally projected to a dorsal glomerulus (DM3) using a dorsolateral route upon entry of the AL (Figure 7.6). In contrast, *psidin*^{IG978} or *psidin*¹ mutant axons deviated from that pattern. Mutant Or47a axons additionally grow along the ventromedial part of the AL, which is usually not invaded by wild type Or47a axons. Along this ventromedial projection route, *psidin* mutant axons eventually form ectopic synapses (Figure 7.6). It overall seemed that *psidin*^{IG978} and *psidin*¹ mutant axons were no longer restricted to their normal projection route, but invaded the entire AL. Consistent with previous observations, the AL was less innervated in *psidin*¹ mutant background, which is due to the reduction in cell number. The quality of the mistargeting phenotype, however, was comparable to the *psidin*^{IG978} background (Figure 7.6). Wild type Or42a axons grow through the subesophageal ganglion (SOG) and eventually reach the AL and project along the ventromedial route to reach their target glomerulus (VM7). *Psidin*^{IG978} mutant neurons are able to grow out of the maxillary palp and extend their axons through the SOG. Furthermore *psidin*^{IG978} mutant axons reached their gross target area, but then seemed to defasciculate and spread out into the vicinity of their innate glomerulus (Figure 7.6). In contrast, *psidin*¹ mutant neurons seemed to be unable to grow out of the maxillary palp and therefore never reach the SOG or AL. Only occasionally, I detected axonal innervation in the AL (Figure 7.6). This is in agreement with the loss of neurons in *psidin*¹ mutant observed earlier (Figure 7.4). Concluding, I found that *psidin*^{IG978} mutants follow the normal wild type path toward the AL.

Psidin seems to be required only at the last stages of axon targeting – since the axons defasciculate abnormally only after they reached the AL.

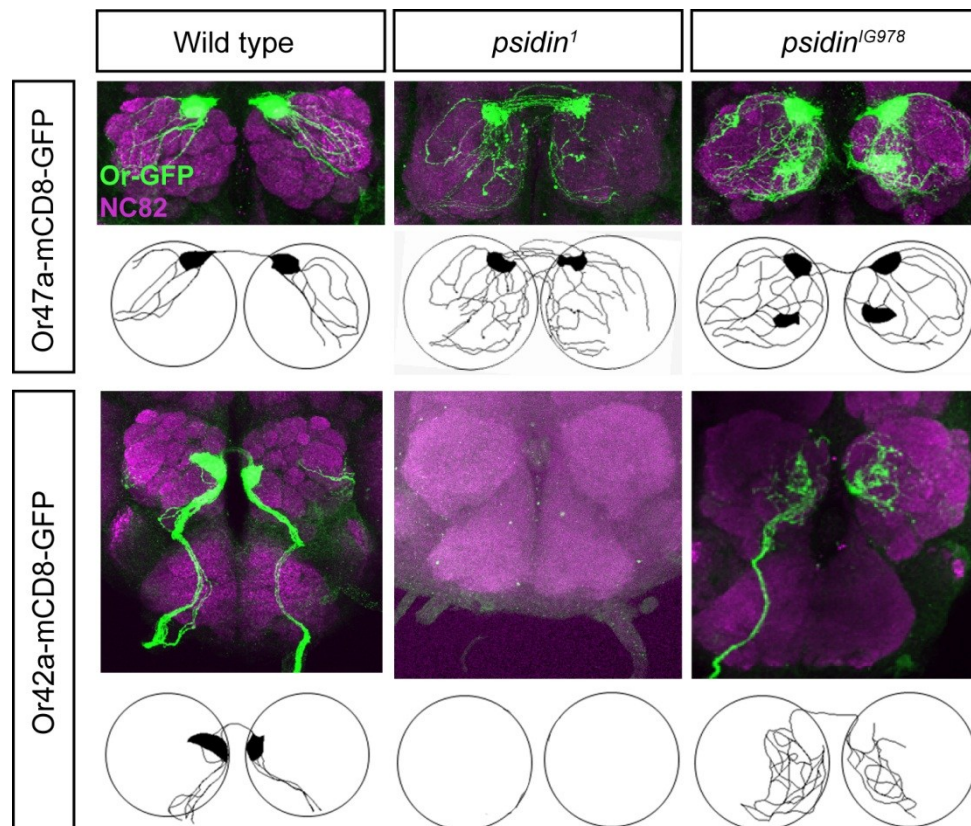


Figure 7.6 | Psidin mutant axons do not follow their normal targeting routes

Axons of one antennal (Or47a) and one maxillary palp (Or42a) ORN class were traced in wild type, *psidin*¹ and *psidin*^{IG978} background using eyFlp mediated clonal analysis. Axons were visualized using Or-GAL4 driving UAS-mCD8-GFP and stained with anti-GFP and NC82. Wild type Or47a axons use the dorsolateral projection route within the AL. *Psidin*¹ mutant axons deviate from that pattern and project also along the ventromedial route, where they eventually form ectopic synapses. Similar mistargeting pattern is visible in *psidin*^{IG978} mutant axons. A somewhat different pattern is found for Or42a neurons. Wild type Or42a axons grow through the SOG and project along the ventromedial route in the AL. In *psidin*¹ mutants no innervation is visible, due to the strong cell loss of Or42a neurons. However, Or42a *psidin*^{IG978} axons follow the wild type path through the SOG, but then defasciculate and innervate in neighboring glomeruli.

7.6 Psidin is not required for the initial outgrowth of ORNs

With the previous experiments I showed that the number of ORNs is severely reduced in *psidin*¹ mutant flies. However, the question whether these *psidin*¹ mutant axons project to the AL and later degenerate or are never able to extend their axons towards the AL remained unanswered. In order to address this question I analyzed the ingrowing ORN axons at the level of the antennal lobe in developing pupae at different stages. At 24h APF wild type axons from the antennal nerve started to surround the developing AL (red circle) (Figure 7.7). There was no difference between wild type axons, *psidin*^{IG978} and *psidin*¹ mutant axons at that stage. At 30h APF more antennal axons surrounded the AL and in addition to that the growing LaN becomes visible in the SOG. In wild type and *psidin*^{IG978} mutant flies the

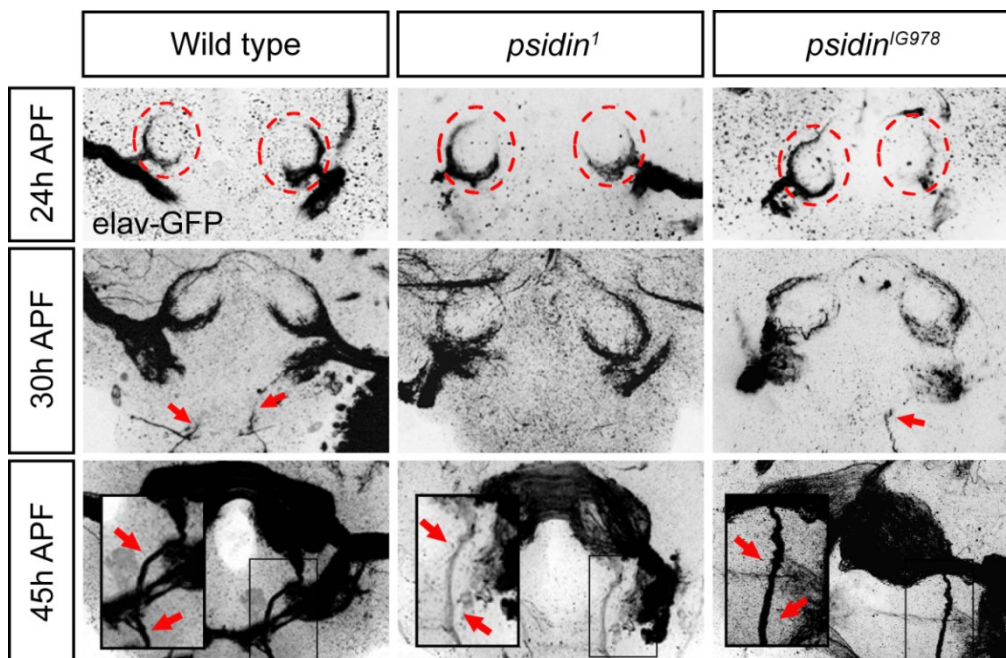


Figure 7.7 | Psidin is not required for initial outgrowth of ORNs

The developing antennal lobe was analyzed at different pupal stages. The panneuronal marker *elav-GAL4* was used to drive the expression of *UAS-mCD8-GFP*. Using *eyFlp* wild type, *psidin*^{IG978} and *psidin*¹ mutant clones were generated. The developing AL at 24h APF (red circles): axons entering the lobe surroundings. Developing AL at 30h APF: LaN is growing from the SOG towards the AL (red arrows). Developing AL at 45h APF: ORNs fully invaded the AL. At 45h APF a clear difference between *psidin*¹ and *psidin*^{IG978} is visible – the LaN is significantly reduced in *psidin*¹ mutants.

LaN was clearly visible (red arrow). In contrast, *psidin*¹ mutant axons coming from the MP were hardly visible in the LaN at 30h APF. Only later, at 45h APF, the LaN was visible in *psidin*¹ mutant flies (Figure 7.7). Compared to wild type or *psidin*^{IG978} mutants the LaN seemed to be greatly reduced in its thickness, which resulted in a weaker GFP signal. Although the antennal nerve showed no such obvious reduction in the innervation, the overall innervation density within the AL was reduced in *psidin*¹ mutant flies (Figure 7.7). In agreement with previous experiments no difference between wild type and *psidin*^{IG978} mutant axons could be observed. I did not observe any developmental delay between the *psidin*^{IG978} mutant and controls. The same holds true for *psidin*¹ mutant flies. Again, I did not find any difference in the developmental timing. *Psidin* mutant neurons are able to extend their axons out of the maxillary palp or antenna towards the AL. The fact that the LaN is severely reduced in its thickness is due to the loss of neurons in the *psidin*¹ background. Apparently a significant number of *psidin*¹ neurons undergoes cell death and are therefore not able to extend their axons. The remaining population of *psidin*¹ neurons, on the other hand, is able to extend their axons through the SOG towards the AL in a normal manner.

7.7 *Psidin* is required cell-autonomously

Next, I addressed the question, whether *Psidin* is required cell-autonomously or non-cell-autonomously in ORN axons. I used forward and reverse MARCM to selectively label mutant or wild type axons, respectively (see page 68 for details on the MARCM technique). In forward MARCM all three tested ORN classes showed the phenotypes described before (Figure 7.3). Using reverse MARCM, where wild type ORNs are labeled among the non-labeled mutant ORNs, the data indicated that *Psidin* is required cell-autonomously, since none of the tested ORN classes showed a phenotype. That means that wild type cells are

able to target normally in the presence of *psidin*¹ or *psidin*^{G978} mutant neurons. In addition, wild type cell also did not show any neuron number reduction, so that wild type neurons have no problem with ORN survival in the presence of *psidin* mutant neurons.

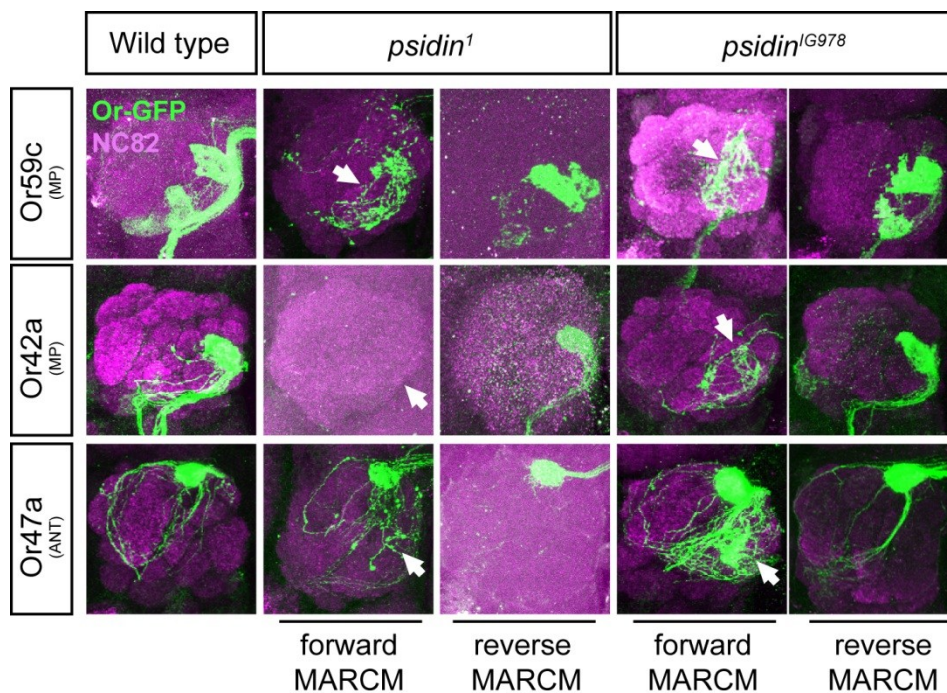


Figure 7.8 | Psidin is required cell autonomously

Comparison of forward MARCM and reverse MARCM analysis for several ORN classes. Forward MARCM labels mutant cells in a wild type background, whereas reverse MARCM labels the wild type population in a mutant background. Or59c, Or42a and Or47a *psidin*¹ and *psidin*^{G978} mutant axons display the before described mistargeting phenotypes of ectopic synapse formation and defasciculation (arrows). However, wild type axons in the same backgrounds target normally in all tested ORN classes.

7.8 Psidin is expressed during the development of the olfactory system

In order to address, whether Psidin is expressed at relevant developmental stages, I performed an *in situ hybridization* in collaboration with Dr. Laura Loschek. Starting with a very early time point, Psidin expression was already detected at 6h APF. Expression was visible in the eye-antennal disc, the primordia of MP and ANT (Figure 7.9A). This correlates

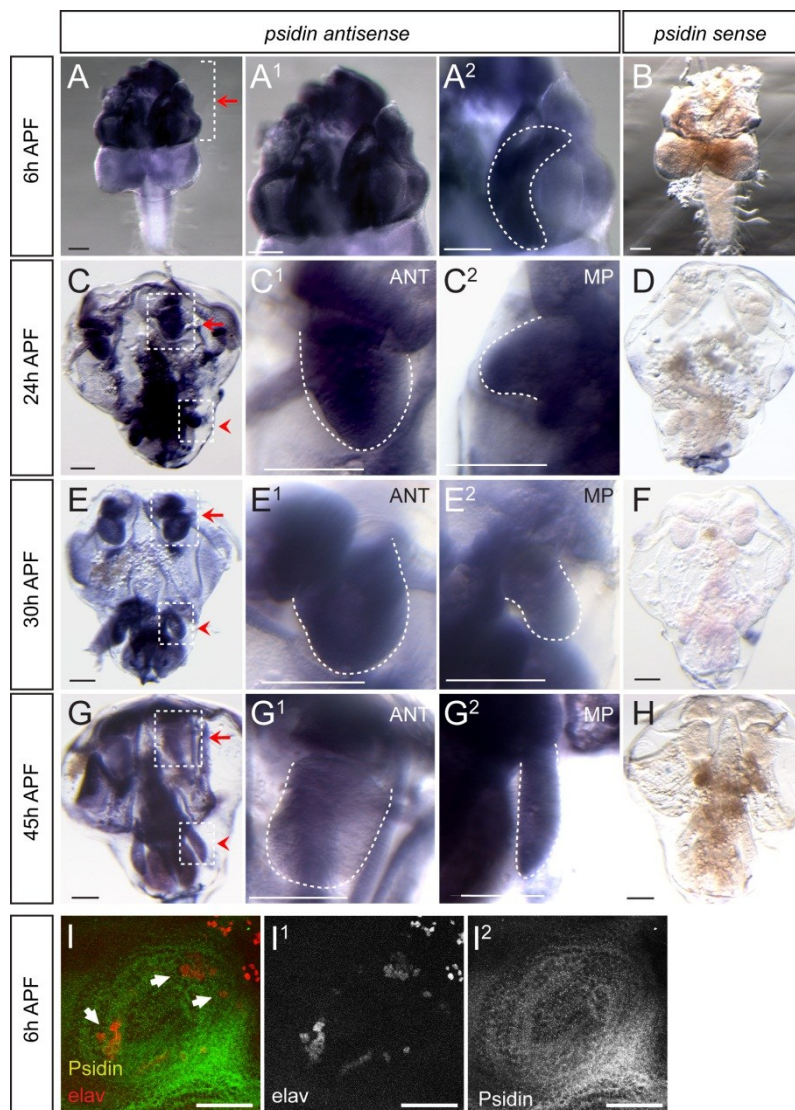


Figure 7.9 | **Psidin is expressed in the developing olfactory organs**

(A-H) In situ hybridization for *psidin* at different developmental stages. (A) At 6h APF *psidin* ISH signal can be detected in the developing eye-antennal discs (arrow). (C, E) The expression stays high in the developing antenna and MPs both at 24h and 30h APF (arrows). (G) *Psidin* expression starts to decline at 45h APF. (B, D, F, and H) Control (sense) probes for *psidin* do not show any signal (ISH done by Dr. Laura Loschek). (I) Staining of a developing antennal disc in 6h APF pupae. Psidin is broadly expressed in the antennal disc and partially overlaps with *elav* expression (arrows). Scale bar is 100 μ m.

well with the time frame of 6-20h APF, in which ORNs develop (Technau, 2008). The expression reached its maximum at around 24 hours APF in both the MP and the ANT (Figure 7.9C). At 30h APF, expression started to decline in the olfactory organs (Figure 7.9D,E). This expression is coherent with a role in the axonal pathfinding of ORNs, known to start around 20h APF and continue over a period of about 30 hours (Technau, 2008). A staining of the developing antennal disc at 6h APF revealed that Psidin partially co-localizes with the neuronal marker *elav* (Figure 7.9I). Thus, Psidin is expressed during the relevant developmental times in ORNs both during ORN differentiation and during axonal targeting, consistent with a functional role of Psidin in both these processes.

7.9 Psidin interacts with *dNAA20* *in vivo* and *in vitro*

My results indicate that Psidin is required at two steps of nervous system development: ORN survival and axonal pathfinding. Therefore, I next investigated the molecular mechanisms Psidin uses to regulate neuron number and axon targeting, respectively. Psidin is the homologue of yeast MDM20, the non-catalytic subunit of the NatB complex. In budding yeast, *natB* subunit mutants show defects including mitochondrial inheritance, budding, and cell division (Hermann et al., 1997). For the human homologue a role in cell cycle control or cell growth was found using analysis in tissue culture (Starheim et al., 2008). Essentially, the authors suggested that the anti-apoptotic protein p21 is involved in regulating downstream targets of NatB. Therefore I studied the *Drosophila* gene *dNAA20*, which encodes the predicted homologue of the catalytic subunit of NatB of yeast and human. I used RNAi in order to study the effect of *dNAA20* knockdown on *psidin* phenotypes *in vivo*. RNAi against *dNAA20* was driven by act-GAL4 in eyFlp clones. The effect of knocking down *dNAA20* on targeting and cell number was analyzed. Expression of *dNAA20* RNAi in

wild type, *psidin*¹ and *psidin*^{G978} background had no impact on the targeting pattern of Or59c and Or42a neurons (Figure 7.10A, Figure 7.11A). However, the expression of *dNAA20* RNAi resulted in a strong functional interaction in the cell number of ORNs. Knockdown of *dNAA20* showed a significant reduction of the respective ORN class in *psidin*^{G978} background. Levels were reduced to levels comparable to Or59c and Or42a *psidin*¹ mutants, respectively. Importantly, Or42a and Or59c neuron numbers in *psidin*¹ null mutants were not further decreased by *dNAA20* RNAi expression (Figure 7.10B, Figure 7.11B). Expression of RNAi against *dNAA20* in wild type clones did not result in targeting or cell number defects of

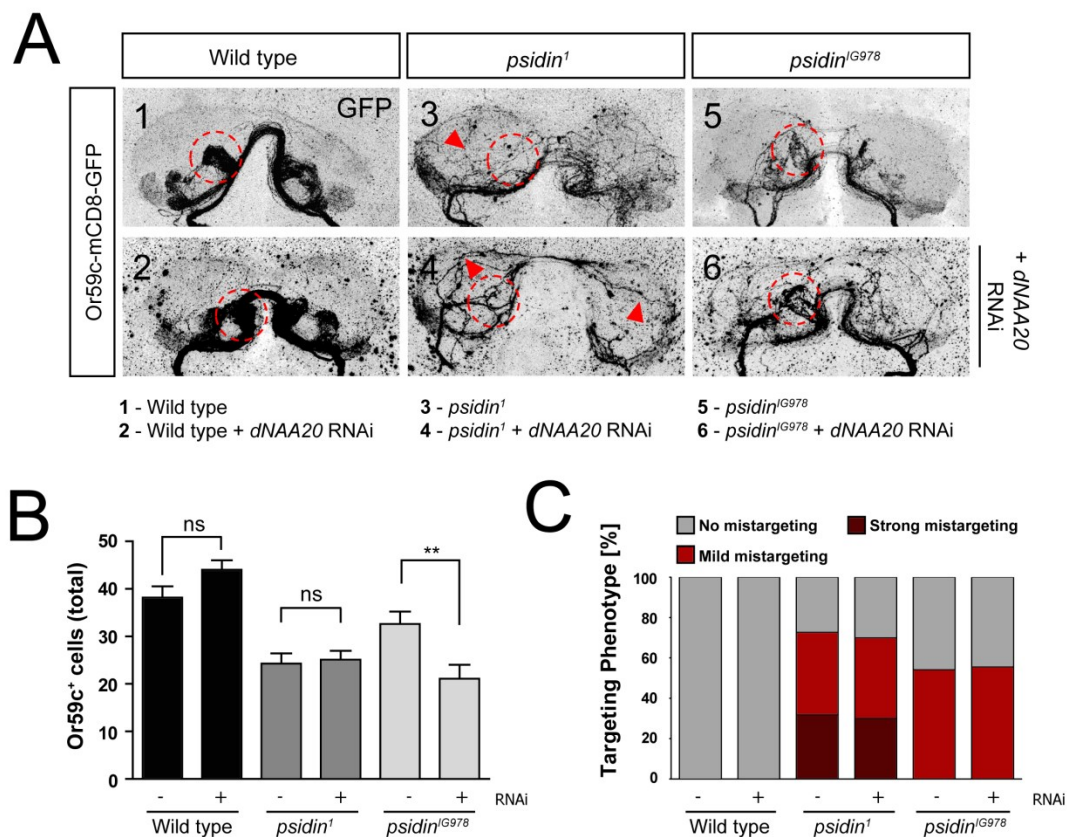


Figure 7.10 | Psidin and *dNAA20* interact in Or59c neurons

RNAi against *dNAA20* was driven by act-GAL4 in eyFlp clones. Axons were visualized using a Or59c::mCD8-GFP direct fusion construct. **(A)** Targeting pattern of Or59c neurons with *psidin*¹ and *psidin*^{G978} background (circles and arrowhead indicate mistargeting) in the presence and absence of RNAi against *dNAA20*. Knock down had no influence on Or59c axons. **(B)** Total cell number of Or59c and positive neurons in wild type, *psidin*¹ and *psidin*^{G978} background, in the presence and absence of *dNAA20* RNAi. Knock down in *psidin*^{G978} neurons reduced cell numbers to levels comparable to *psidin*¹ alone. **(C)** Quantification of the targeting phenotype. Bar graphs: One-way ANOVA, Bonferroni post-test for normally distributed values (* $p < 0.05$, ** $p < 0.01$, *** $p < 0.001$). Error bars \pm SEM.

Or42a or Or59c neurons, possibly because the amount of dNAA20 still present after knock-down was sufficient to maintain wild type cell numbers. In contrast to the reduction in cell number in *psidin*^{G978} mutants, Or59c and Or42a ORNs did not show any enhancement in mistargeting or ectopic synapse formation when *dNAA20* RNAi was expressed in *psidin*^{G978} and *psidin*¹ mutants (Figure 7.10, Figure 7.11). I could verify the knock-down of *dNAA20* using S2 cell culture and western blot analysis. Protein levels of dNAA20 were reduced by 80% upon co-expression of RNAi against dNAA20-myc (Figure 7.12). These results indicate that *dNAA20* is dispensable for ORN targeting, but it is required for the formation of the correct number of ORNs in a Psidin-dependent manner. These data are consistent with a role in cell cycle progression similar to the function of the yeast and human NatB complexes. *In vitro* experiments in both yeast and human cell lines demonstrated that the catalytic and non-catalytic subunits of NatB form a physical complex (Polevoda et al., 2003; Starheim et al., 2008). The data suggest that Psidin and dNAA20 might act in the same molecular pathway *in vivo*.

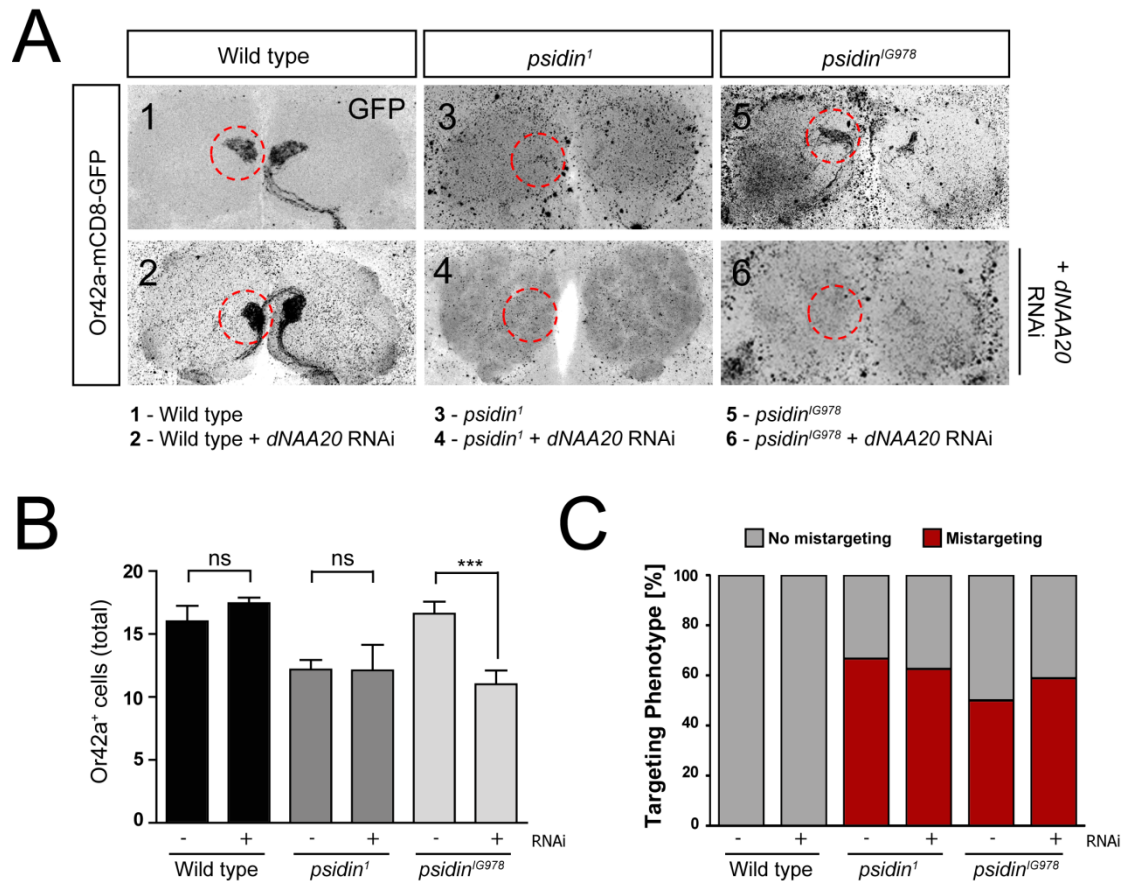


Figure 7.11 | Psidin and *dNAA20* interact in Or42 neurons

RNAi against *dNAA20* was driven by act-GAL4 in eyFlp clones. Axons were visualized using a Or59c::mCD8-GFP direct fusion construct. **(A)** Targeting pattern of Or42a neurons with *psidin*¹ and *psidin*^{G978} background in the presence and absence of RNAi against *dNAA20*. Knock down in *psidin*^{G978} neurons reduced the cell number, which in parallel caused a reduced innervation in the AL (circles). **(B)** Total cell number of Or42a positive neurons in wild type, *psidin*¹ and *psidin*^{G978} background, in the presence and absence of *dNAA20* RNAi. Knock down in *psidin*^{G978} neurons caused a reduction of neuron number. Bar graphs: One-way ANOVA, Bonferroni post-test for normally distributed values (* $p < 0.05$, ** $p < 0.01$, *** $p < 0.001$). Error bars \pm SEM.

Next, I addressed whether Psidin and dNAA20 also interact physically as their human and yeast homologues using co-immunoprecipitation assays (Figure 7.13). An N-terminal fusion of Psidin to an HA-protein tag and N-terminal myc fusion of dNAA20 were expressed in S2 cells. The pull-down of Psidin using anti-HA antibody resulted in co-immunoprecipitation of dNAA20 (Figure 7.13). These data show that also in *Drosophila*, Psidin and dNAA20 form a complex. Given that *psidin*^{IG978} contains a point mutation that selectively influences axon targeting, but not ORN survival, it was interesting to investigate whether *psidin*^{IG978} still interacts with dNAA20 as I would have predicted. I found that Psidin^{IG978} still pulls down dNAA20 at levels comparable to Psidin wild type (Figure 7.13), consistent with the fact that the *psidin*^{IG978} mutant allele in the presence of dNAA20 (or absence of dNAA20 RNAi) does not affect the cell number of ORNs.

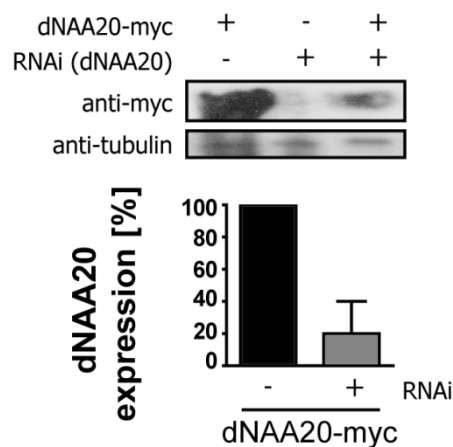


Figure 7.12 | Knock down of *dNAA20* in S2 cells

Expression of UAS-Psidin-HA and UAS-dNAA20-myc was driven by ub-GAL4 in S2 cells. Protein levels of dNAA20-myc are significantly (80%) reduced upon co-expression of RNAi against *dNAA20*. Bar graphs: One-way ANOVA, Bonferroni post-test for normally distributed values (* $p < 0.05$, ** $p < 0.01$, *** $p < 0.001$). Error bars \pm SEM.

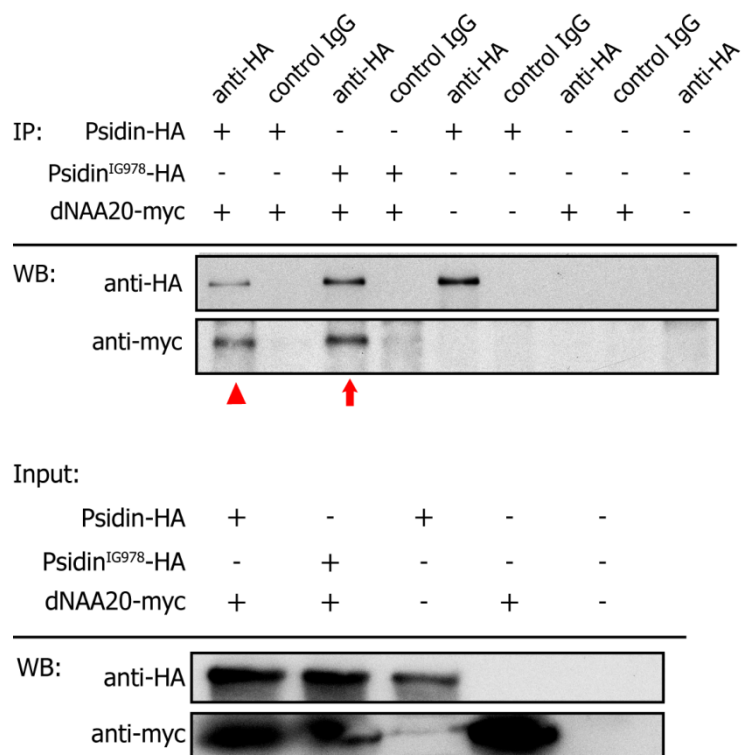


Figure 7.13 | Psidin and dNAA20 interact *in vitro*

UAS-Psidin-HA and UAS-dNAA20-myc were expressed in S2 cells under the control of a ubiquitous GAL4 (ub-GAL4). Using Co-IP, dNAA20 pulled down together with Psidin (arrowhead). Also Psidin^{IG978} is able to bind to dNAA20 at levels comparable to wild type Psidin (arrow).

7.10 NatB interaction domain is required for Psidin/dNAA20 interaction

My next aim was to map the interaction domain between Psidin and dNAA20 in order to separate NatB-dependent and independent functions of Psidin. Therefore, several small and big deletions of the predicted NatB interaction domain were generated (Figure 3.11). The following experiments were done in collaboration with Ramona Gerhards, who conducted these experiments as part of her bachelor thesis. The Psidin deletion constructs were co-expressed with dNAA20-myc. Cell lysates were used for a Co-IP of Psidin and dNAA20. The deletion of the entire NatB interaction domain resulted in a complete loss of dNAA20 binding to Psidin (Figure 7.14). Smaller deletions (Psidin^{ΔNatB23}, Psidin^{ΔNatB2}) pulled down significantly less amounts of dNAA20 compared to wild type. Only the deletion Psidin^{ΔNatB1} was able to pull down dNAA20 at levels comparable to wild type Psidin. Interestingly, the deletion Psidin^{ΔNatB1} covers a region around the mutation E320K found in the *psidin*^{G978} allele. The finding that *psidin*^{G978} has no defect in ORN cell number is in line with the data that the deletion around the mutation E320K is not sufficient to disrupt Psidin/dNAA20 binding. This would argue that the amino acid stretch deleted in Psidin^{ΔNatB1} is dispensable for Psidin/dNAA20 interaction.

Figure 7.14 | NatB domain is required for Psidin and dNAA20 interaction

Psidin deletion constructs were overexpressed in S2 cells together with dNAA20. **(A)** Different Psidin deletions were co-expressed with dNAA20 and used to pull down dNAA20 using Co-IP. Representative examples of co-immunoprecipitated dNAA20-myc using various Psidin deletions. Upper blot shows the different Psidin deletions (anti-HA blot). Lower blot displays the amount of dNAA20 that was pulled down together with the Psidin variants (anti-myc blot). As a reference wild type Psidin pull-down of dNAA20 was used (arrowhead, left lane) to compare the pull-down of dNAA20 with Psidin deletions (arrow, right lane). Deletion of the entire “NatB interaction domain” in Psidin^{ΔNatBfull} leads to loss of dNAA20 (arrow) pull down. Smaller deletions of this domain (Psidin^{ΔNatB23}, Psidin^{ΔNatB2}) showed a reduced pull down of dNAA20 (arrow). Only Psidin^{ΔNatB1} was able to pull down dNAA20 (arrow) at levels close to wild type Psidin (arrowhead). **(B)** Amount of Psidin^X-HA and dNAA20-myc that were used for the Co-IP. Although the deletion isoform seem to be expressed at normal levels, they seem to be very unstable given the low amount of protein that is captured by the HA antibody. Degree of Psidin/dNAA20 binding also seems to influence the stability of dNAA20, since the amounts of detected dNAA20 is lower if co-transfected with a deletion isoform.

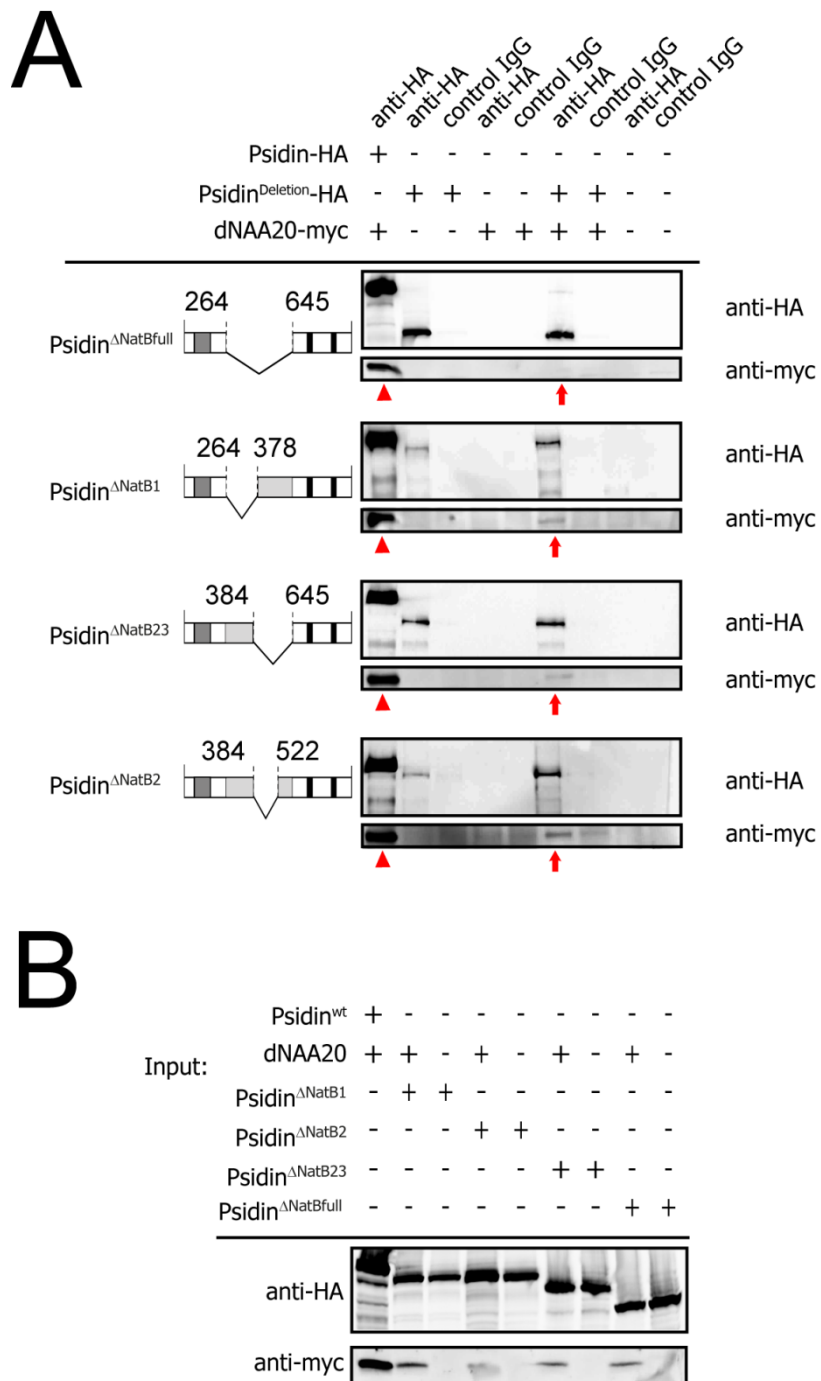


Figure 7.14 | NatB domain is required for Psidin and dNAA20 interaction

(Figure legend see previous page)

7.11 Psidin/dNAA20 interaction is regulated by serine S678

A previous study could identify a serine residue in human Mdm20 that is phosphorylated *in vivo* (Troost et al., 2009). In order study this potential phosphorylation site in *Drosophila*, I generated a phosphomimetic and a non-phosphorylatable Psidin isoform, respectively. Both isoform were expressed in eyFlp generated clones and could rescue the targeting phenotype of *psidin*¹ mutant axons. This is in contrast to the expression of Psidin^{IG978}, which is not able to rescue targeting defects (Figure 7.15A). At the same time,

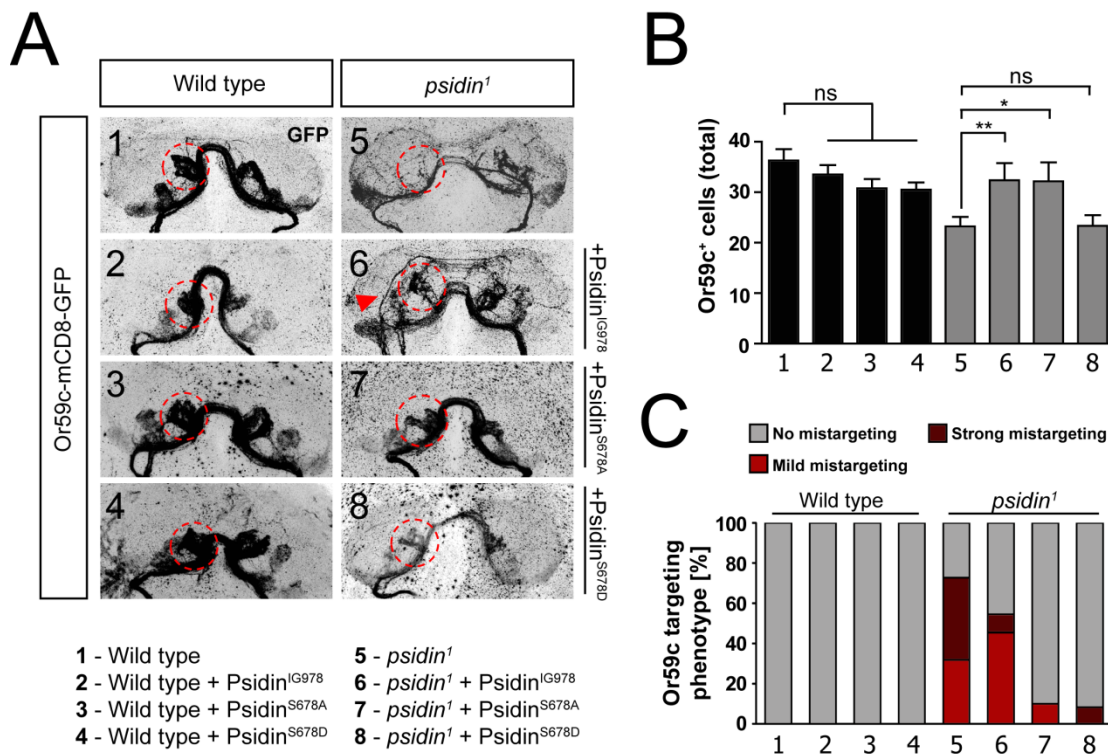


Figure 7.15 | Psidin phosphorylation state regulates ORN survival *in vivo*

Psidin isoforms were expressed in eyFlp clones using act-GAL4 as a driver. **(A)** Both phosphomutants Psidin^{S678A} and Psidin^{S678D} are able to rescue the mistargeting phenotype of *psidin*¹ mutant neurons. Contrary, expression of Psidin^{IG978} only rescues the strong mistargeting phenotype in *psidin*¹, overall mimicking the *psidin*^{IG978} allele (arrowhead and circle). **(B)** At the same time only one of the non-phosphorylatable Psidin isoform (S678A) is able to rescue the ORN cell number. The phosphomimetic isoform (S678D) fails to do so. As seen before Psidin^{IG978} can selectively rescue the ORN cell number. **(C)** Quantification of the targeting phenotype. Expression of both phosphomutants rescues the targeting phenotype of *psidin*¹ mutants, whereas Psidin^{IG978} expression only rescue to a level of the *psidin*^{IG978} allele. Bar graphs: One-way ANOVA, Bonferroni post-test for normally distributed values (* p<0.05, ** p<0.01, *** p<0.001). Error bars ± SEM.

only one phosphovariant (S678A) was able to restore ORN wild type cell numbers, whereas the other (S678D) failed to do so (Figure 7.15B). As seen in previous experiments, both isoforms are able to rescue the targeting phenotype of *psidin*¹ mutants *in vivo*. Nevertheless, only Psidin^{S678A} is able to restore ORN cell numbers to wild type levels, whereas Psidin^{S678D} fails to do so. Using these different Psidin variants, I was able to selectively only rescue the targeting phenotype (Psidin^{S678D}) or only the ORN cell loss (Psidin^{I^{G978}}).

Since it seems to be likely that ORN survival is linked to a functional NatB-complex, I next tested whether these two phosphomutants are able to interact with dNAA20. Using Co-IP with S2 cell lysates I could show that only the non-phosphorylatable isoform Psidin^{S678A} is able to pull down dNAA20. On the other hand, Psidin^{S678D} shows a significant reduction of dNAA20 pull-down compared to wild type (Figure 7.16). This is in agreement with the previous result that Psidin^{S678D} is unable to rescue the ORN cell loss.

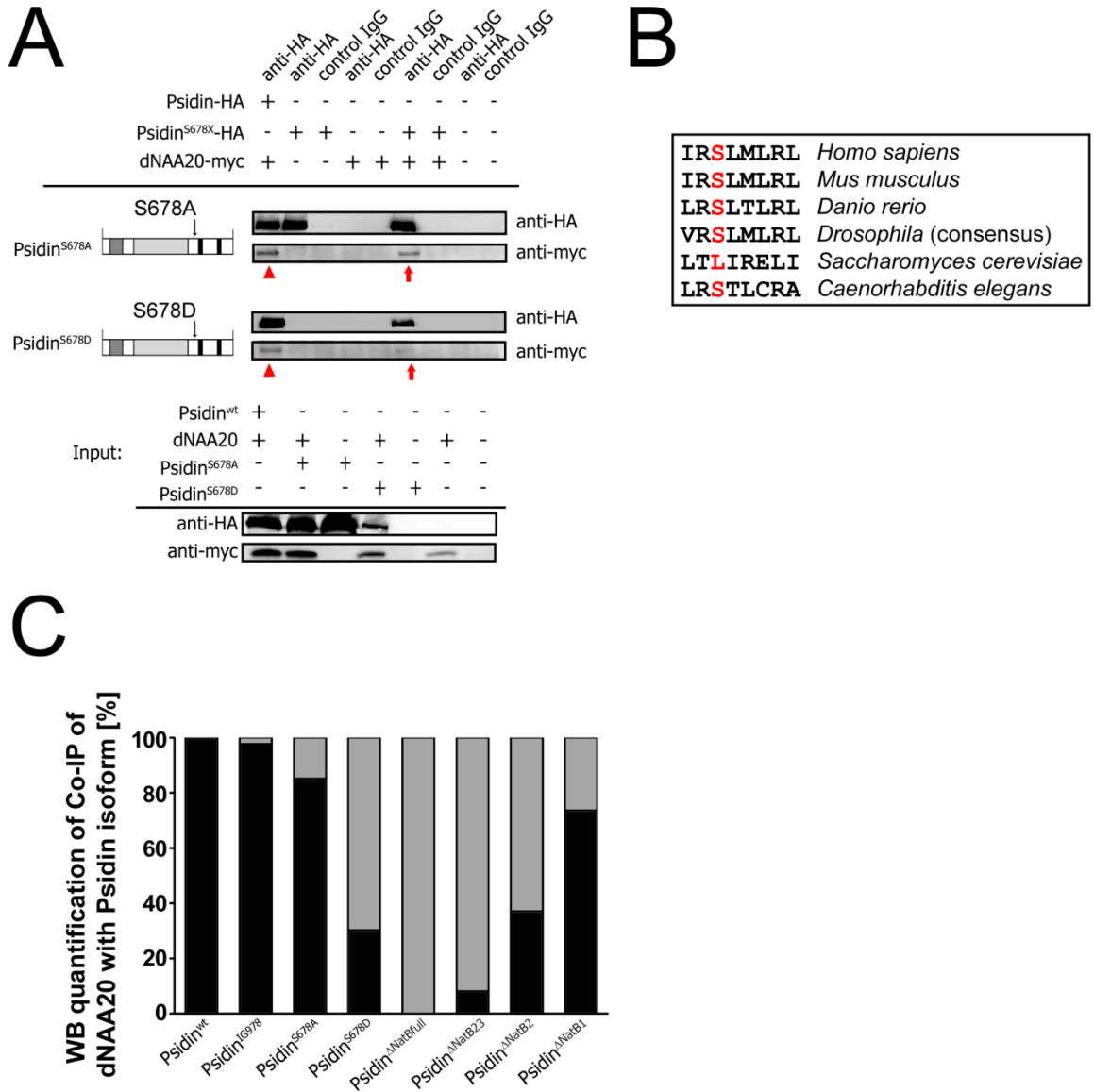


Figure 7.16 | S678 in Psidin is used to regulate Psidin/dNAA20 interaction

(Figure legend see next page)

Figure 7.16 | Serine 678 regulates Psidin/dNAA20 interaction

(A) Psidin^{S678A} and Psidin^{S678D} phosphomutants were co-expressed with dNAA20 and used to pull down dNAA20 using Co-IP. Representative examples of co-immunoprecipitated dNAA20-myc with Psidin phosphomutants. Upper blot shows the Psidin phosphomutant (anti-HA blot). Lower blot displays the amount of dNAA20 that was pulled down together with the phosphomutant (anti-myc blot). As a reference wild type Psidin pull-down of dNAA20 was used (arrowhead, left lane) to compare the pull-down of dNAA20 with Psidin deletions (arrow, right lane). Psidin^{S678A} was able to pull down dNAA20 (arrow) at levels similar to wild type Psidin (arrowhead). Contrary, Psidin^{S678D} showed a reduced pull down of dNAA20 (30% of wild type Psidin). **(B)** The serine residue 678 is highly conserved in *Drosophila* and higher organisms. Interestingly, this serine residue can't be found in yeast. **(C)** Quantification of the Western blots showing the normalized pull-down of dNAA20 with different Psidin isoforms. Psidin^{IG978}, Psidin^{S678A}, Psidin^{ΔNatB1} pulled down dNAA20 at wild type levels. Contrary Psidin^{S678D}, Psidin^{ΔNatBfull}, Psidin^{ΔNatB23} and Psidin^{ΔNatB2} show a reduced or no pull down of dNAA20, respectively.

7.12 Psidin regulates actin dynamics

After investigating Psidin's role as non-catalytic part of the NatB-complex I went on to elucidate its role in growth cone and axon actin dynamics. Psidin was recently identified as a novel actin-binding protein (Kim et al., 2011). The authors found that Psidin binds actin and competes with Tropomyosin for actin interaction. I therefore tested the possibility of a potential interaction between Psidin and Tropomyosin during axon targeting. I generated eyFlp clones to analyze the targeting pattern of Or59c neurons mutant for *tropomyosin-1* (*tm1*) or *psidin*. Neurons mutant for *psidin*¹ or *psidin*^{55D4} displayed a strong targeting defect

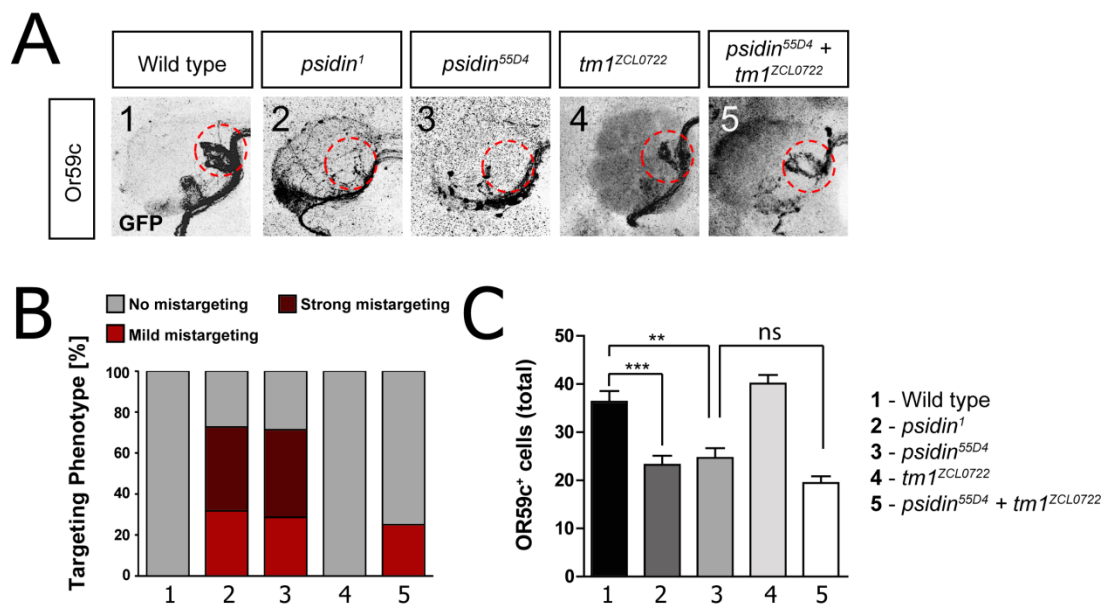


Figure 7.17 | Psidin and Tropomyosin interact during axon targeting

Eyflp mediated clonal analysis was used to analyze the targeting pattern of Or59c neurons. Axons were visualized using a Or59c::mCD8-GFP direct fusion. **(A)** Or59c neurons in a *psidin*¹ and *psidin*^{55D4} mutant background showed a complete loss of innervation at their innate glomerulus (red circles). The tropomyosin mutant *tm1*^{ZCL0722} didn't show any targeting defect. The targeting pattern of *psidin* single mutants was restored in *psidin*^{55D4} + *tm1*^{ZCL0722} double mutants. **(B)** Quantification of the targeting defect of Or59c neurons. Single mutants of *tm1*^{ZCL0722} show no targeting defect, whereas *psidin*¹ and *psidin*^{55D4} single mutants showed a pronounced targeting defect. The targeting defect of *psidin*^{55D4} mutants was significantly rescued in the double mutant *psidin*^{55D4} + *tm1*^{ZCL0722}. **(C)** Quantification of Or59c neuron number. Cell loss in *psidin*^{55D4} background was not rescued in the double mutant. The *tm1*^{ZCL0722} background didn't show any significant reduction of Or59c neurons. Bar graphs: One-way ANOVA, Bonferroni Post-test (* p<0.05, ** p<0.01, *** p<0.001)

as shown above (Figure 7.17A). These neurons failed to innervate their innate target glomerulus (Figure 7.17A, red circles). *Tm1^{ZCL0722}* mutant neurons, on the other hand, did not show any targeting defect (Figure 7.17A). To test for a possible interaction between Psidin and Tropomyosin, I used a double mutant (*psidin^{55D4}* + *tm1^{ZCL0722}*) and analyzed the targeting pattern of Or59c neurons in mutant clones. Interestingly, the double mutant restored the normal targeting pattern (Figure 7.17A) almost to wild type levels (Figure 7.17B, 70% vs. 25%). In contrast, this double mutant did not restore the cell number of Or59c expressing neurons. Cell numbers remained comparable to the *psidin¹* or *psidin^{55D4}* single mutants (Figure 7.17C). These findings are consistent with the hypothesis that Psidin does not function as a NatB component but rather as an actin regulator in the context of axonal targeting.

Tropomyosin acts primarily as a stabilizer of F-actin (Cooper, 2002). To test whether its genetic interaction with *psidin* is due to actin-stabilizing functions, I next asked whether other molecules involved in F-actin stabilization and destabilization show similar genetic interactions with *psidin*. Lim kinase (LimK) is an important regulator of actin dynamics and was previously implicated in ORN targeting (Moriyama et al., 1996; Aizawa et al., 2001). Wild type LimK phosphorylates Cofilin, inactivating its function in F-actin disassembly. In contrast, kinase inactive LimK acts as a dominant negative regulator increasing the amount of active Cofilin and thereby reducing F-actin levels (Maciver et al., 1998). I expressed wild type LimK, kinase inactive LimK and RNAi against LimK under the control of act-GAL4 in eyFlp generated *psidin* mutant and control clones (Figure 7.18). Overexpression of wild type LimK in wild type neurons caused 88% of the Or59c neurons to mistarget (Figure 7.18A), which is comparable to *psidin* mutants (Figure 7.17B). Axons showed a strong deviation from the normal growth pattern, invading the AL from the dorsolateral and ventromedial side. In contrast,

expression of LimK RNAi or of a kinase-inactive LimK affected the targeting of only 10% of ORNs (Figure 7.18B). It therefore seems that increased actin filament stability strongly impairs ORN axon targeting. Expression of wild type LimK in *psidin*¹ mutants slightly increased the targeting phenotype (87% vs. 72%) (Figure 7.18B). Consistent with the idea that Psidin promotes actin dynamics and instability, overexpression of LimK RNAi or kinase-inactive LimK (i.e. conditions that promote F-actin destabilization) significantly rescued the *psidin*¹ mutant axonal targeting phenotype (38% vs. 72%) (Figure 7.18B).

Next, I analyzed an important downstream target of LimK, Cofilin (Twinstar, Tsr) and its functional interaction with Psidin *in vivo*. I overexpressed two different forms of *tsr*, a constitutive active (TsrS3A) and a constitutive inactive version (TsrS3E) in wild type and *psidin*¹ mutant clones. Overexpression of either of the two *tsr* alleles in wild type clones resulted in mistargeting of MP ORN axons in about 20% of the brains (TsrS3A: 20%, TsrS3E: 23%, Figure 7.19). Constitutive active Tsr overexpressed in *psidin*¹ mutants reduced the *psidin*¹ Or59c mistargeting phenotype by 14% compared to *psidin*¹ alone. Constitutive inactive Tsr aggravated the *psidin*¹ phenotype slightly (8% increase, Figure 7.19).

It can be concluded that the *psidin* mutant targeting phenotype can be rescued by promoting actin destabilization via LimK/Cofilin or by decreasing the amount of the actin filament stabilizer Tropomyosin-1 in the neuron. Therefore, Psidin might shift the cytoskeletal balance to an increase in the amount of dynamic actin within ORNs.

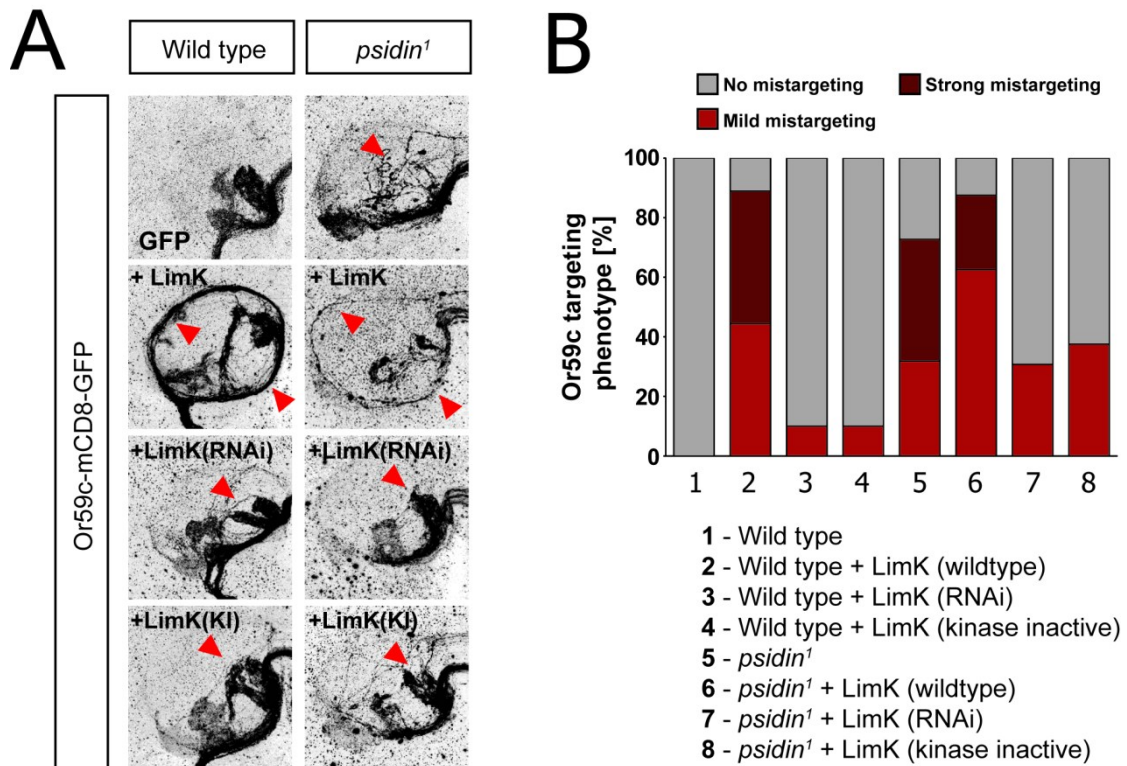


Figure 7.18 | Psidin genetically interacts with LimK

Or59c axons were visualized using a direct fusion Or59c::mCD8-GFP. The different transgenes were expressed in eyFlp clones under the control of act-GAL4. **(A,B)** Overexpression of wild type LimK leads to a severe mistargeting defect (87%). Expression of a kinase inactive LimK variant only mildly affected the targeting (10%). Knock-down of LimK using RNAi only mildly affected targeting (10%). Stabilizing F-actin even more by overexpressing LimK in a *psidin*¹ background mildly aggravates the targeting defect. Contrary destabilization of F-actin (inactivation of LimK) rescues the targeting phenotype.

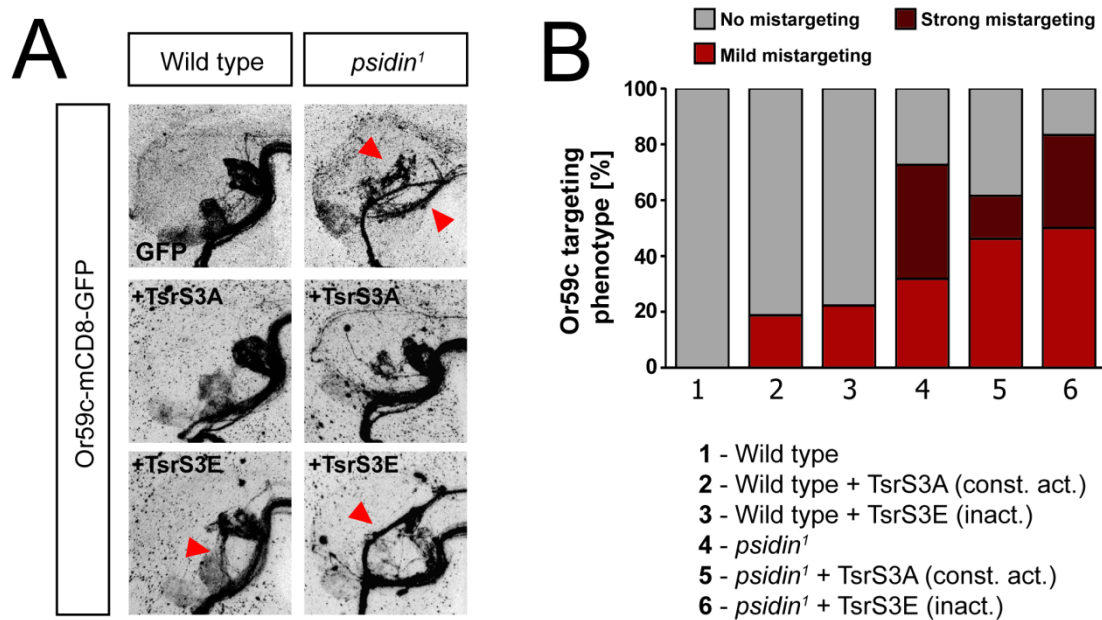


Figure 7.19 | Psidin genetically interacts with Cofilin (twinstar)

Or59c axons were visualized using a direct fusion Or59c::mCD8-GFP. The different transgenes were expressed in eyFlp clones under the control of act-GAL4. **(A,B)** Overexpression of constitutive active (TsrS3A) and constitutive inactive (TsrS3E) Cofilin leads to a mild targeting phenotype (20%). Expression of a TsrS3A rescued the targeting (72% vs 58%), whereas the opposite, expression of TsrS3E aggravates the phenotype (72% vs. 80%) (arrowhead).

7.13 Loss of Psidin decreases the size of lamellipodia in growth cones

The following experiment was done in collaboration with Dr. Natalia Sánchez-Soriano in the laboratory of Prof. Andreas Prokop at the University of Manchester, UK. To directly test whether Psidin regulates actin dynamics in axons and growth cones, *psidin* loss-of-function mutant phenotypes were analyzed at the sub-cellular level. Embryonic primary neurons are ideally suited to dissect the regulatory mechanisms underpinning cytoskeletal dynamics in general and of F-actin networks in particular (Sánchez-Soriano et al., 2010; Matusek et al., 2008; Gonçalves-Pimentel et al., 2011). The analysis of several cell parameters revealed that *psidin*¹ and *psidin*^{IG978} mutant neurons displayed significantly smaller lamellipodia (Figure 7.20A,B, insets). Notably, neurites were significantly longer (Figure 7.20B), which is consistent with similar observations for other actin-regulating proteins with known pathfinding defects *in vivo* (Sánchez-Soriano et al., 2010). Consistent with Psidin's role as a positive regulator of actin dynamics and with my data on axon targeting of ORNs *in vivo*, the double mutant of *psidin*^{55D4} and *tm1*^{ZCL0722} fully rescued all parameters including lamellipodia size (Figure 7.20A,B). Primary neurons derived from wild type or *psidin* mutant embryos were analyzed after 6 hour in culture and were stained with phalloidin and anti-tubulin antibody to visualize Actin and Tubulin, respectively (Figure 7.20C). Overexpressed HA-tagged Psidin partially co-localized with actin filaments at growth cone lamellipodia (Figure 7.20A). All these observations support a model in which Psidin positively regulates actin protrusions of growth cones as an essential prerequisite for the correct navigation of growing axons.

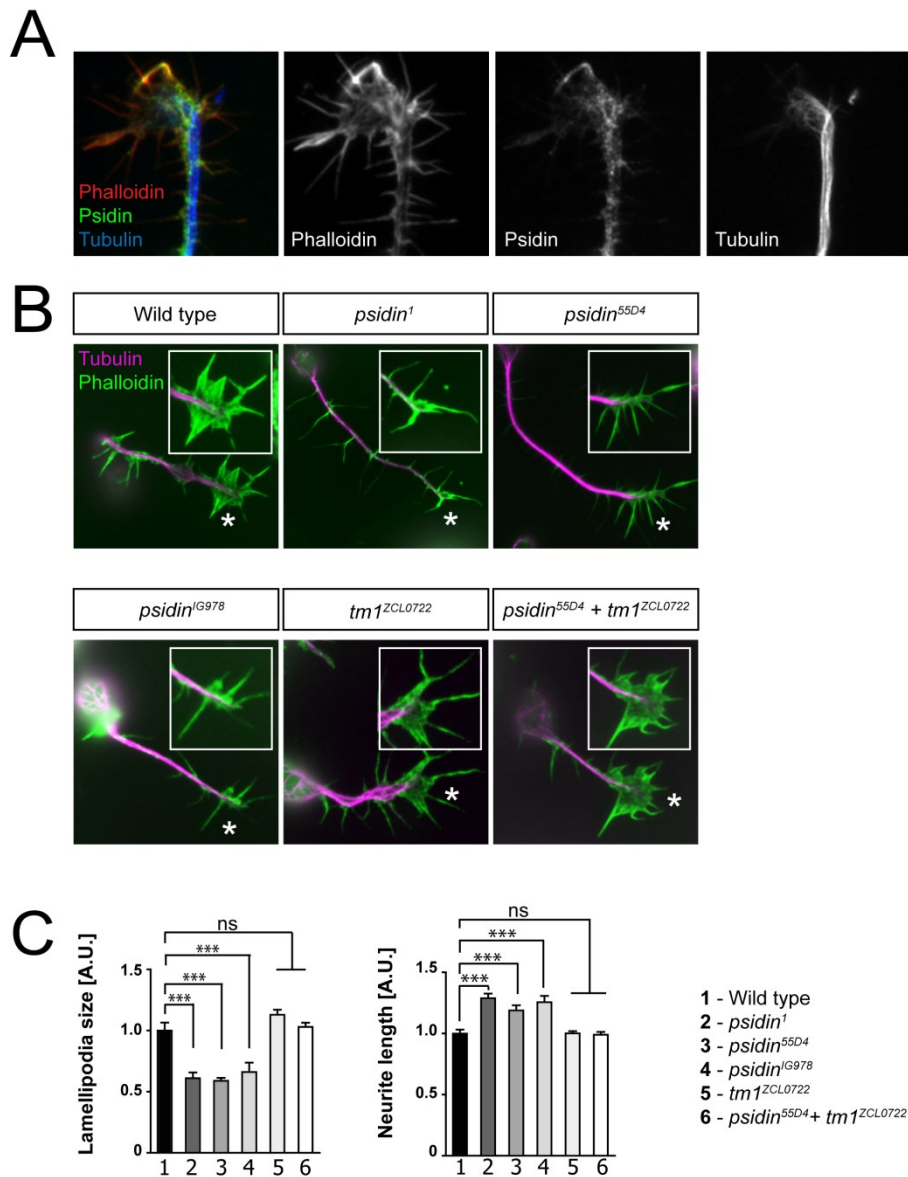


Figure 7.20 | Reduced Lamellipodia in *psidin* loss of function neurons

Drosophila embryos mutant for homozygous mutant for *Psidin* or *Tropomyosin* were cultured and analyzed after six hours. **(A)** Localization of Psidin and Actin in the growth cone. Psidin partially co-localizes with actin in the growth cone, whereas Tubulin only localizes to the shaft of the axon. **(B)** Growth cones of wild type, *psidin*^{G978}, *psidin*¹ and *psidin*^{55D4} + *tm1*^{ZCL0722} mutant neurons. Growth cones appear to be significantly smaller in *psidin* mutants, but normal in the double mutant. **(C)** Quantification of lamellipodia size and neurite length. Lamellipodia size is significantly reduced in *Psidin* mutants, but rescued in the double mutant. As a secondary effect, neurite length is increased in *psidin* mutants, but again rescued in the double mutant. Bar graphs: One-way ANOVA, Bonferroni post-test for normally distributed values (* $p < 0.05$, ** $p < 0.01$, *** $p < 0.001$). Error bars \pm SEM.

7.14 Psidin^{IG978} maintains ability to bind F-actin

I have shown above that Psidin^{IG978} binds dNAA20 at levels comparable to wild type Psidin (see Figure 7.13). In order to further investigate the effect of the E320K mutation in Psidin, I performed an *in vitro* actin binding assay. It was previously shown that wild type

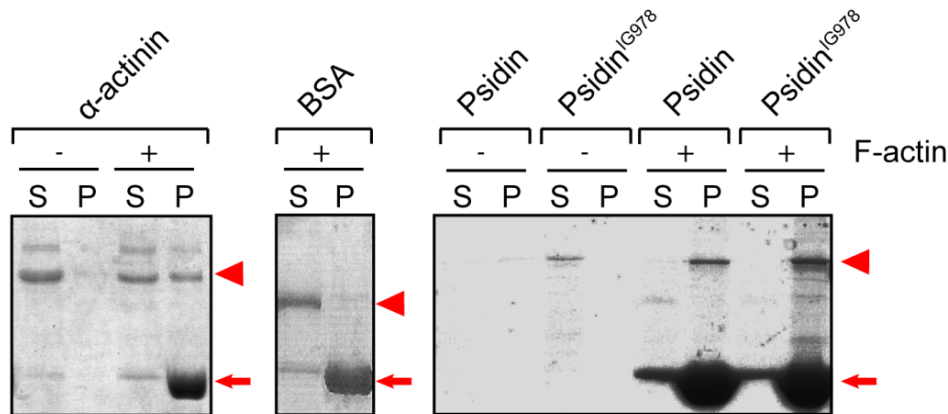


Figure 7.21 | Psidin^{IG978} is able to bind F-actin

Positive control α -actinin (arrowhead) is present in the pellet together with F-actin (arrow). Contrary, the negative control BSA (arrowhead) can only be found in the supernatant (arrow). Psidin and Psidin^{IG978} was overexpressed under the control of a ubiquitous GAL4 (ub-GAL4) and purified from S2 cells. Both, Psidin and Psidin^{IG978} can be found in the pellet (arrowhead) in the presence of F-actin indicating that both bind F-actin.

Psidin binds F-actin (Kim et al., 2011). I purified Psidin^{IG978} from S2 cells and determined its actin binding capabilities. In this assay I tested the ability of Psidin and Psidin^{IG978} to bind F-actin. Purified Psidin and Psidin^{IG978} are incubated with F-actin. After the incubation, supernatant and pellet are separated and analyzed on an SDS-gel. As a positive control I used α -actinin, which can only be found in the pellet in the presence of F-actin. The negative control BSA cannot be found in the F-actin pellet. Both Psidin proteins are found in the F-actin pellet. Therefore, Psidin^{IG978} is able to bind F-actin at levels that are comparable to wild type Psidin. Therefore I concluded that the observed defects in axon targeting in *psidin*^{IG978} mutants are not due to changed F-actin binding capabilities of Psidin^{IG978}.

7.15 Fly-like yeast Mdm20 can rescue Mdm20 function during cell division

The mutation I found in the *psidin*^{I^{G978}} mutant revealed a point mutation in a residue that is highly conserved in *Drosophila* as well as in higher organisms including humans (Figure 7.22A). In yeast, however, the wild type amino acid resembles exactly the mutation found in *psidin*^{I^{G978}} (yeast contains a lysine and *Drosophila* a glutamate at the position in question). NatB complexes are found in yeast, *Drosophila*, but also higher organisms. This complex usually consists of two subunits, a catalytic and a non-catalytic one. The *psidin*^{I^{G978}} phenotype is specific for Psidin's function in actin dynamic, since Psidin^{I^{G978}} interacts normally with dNAA20. I therefore ask the question, whether the residue in question has a special function in yeast. Later during evolution Psidin might have acquired additional functions leading to an amino acid change in *Drosophila*. I therefore engineered a "fly-like" yeast Psidin (Mdm20^{K^{304E}}) and asked the question whether this protein can rescue the Mdm20 phenotype in yeast. This experiment was done in collaboration with Susanne Gutmann and Zuzana Storchova at the MPI Biochemistry, Martinsried. *Mdm20* mutants show severe defects during cell division (Figure 7.22B). Actin spindles are not formed properly during the budding process. Actin cables are strongly segmented in *Mdm20* mutants. Expression of the "fly-like" yeast Psidin (Mdm20^{K^{304E}}) restores these actin cables to wild type morphology (Figure 7.22B, arrowheads). Also growth parameters and polarization of yeast cells was not affected in Mdm20^{K^{304E}} expressing cells (Figure 7.22C,D). This indicates that changing the residue in question had no effect on the functionality of the protein in yeast.

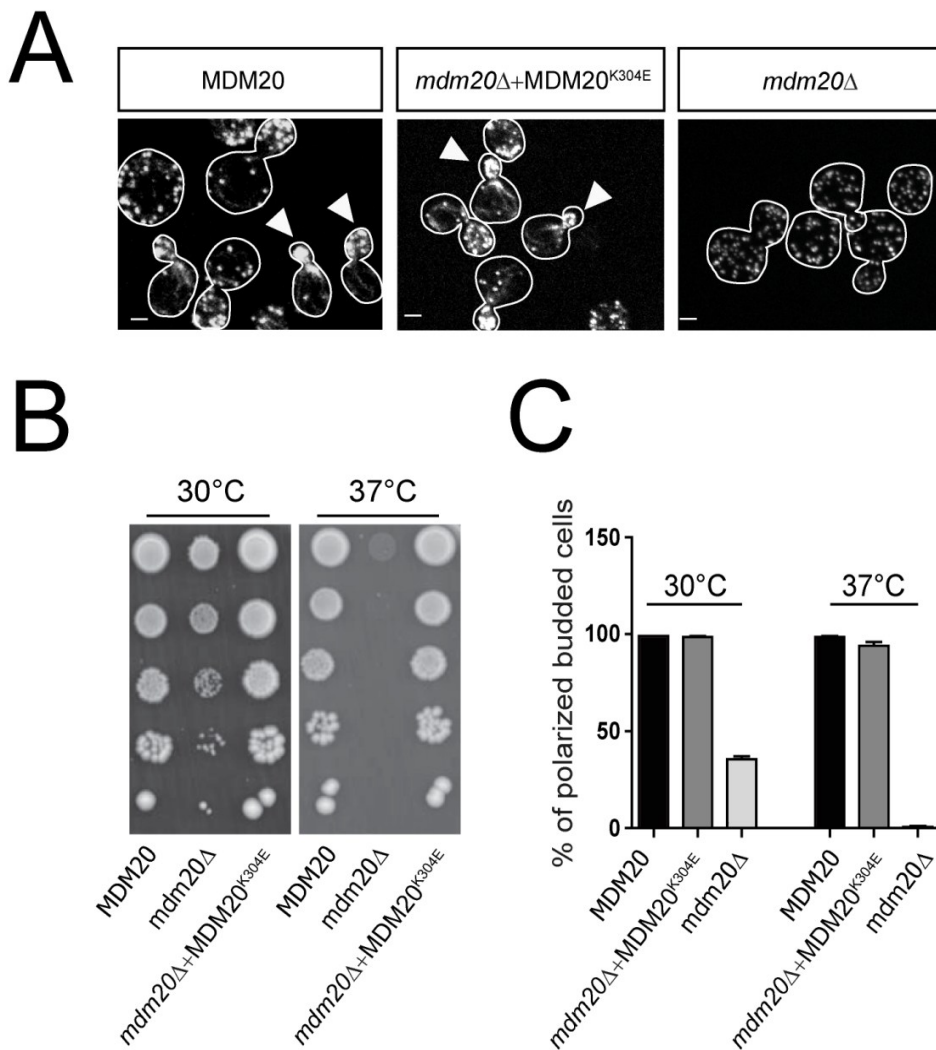


Figure 7.22 | Fly like Mdm20 can rescue Mdm20 mutants during cell division

(A) Mimicking a 'fly-like' MDM20 by replacing lysine with glutamate did not change the functionality of the yeast MDM20 protein compared to wild type. Budding yeast with 'fly-like' MDM20 shows normal actin cables during cell division. (B) MDM20^{K204E} does not show any growth defects and functions comparable to MDM20 wild type protein. (C) The percentage of polarized yeast cells is not affected in MDM20^{K304E} expressing cells under different growth conditions. Bar graphs: One-way ANOVA, Bonferroni post-test for normally distributed values (* $p < 0.05$, ** $p < 0.01$, *** $p < 0.001$). Error bars \pm SEM.

8 Discussion

The work presented in this thesis demonstrates for the first time that Psidin is involved in two aspects of the development of *Drosophila melanogaster's* olfactory system – the process of axon guidance and the survival of neurons.

8.1 Psidin as regulator of actin dynamics

Axon guidance is controlled by a great variety of extracellular biochemical cues. The key effectors of these guidance cues are actin- and microtubule-associated proteins, which control cytoskeletal dynamics. In this thesis I was able to demonstrate that Psidin is part of the actin housekeeping machinery in neurons and is required for neuronal circuit formation. This is in line with the findings of a previous study (Kim et al., 2011), describing Psidin as an actin binding molecule. Furthermore, I was able to show that the loss of Psidin results in smaller growth cones with significantly smaller lamellipodia in primary neurons. This phenotype is completely rescued by the parallel removal of the actin stabilizer Tropomyosin-1. This suggests that Psidin and Tropomyosin have opposing roles in actin dynamics. A similar role for Psidin was recently reported in oocyte migration (Kim et al., 2011). Additionally, it is apparent that Psidin interacts genetically with other proteins that also control actin dynamics. Cofilin and LimK are well-known effectors of the cytoskeleton (Sarmiere and Bamburg, 2004). More specifically, the actin destabilizing molecule Cofilin is a direct target of LimK. Here, LimK phosphorylates Cofilin and thereby inactivates it (Aizawa et al., 2001; Ohashi et al., 2000). Hence, I used overexpression of LimK and Cofilin isoforms to artificially shift the F-actin balance towards more stable or less stable F-actin conditions,

respectively. The knock-down of LimK or expression of hyperactive Cofilin (promoting conditions for less stable F-actin), rescued the *psidin*¹ targeting phenotype in Or59c neurons. Overall using LimK to manipulate actin dynamics had a stronger impact on Or59c targeting compared to Cofilin in the same context. Although it has been shown that LimK acts upstream of Cofilin (Ang et al., 2006) and supposedly in one pathway, the effect on targeting was much stronger using LimK than using Cofilin. The overexpression of different Cofilin isoforms had only a mild influence on the Or59c targeting defect. This can be explained by the fact that Cofilin is a downstream actin regulator, which limits its effectiveness in modulating actin dynamics. It is likely that its overexpression can be compensated by a number of other actin modulating proteins. Contrary, LimK is upstream of Cofilin and it is therefore possible that this kinase has other, not yet identified downstream targets. This is in agreement with the finding that overexpression of LimK in wild type neurons leads to strong targeting defects, but at the same time overexpression of inactive Cofilin in wild type neurons has only a minor effect. This argues for a Cofilin independent pathway of Limk, which could explain its overall stronger impact on ORN targeting.

To conclude, I could show that Psidin acts as an F-actin destabilizing protein and antagonist of Tropomyosin. Creating conditions that artificially shifted the balance towards more stable F-actin aggravated the *psidin* phenotype, whereas artificial destabilization of F-actin was able to rescue the *psidin* phenotype. This strongly argues for Psidin's functions as opponent of the actin stabilizer Tropomyosin. In addition, Psidin is required to maintain the lamellipodium in neuronal growth cones. Here Psidin act as part of the actin housekeeping machinery and maintains F-actin in the lamellipodium in a highly dynamic and responsive state.

8.2 Psidin is required differentially in olfactory neurons

The loss of Psidin results in a strong lamellipodia phenotype in primary neurons. Interestingly, a lamellipodial localization has also been proposed in a previous work (Kim et al., 2011). Again the parallel removal of Tropomyosin is able to restore lamellipodia size. As described in the introduction, the growth cone functions as an important signaling hub during axon guidance. This is in agreement with the strong phenotype in primary neurons. Nevertheless, ORN classes are affected differently in *psidin* mutants.

Although ORNs are equally affected by the lamellipodia phenotype, certain ORN classes seem to have a higher requirement for Psidin than others. ORNs projecting dorsolaterally or ventromedially showed a stronger mistargeting phenotype than centrally projecting neurons (Table 5.1). I therefore propose a mechanism were neurons have to face

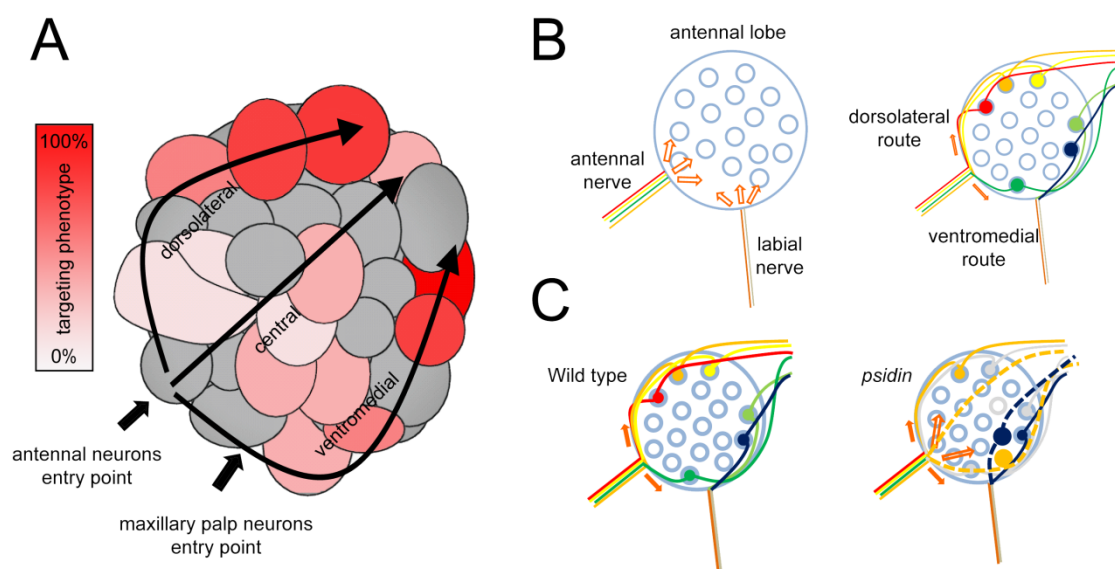


Figure 8.1 | Psidin is required differentially in ORN classes

(A) ORN targeting is affected differentially in *psidin* mutants. ORN axons reach the AL at two different entry points (arrows) – antennal and maxillary palp entry point. Axons then split into three main projection routes (dorsolateral, central and ventromedial) and target their innate glomeruli. Axons targeting central glomeruli are less affected, whereas axons targeting dorsally or ventrally are strongly affected. **(B)** Axons growing along the dorsolateral and ventromedial route are strongly affected in *psidin* mutants. Centrally projecting neurons (not depicted) are less affected. **(C)** In *psidin* mutants axons are unable to respond to instructive guidance cues. As a consequence, axons don't follow their normal projection route and grow across the entire AL. Mutant axons are shifted towards the ventromedial and central parts of the AL.

“decision points” during development (Figure 8.1). Depending on the ORN class, axons growing along the dorsolateral and ventromedial route are repelled towards the upper or lower part of the AL, respectively (see also Figure 7.6). At this time point, functional lamellipodia are highly required. Only they can enable growth cones to respond to “turning instructions” (Koestler et al., 2009b). It seems therefore plausible that Psidin is more required in neurons that target dorsolaterally or ventromedially. Axons projecting centrally are likely not to receive “turning instructions”. In these axons, microtubule driven growth can compensate for the lamellipodium phenotype (Alves-Silva et al., 2012). The model I proposed correlates with the phenotype of Or47a axons mutant for *psidin*¹ and *psidin*^{IG978} (Figure 7.6 and Figure 8.1). Wild type Or47a axons grow along the dorsolateral route and innervate a dorsal glomerulus. Contrary, Or47a *psidin* mutant axons are no longer restricted to this dorsolateral route. *Psidin*¹ mutant axons deviated from this path and are no longer repelled from the lower part of the AL. Moreover they use the entire AL in order to grow towards the target glomerulus. This experiment also revealed, that Psidin is required during the final stages of axon targeting, since *psidin* mutant axons have no problem reaching the AL. In a similar manner, Or42a mutant neurons show a defasciculation phenotype once they reach their target glomerulus. Psidin is only required for the final stages of ORN axon guidance (Figure 7.6). In agreement with these experiments, I did not observe any developmental delay in *psidin* mutant axons (Figure 7.7). Using the pan-neuronal driver *elav-GAL4* to label all neurons revealed that mutant neurons have no problems during their initial outgrowth. Only the cell number is significantly reduced in *psidin*¹ mutants, resulting in a thinner LaN at around 45h APF (Figure 7.7). Since mutant neurons are able to grow in a straight line through the SOG towards the AL, it is likely that microtubule driven growth alone is sufficient to sustain normal axon extension at this time point.

Further along the same line is the finding that Psidin acts cell autonomously (Figure 7.8) in *Drosophila* ORNs. I was able to demonstrate that wild type neurons show no targeting defect in a *psidin* mutant background. This finding indicates that correct ORN targeting largely depends on the growth cone of each individual neuron. Although neurons might reach the AL in a collaborative effort (interclass adhesion between multiple ORN classes), during the final stages each neuron has to respond individually to guidance cues. I therefore want to propose a model in which Psidin acts as a housekeeping protein of the actin machinery for three reasons:

Firstly, I demonstrated that Psidin interacts with a number of actin regulatory proteins such as Tropomyosin, Cofilin and LimK. Although these proteins use different molecular pathways, their very downstream effector molecules are likely to be similar. This implies that Psidin can potentially be activated/deactivated by a large number of upstream molecules.

Secondly, not all ORN types require Psidin equally. Neurons that target dorsolateral and ventromedial glomeruli are strongly affected, whereas axons that innervate central glomeruli of the AL show no or only mild mistargeting phenotypes. This might sound contradictory at first, but makes sense if one takes into consideration that ORN classes face different guidance decisions during their endeavor towards the AL. Upon entry of the peripheral AL, axons projecting dorsolateral or ventromedial are confronted with a “decision point”, which instructs their growth cones to turn into one or the other direction (Jhaveri et al., 2004). Importantly, at this time point growth cones with smaller lamellipodia are simply not able to respond to such cues. Contrary, centrally projection axons are not challenged with such a decision and continue to grow. This would explain the observed mistargeting defects in the *psidin*¹ mutants.

Thirdly, an intact F-actin network *in vivo* is not required for axon extension per se (Sánchez-Soriano et al., 2007). This is in line with the finding that the loss of Psidin doesn't result in a general defect of axon outgrowth. *Psidin* mutant axons have no problems reaching the AL, but rather at a later time point, where axons have to change their growth direction. In axons growing in a more or less straight line, microtubule driven growth can be the main source of axon extension (Alves-Silva et al., 2012). This model can provide an explanation for the differentially affected ORN classes, especially for the unaffected centrally projecting axons (Figure 8.1).

To summarize, as housekeeping protein of the actin machinery, Psidin maintains lamellipodia size and keeps F-actin in a dynamic state. It therefore provides the growth cone with the necessary flexibility to respond to guidance cues. Under normal conditions, the actin cytoskeleton is always in a state of fine-tuned balance of polymerization versus depolymerization. Various proteins can shift that balance in either of the two directions. Guidance cues can trigger local changes in this balance. Accordingly, a growth cone can only respond to guidance cues, if the actin cytoskeleton is dynamic enough to allow F-actin breakdown. Psidin destabilizes F-actin fibers and therefore keeps the cytoskeleton in a responsive state. This study might provide additional evidence for the pivotal role of actin and cytoskeleton dynamics, and showed that neurons with challenging targeting routes are more likely to be affected by malfunctioning or absent guidance cues.

8.3 Psidin is expressed in developing olfactory organs

In-situ hybridization revealed that Psidin is highly expressed in the developing ANT and MP. Further analysis showed that the expression seems to decrease over time, possibly

reaching a minimal level at adult stages. A similar broad expression pattern was shown earlier for Psidin (Brennan et al., 2007), but also for hMdm20 (Starheim et al., 2008). Despite that, both studies also observed that a smaller, but significant fraction of Psidin/hMdm20 is localized in other cell compartments. In addition to that the authors speculated about a second function for Psidin – a function independent of the NatB-complex. During development Psidin would first be required as part of the NatB-complex. Here, Psidin is highly expressed, most likely to recruit proteins to the catalytic subunit of the NatB-complex. During these developmental stages Psidin is highly required, together with the catalytic subunit dNAA20. This is in line with the expression pattern of dNAA20 (Fly Atlas website), which displays a high expression during developmental stages.

Later during ORN targeting Psidin is additionally required as actin regulator. Given its peak expression during the relevant stages of ORN targeting, it is likely that Psidin at this time point is highly required due to the dynamics of migrating neurons. This idea is underlined with the expression pattern observed in primary neurons (Figure 7.20). Here, a significant portion of Psidin localizes to the lamellipodium of the growth cone and also partially co-localizes with the actin cytoskeleton. This argues for Psidin's function as actin binding protein. Later, at adult stages it will only maintain a residual activity as actin regulator and continue to functions as part of the NatB complex.

This is in strong agreement with the hypothesis that Psidin is acting as housekeeping protein and regulator of the actin machinery, with a special requirement during development. Given the broad expression pattern and a peak expression during the development of the olfactory appendages, Psidin seems to be a perfect candidate for such a housekeeping protein.

8.4 Psidin as non-catalytic part of the NatB-complex

As stated above, several studies speculated about a second function of Psidin – similar to its role in yeast. The hypomorphic allele *psidin*^{IG978} provided an excellent tool to investigate this potential second function. In contrast to *psidin*¹ and *psidin*^{55D4} mutants, *psidin*^{IG978} mutants did not show any reduction in the ORN cell number. Although *psidin*^{IG978} selectively affects axon targeting, I was able to demonstrate that the protein Psidin^{IG978} is still capable of binding F-actin *in vitro*. It would be interesting to further investigate the consequences of the E320K mutation on Psidin's actin binding function.

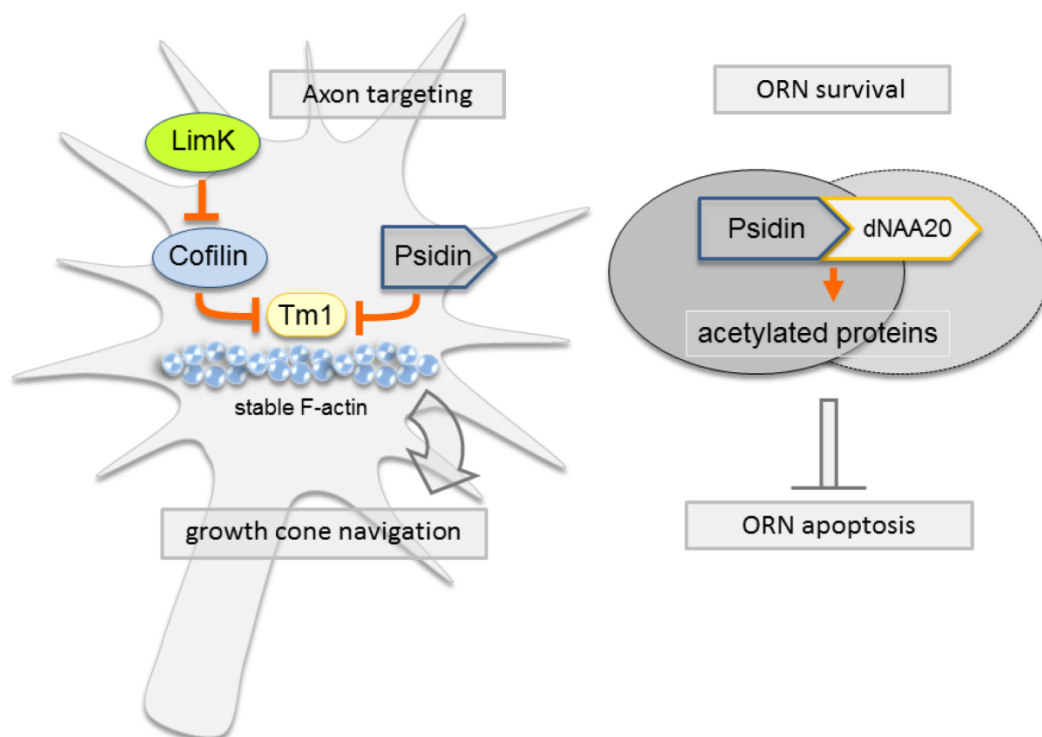


Figure 8.2 | Psidin's two independent functions during ORN targeting and survival

Psidin functions as actin destabilizing protein and antagonist of Tropomyosin. It is differentially required in ORN classes. In its second function Psidin acts as part of the NatB-complex together with the catalytic subunit of this complex dNAA20. As part of the NatB complex Psidin ensures ORN survival during early stages of ORN development.

It might be possible that this mutation interferes with a direct binding of Psidin and Tropomyosin. Although it was shown that Psidin competes with Tropomyosin for F-actin binding (Kim et al., 2011), it still remains unclear whether both proteins interact directly. Furthermore, the regulation of actin dynamics can't be the sole function of Psidin, since the parallel removal of Tropomyosin rescues the targeting defects (normal actin dynamics are restored), but fails to rescue the loss of ORNs. During this work I was able to prove that Psidin indeed has a second function as part of the NatB-complex. Psidin uses the evolutionary well conserved pathway as part of the NatB-complex and interactor of dNAA20 to maintain the neuron number. Since overexpression of the anti-apoptotic protein p35 in *psidin*¹ mutants rescued the cell number, but not the targeting defect, it is likely that a functional NatB-complex is inhibiting apoptosis and thereby ensuring ORN survival (Starheim et al., 2008; Polevoda and Sherman, 2003a). The analysis of the *psidin*^{IG978} allele indicated already that Psidin has two independent functions, since *psidin*^{IG978} mutants showed no significant reduction in ORN cell number. Therefore, the newly established allele *psidin*^{IG978} provided an excellent tool to separate the two Psidin functions. Interestingly, knock-down of dNAA20 in Or42a and Or59c *psidin*^{IG978} mutants resulted in an ORN cell number reduction reminiscent of *psidin*¹ mutant levels. At the same time, the knock-down of dNAA20 didn't affect the targeting phenotype of *psidin* mutants. In addition, the ORN cell number was not further reduced in *psidin*¹ mutants upon knock-down of dNAA20. This argues for an interaction of Psidin and dNAA20 in the same pathway. Unexpectedly, the knock-down of dNAA20 had no effect on the cell number of wild type neurons. Given that two subunits are required for the formation of the NatB-complex, it is reasonable to assume that the removal of one of the subunits is sufficient to block NatB-complex formation. Although, the knock-down efficiency was high (80%) in S2 cells, the resulting reduction of dNAA20 protein

levels was not sufficient to cause a cell number reduction in wild type neurons *in vivo*. Therefore, one explanation could be that the RNAi has a reduced efficiency *in vivo*. However, a more likely explanation is that the *psidin*^{G978} allele provides a sensitized background for the RNAi knock-down. Although the ORN number is not significantly reduced, there is a trend towards a reduction (Figure 7.4). This indicates, that Psidin protein levels in the *psidin*^{G978} background might be slightly reduced and therefore interaction with dNAA20 mildly impaired. At this point the sensitized background could explain why cell numbers are reduced upon RNAi knock-down. In wild type cells, such a reduction of Psidin protein levels is not present. Further substantiating the interaction, I was able to demonstrate the interaction between Psidin and dNAA20 in two different ORN classes (Or59c and Or42a) *in vivo*. In line with this hypothesis, Psidin deletion constructs driven by the GAL4/UAS system in S2 cells also showed reduced expression levels compared to wild type Psidin. This evidence points out that the interaction of dNAA20 and Psidin seems to stabilize the respective protein levels. Similar, Psidin^{S678D} (non-phosphorylatable isoform, no interaction with dNAA20) shows reduced expression in S2 cells compared to Psidin^{S678A} (non-phosphorylatable isoform, normal interaction with dNAA20) (Figure 7.14). A similar observation was reported previously (Ohyama et al., 2011), arguing for some degree of interdependency in the expression level of both proteins.

8.5 Psidin has a minimal interaction domain with dNAA20

At this point it was tempting to investigate a potential interaction domain between Psidin and dNAA20, since there has been no precise prediction of a NatB interaction domain so far. I generated several deletions of the putative NatB interaction domain and found that the complete deletion of this predicted domain abolished the interaction between Psidin

and dNAA20 *in vitro* (Figure 7.14). Although the deletion of smaller parts of the interaction domain (Psidin^{ΔNatB23} and Psidin^{ΔNatB3}) strongly affected the dNAA20 pull-down, deletion of more C-terminal regions had a greater effect on the pull-down. The respective deletion (Psidin^{ΔNatB23}) might simply be bigger than other. On the other hand, N-terminal parts are in close proximity towards a regulatory serine in Psidin (see below). This proximity could provide a regulatory mechanism, where this serine residue is phosphorylated and then blocks the nearby interaction domain. Interestingly, the deletion of parts of the domain around the mutation found in *psidin*^{IG978} had no effect on the interaction. In line with this, Psidin^{IG978} is able to bind dNAA20 *in vitro* to levels comparable to wild type Psidin. This goes hand in hand with the finding that *psidin*^{IG978} mutant displays no ORN cell loss. To this end, experiments showed that the mutation E320K, as well as the region around the residue E320 is dispensable for Psidin's ability to interact with dNAA20. Furthermore, only protein deletions downstream of E320 are able to disrupt the binding.

All together I showed that there is a minimal interaction domain, which allows Psidin to interact with dNAA20. The mutation E320K itself, as well as the protein regions around this residue are dispensable for the interaction. This is supported by the finding that Psidin^{IG978} can interact with dNAA20 *in vitro*, and *psidin*^{IG978} mutants displayed no ORN cell loss *in vivo*.

8.6 Psidin is regulated by the conserved serine 678

Further experiments showed that a conserved serine residue (S678) downstream of the interaction domain is used to regulate the interaction of Psidin and dNAA20. This particular serine was found to be phosphorylated in human Mdm20 (Trost et al., 2009) and

is highly conserved in higher organisms. *In vivo* and *in vitro* experiments illustrated that the phosphorylation of S678 interferes with the binding of Psidin and dNAA20. The phosphomimetic mutant Psidin^{S678D} showed a severe reduction of dNAA20 binding, whereas the non-phosphorylatable form Psidin^{S678A} interacted normally with dNAA20 *in vitro*. Independent of dNAA20 binding, both mutants were able to rescue the targeting phenotype in *psidin*¹ mutants *in vivo*. This strongly suggests that Psidin is required in two modes: non-phosphorylated as part of the NatB-complex and phosphorylation independent as a regulator of actin dynamics in processes like axon targeting or cell migration. Additionally, this conserved residue is located just downstream of the NatB interaction domain providing a reasonable mechanism to control Psidin/dNAA20 interaction. Upon phosphorylation of the serine residue, local steric changes could result in the blockage of the interaction domain, preventing Psidin and dNAA20 to bind. Future experiment may further elucidate, which specific kinase is interacting with Psidin.

8.7 Psidin's function in an evolutionary context

Given the striking difference in conservation of the E320 residue as well as the S678 residue, it was tempting to investigate, how the protein may have evolved from yeast to higher organisms. It is known that the yeast Psidin homologue, Mdm20, is required for proper actin cable formation during cell division (Hermann et al., 1997). Furthermore, it was shown that the defect observed in $\Delta Mdm20$ strains, could be rescued by certain Tropomyosin mutants that mimic N-acetylation (Singer and Shaw, 2003). This implies that the ancestral Psidin in yeast was also involved in cell division, which is reminiscent of the function of *Drosophila* Psidin in ORN survival. In addition, it was shown that Tropomyosin is a direct target of the NatB-complex in yeast, whereas it is unknown whether N-acetylation is

required for *Drosophila* Tropomyosin. Given that the removal of Tropomyosin can rescue the *psidin*¹ targeting phenotype, it seems at least very unlikely.

These observations imply that Mdm20 in yeast might solely be required as part of the NatB-complex. Here, the NatB-complex acetylates Tropomyosin, thereby facilitating actin cable formation. Interestingly, the mutation in *psidin*^{IG978} (E320K) exactly resembles the wild type residue in yeast (K304). The engineered “fly-like” Mdm20 carrying a lysine at position 304, was able to restore the actin cable formation just as wild type yeast Mdm20. This demonstrated that this residue is not important in yeast to ensure a functional NatB-complex. Along the same line is the finding that *psidin*^{IG978} is able to interact with dNAA20 in *Drosophila*.

From an evolutionary point of view, it is possible that Mdm20 and later Psidin acquired the additional function to directly regulate actin dynamics. Evolutionary constraints might have required Psidin to directly influence actin stability rather than the indirect control via N-acetylation of Tropomyosin. This could also explain why Tropomyosin doesn't seem to be a direct target of the NatB-complex anymore. Thinking further along the same line, this model could also explain why the highly conserved serine residue can't be found in yeast. If Psidin acquired that additional function (being an actin binding protein), it might have been necessary to regulate its ability to form the NatB-complex. Given that this serine is highly conserved in any higher organism seems to argue for that necessity (Figure 7.16).

Comparing the characteristics of yeast and neurons, one can find that the cell division of budding yeast is reminiscent of a dividing cell or neuron. Nevertheless, the challenges of axons bridging large distances to find their synaptic partners in the context of an entire organism seems to be more challenging compared to a simple yeast cells. It seems

logical that direct regulation of actin dynamics is required in any neuron that has to extend its axon over large distances.

For further studies it would be interesting to identify direct targets of the NatB-complex in *Drosophila*. It would be especially interesting to see which NatB-dependent mechanisms prevent apoptosis in ORNs. Although there is a consensus target sequence for the NatB-complex (Polevoda and Sherman, 2003b), it has proven difficult to identify single proteins as NatB targets. In yeast alone one can find up to three different Nat-complexes (Polevoda and Sherman, 2003b). Although their consensus target sequences are somewhat different it remains unknown how redundant the different systems are. In addition to that more than 60% of all proteins undergo co- or posttranslational acetylation, a modification that can only be analyzed using mass spectrometry (Polevoda et al., 2003; Singer and Shaw, 2003). It will therefore be difficult to identify a single key target responsible for the cell number phenotype. Another valid possibility is that not a single protein, but rather multiple proteins are responsible for the cell loss. One could easily imagine that during the early steps of development a number of proteins are necessary to maintain ORN cell numbers.

8.8 Concluding remarks

Summarizing the work presented in this thesis, I showed that Psidin is a regulator of neuronal development with key functions during neuronal survival and axon targeting in *Drosophila melanogaster*. Psidin is an actin destabilizing protein in neurons and an antagonist of Tropomyosin. It is required to maintain a dynamic F-actin network in lamellipodia of neurons. Only a dynamic F-actin network enables axon growth cones to

respond properly to guidance cues. In its second function as non-catalytic part of the NatB-complex, Psidin ensures the survival of ORNs during early development. Here, Psidin interacts and binds dNAA20 and forms the NatB-complex. The formation of this complex is regulated by a conserved serine (S678) in the C-terminal region of Psidin. It is only interacting with dNAA20 in its unphosphorylated form. Although phosphorylation has a dramatic impact on NatB-complex formation and ORN survival, ORN targeting seems to be phosphorylation independent. Given that, it is likely that Psidin is part of the actin housekeeping machinery. Further studies of Psidin and its homologues could provide more detailed insights into the mechanisms underlying regeneration and degeneration of the nervous system. They could also provide more detailed knowledge about the integration of guidance cues at the growth cone level and their related neurologic diseases.

9 Acknowledgements

First and foremost I would like to thank Ilona for having me as a student in her lab and giving me this exciting project. I especially would like to thank you for believing in the success of this project and my will to master my daily commute. Without your supervision and feedback this project never would have been successful. Your constant support made me find strength in the hard times and your amazing enthusiasm made me appreciate the good times.

I am grateful to my Doktorvater Rüdiger Klein for his continuous support and helpful scientific feedback. My gratitude goes to all members of my thesis advisory committee for helping me to stay focused throughout this work. Thanks to Takashi Suzuki and Christian Klämbt for your great scientific advice and helpful discussions.

I owe special thanks to all current and previous Kadow lab members. Thank you for creating the best working atmosphere in the world! Never forgotten will be the members of the Klein lab for great technical support and fun in the department – especially for letting me ‘borrow’ reagents.

I also would like to thank all the other people that were involved in the project – without them I never would have finished it: Verena Schilling, Laura Loschek and Christiane Knappmeyer.

Special thanks go to ‘The Office’ for the many scientific and non-scientific discussions we shared: To Juhi for all the discussions about the project and education in Indian culture; to Siju for sharing his post-doctoral wisdom with us; to Lasse for lecturing us on so many topics and to Cristina for bringing fun to the lab-E! Thanks to all of you, I enjoyed coming to work every day. *It was the best of times; it was the worst of times.*

Finally many thanks to Ramona Gerhards, who worked incredible hours as my HiWi and later as a bachelor student. I’m grateful that we worked together on this project.

Ein ganz besonderer Dank geht an Julia, die einem selbst an schweren Tagen zeigte, dass es immer irgendwie weitergeht und immer ein offenes Ohr hatte. Ein großes

Dankeschön auch an all die Menschen, die einem immer wieder in Erinnerung rufen, dass es ein Leben außerhalb des Labors gibt.

Großer Dank gilt meiner Familie, die mich die vielen Jahre hindurch bedingungslos unterstützt hat und immer da ist, wenn man sie braucht. Vielen Dank, dass ihr nie den Glauben an mich verloren habt.

ንክብርቱ ባዓልቲ በይተይ። ንኩሉ ኣብ ዝሓለፈ ጊዜይ ዘይሕለል ተስፋን ሓይልን ዝሃብኪን ብጣዕሚ የመስግነኪ። ኣብ ቀጻሊ ሂወትና፡ ዓጻፋ ክኸፍለኪ ባዓል ሙሉእ ተስፋ ኢየ። ብልቢ ድማ የፍቅረኪ። የቐንዖለይ!

10 Literature

- Abuin, L., Bargeton, B., Ulbrich, M. H., Isacoff, E. Y., Kellenberger, S., and Benton, R. (2011). Functional architecture of olfactory ionotropic glutamate receptors. *Neuron* 69, 44–60. Available at: <http://www.pubmedcentral.nih.gov/articlerender.fcgi?artid=3050028&tool=pmcentrez&rendertype=abstract> [Accessed March 26, 2012].
- Agarwal, N., Adhikari, a S., Iyer, S. V., Hekmatdoost, K., Welch, D. R., and Iwakuma, T. (2012). MTBP suppresses cell migration and filopodia formation by inhibiting ACTN4. *Oncogene*, 1–9. Available at: <http://www.ncbi.nlm.nih.gov/pubmed/22370640> [Accessed March 9, 2012].
- Aizawa, H., Wakatsuki, S., Ishii, a, Moriyama, K., Sasaki, Y., Ohashi, K., Sekine-Aizawa, Y., Sehara-Fujisawa, a, Mizuno, K., Goshima, Y., et al. (2001). Phosphorylation of cofilin by LIM-kinase is necessary for semaphorin 3A-induced growth cone collapse. *Nature neuroscience* 4, 367–373. Available at: <http://www.ncbi.nlm.nih.gov/pubmed/11276226>.
- Alves-Silva, J., Sánchez-Soriano, N., Beaven, R., Klein, M., Parkin, J., Millard, T. H., Bellen, H. J., Venken, K. J. T., Ballestrem, C., Kammerer, R. A., et al. (2012). Spectraplakins Promote Microtubule-Mediated Axonal Growth by Functioning As Structural Microtubule-Associated Proteins and EB1-Dependent +TIPs (Tip Interacting Proteins). *The Journal of neuroscience : the official journal of the Society for Neuroscience* 32, 9143–9158. Available at: <http://www.ncbi.nlm.nih.gov/pubmed/22764224> [Accessed July 6, 2012].
- Ang, L.-H., Chen, W., Yao, Y., Ozawa, R., Tao, E., Yonekura, J., Uemura, T., Keshishian, H., and Hing, H. (2006). Lim kinase regulates the development of olfactory and neuromuscular synapses. *Developmental biology* 293, 178–190. Available at: <http://www.ncbi.nlm.nih.gov/pubmed/16529736> [Accessed May 24, 2011].
- Ang, L.-H., Kim, J., Stepensky, V., and Huey, H. (2003). Dock and Pak regulate olfactory axon pathfinding in *Drosophila*. *Development* 130, 1307–1316. Available at: <http://dev.biologists.org/cgi/doi/10.1242/dev.00356> [Accessed April 5, 2012].
- Bai, L., Goldman, A. L., and Carlson, J. R. (2009). Positive and negative regulation of odor receptor gene choice in *Drosophila* by *acj6*. *The Journal of neuroscience : the official journal of the Society for Neuroscience* 29, 12940–12947. Available at: <http://www.ncbi.nlm.nih.gov/pubmed/19828808>.

- Bartles, J. R. (2000). Parallel actin bundles and their multiple actin-bundling proteins. *Current opinion in cell biology* 12, 72–78. Available at: <http://www.pubmedcentral.nih.gov/articlerender.fcgi?artid=2853926&tool=pmcentrez&rendertype=abstract>.
- Bashaw, G. J. (2007). Semaphorin directs axon traffic in the fly olfactory system. *Neuron* 53, 157–159. Available at: <http://www.ncbi.nlm.nih.gov/pubmed/17224397>.
- Benton, R., Sachse, S., Michnick, S. W., and Vosshall, L. B. (2006). Atypical membrane topology and heteromeric function of *Drosophila* odorant receptors in vivo. *PLoS biology* 4, e20. Available at: <http://www.pubmedcentral.nih.gov/articlerender.fcgi?artid=1334387&tool=pmcentrez&rendertype=abstract> [Accessed March 24, 2012].
- Benton, R., Vannice, K. S., Gomez-Diaz, C., and Vosshall, L. B. (2009). Variant ionotropic glutamate receptors as chemosensory receptors in *Drosophila*. *Cell* 136, 149–162. Available at: <http://www.pubmedcentral.nih.gov/articlerender.fcgi?artid=2709536&tool=pmcentrez&rendertype=abstract> [Accessed March 12, 2012].
- Berger, J., Suzuki, T., Senti, K. A., Stubbs, J., Schaffner, G., and Dickson, B. J. (2001). Genetic mapping with SNP markers in *Drosophila*. *Nat Genet* 29, 475–481. Available at: http://www.ncbi.nlm.nih.gov/entrez/query.fcgi?cmd=Retrieve&db=PubMed&dopt=Citation&list_uids=11726933.
- Brand, A. H., and Perrimon, N. (1993). Targeted gene expression as a means of altering cell fates and generating dominant phenotypes. *Development* 119, 401–415.
- Brennan, C. a, Delaney, J. R., Schneider, D. S., and Anderson, K. V. (2007). Psidin is required in *Drosophila* blood cells for both phagocytic degradation and immune activation of the fat body. *Current biology : CB* 17, 67–72. Available at: <http://www.ncbi.nlm.nih.gov/pubmed/17208189> [Accessed July 29, 2011].
- Brown, M. E., and Bridgman, P. C. (2004). Myosin function in nervous and sensory systems. *Journal of neurobiology* 58, 118–130. Available at: <http://www.ncbi.nlm.nih.gov/pubmed/14598375> [Accessed May 12, 2012].
- Bugyi, B., and Carlier, M.-F. (2010). Control of actin filament treadmilling in cell motility. *Annual review of biophysics* 39, 449–470. Available at: <http://www.ncbi.nlm.nih.gov/pubmed/20192778> [Accessed March 1, 2012].
- Burkhard, P., Stetefeld, J., and Strelkov, S. V. (2001). Coiled coils: a highly versatile protein folding motif. *Trends in cell biology* 11, 82–88. Available at: <http://www.ncbi.nlm.nih.gov/pubmed/11166216>.

- Buzan, J. M., and Frieden, C. (1996). Yeast actin: polymerization kinetic studies of wild type and a poorly polymerizing mutant. *Proceedings of the National Academy of Sciences of the United States of America* 93, 91–95. Available at: <http://www.pubmedcentral.nih.gov/articlerender.fcgi?artid=40184&tool=pmcentrez&rendertype=abstract>.
- Cayirlioglu, P., Kadow, I. G., Zhan, X., Okamura, K., Suh, G. S. B., Gunning, D., Lai, E. C., and Zipursky, S. L. (2008). Hybrid neurons in a microRNA mutant are putative evolutionary intermediates in insect CO₂ sensory systems. *Science (New York, N.Y.)* 319, 1256–1260. Available at: <http://www.pubmedcentral.nih.gov/articlerender.fcgi?artid=2714168&tool=pmcentrez&rendertype=abstract> [Accessed September 28, 2011].
- Chacón, M. R., and Fazzari, P. (2011). FAK: Dynamic integration of guidance signals at the growth cone. *Cell Adhesion & Migration* 5, 52–55. Available at: <http://www.landesbioscience.com/journals/celladhesion/article/13681/> [Accessed March 10, 2012].
- Chauvet, S., and Rougon, G. (2009). The growth cone: an integrator of unique cues into refined axon guidance. *F1000 biology reports* 1, 27. Available at: <http://www.pubmedcentral.nih.gov/articlerender.fcgi?artid=2924699&tool=pmcentrez&rendertype=abstract> [Accessed April 16, 2012].
- Chou, Y.-H., Spletter, M. L., Yaksi, E., Leong, J. C. S., Wilson, R. I., and Luo, L. (2010). Diversity and wiring variability of olfactory local interneurons in the *Drosophila* antennal lobe. *Nature neuroscience* 13, 439–449. Available at: <http://www.pubmedcentral.nih.gov/articlerender.fcgi?artid=2847188&tool=pmcentrez&rendertype=abstract> [Accessed March 19, 2012].
- Cohan, C. S., Welnhof, E. a, Zhao, L., Matsumura, F., and Yamashiro, S. (2001). Role of the actin bundling protein fascin in growth cone morphogenesis: localization in filopodia and lamellipodia. *Cell motility and the cytoskeleton* 48, 109–120. Available at: <http://www.ncbi.nlm.nih.gov/pubmed/11169763>.
- Cooper, J. A. (2002). Actin Dynamics : Tropomyosin Provides Stability. *Curr Biol* 12, 523–525.
- Cooper, J. A., Buhle, E. L., Walker, S. B., Tsong, T. Y., and Pollard, T. D. (1983). Kinetic evidence for a monomer activation step in actin polymerization. *Biochemistry* 22, 2193–2202. Available at: <http://www.ncbi.nlm.nih.gov/pubmed/6860660>.
- Cooper, J. a, Wear, M. a, and Weaver, a M. (2001). Arp2/3 complex: advances on the inner workings of a molecular machine. *Cell* 107, 703–705. Available at: <http://www.ncbi.nlm.nih.gov/pubmed/11747805>.
- Couto, A., Alenius, M., and Dickson, B. J. (2005). Molecular, anatomical, and functional organization of the *Drosophila* olfactory system. *Curr Biol* 15, 1535–1547. Available at: http://www.ncbi.nlm.nih.gov/entrez/query.fcgi?cmd=Retrieve&db=PubMed&dopt=Citation&list_uids=16139208.

- Dent, E. W., Gupton, S. L., and Frank B., G. (2011). The Growth Cone Cytoskeleton in Axon Outgrowth and Guidance. *Cold Spring Harbor perspectives in biology*.
- Diefenbach, T. J. (2002). Myosin 1c and myosin IIB serve opposing roles in lamellipodial dynamics of the neuronal growth cone. *The Journal of Cell Biology* 158, 1207–1217. Available at: <http://www.jcb.org/cgi/doi/10.1083/jcb.200202028> [Accessed April 19, 2012].
- Dobritsa, A. A., Naters, W. V. D. G. V., Warr, C. G., Steinbrecht, R. A., Carlson, J. R., Haven, N., and Vic, C. (2003). Integrating the Molecular and Cellular Basis of Odor Coding in the *Drosophila* Antenna. *Neuron* 37, 827–841.
- Dübendorfer, and Eichenberger-Glinz (1980). Development and interactions in the ectoderm of *Drosophila melanogaster*. *Development*.
- D'Andrea, L. (2003). TPR proteins: the versatile helix. *Trends in Biochemical Sciences* 28, 655–662. Available at: <http://linkinghub.elsevier.com/retrieve/pii/S0968000403002731> [Accessed March 9, 2012].
- Endo, K., Aoki, T., Yoda, Y., Kimura, K., and Hama, C. (2007). Notch signal organizes the *Drosophila* olfactory circuitry by diversifying the sensory neuronal lineages. *Nature neuroscience* 10, 153–160. Available at: <http://www.ncbi.nlm.nih.gov/pubmed/17220884>.
- Fass, J., Gehler, S., Sarmiere, P., Letourneau, P., and Bamberg, J. R. (2004). Special Review Based on a Presentation made at the 16th International Congress of the IFAA Regulating filopodial dynamics through actin-depolymerizing factor / cofilin. 173–183.
- Firestein, S. (2001). How the olfactory system makes sense of scents. *Nature* 413, 211–218. Available at: <http://www.ncbi.nlm.nih.gov/pubmed/11557990>.
- Footer, M. J., Kerssemakers, J. W. J., Theriot, J. a, and Dogterom, M. (2007). Direct measurement of force generation by actin filament polymerization using an optical trap. *Proceedings of the National Academy of Sciences of the United States of America* 104, 2181–2186. Available at: <http://www.pubmedcentral.nih.gov/articlerender.fcgi?artid=1892916&tool=pmcentrez&rendertype=abstract>.
- Forscher, P., and Smith, S. J. (1988). Actions of cytochalasins on the organization of actin filaments and microtubules in a neuronal growth cone. *The Journal of cell biology* 107, 1505–1516. Available at: <http://www.pubmedcentral.nih.gov/articlerender.fcgi?artid=2115246&tool=pmcentrez&rendertype=abstract>.

- Fujisawa, H., and Kitsukawat, T. (1998). Receptors for collapsin/semaphorins. *Curr Opin Neurobiol*, 587–592.
- Gallo, G., and Letourneau, P. C. (2004). Regulation of growth cone actin filaments by guidance cues. *Journal of neurobiology* 58, 92–102. Available at: <http://www.ncbi.nlm.nih.gov/pubmed/14598373> [Accessed April 1, 2012].
- Gao, Q., Yuan, B., and Chess, a (2000). Convergent projections of *Drosophila* olfactory neurons to specific glomeruli in the antennal lobe. *Nature neuroscience* 3, 780–785. Available at: <http://www.ncbi.nlm.nih.gov/pubmed/10903570>.
- Gehler, S., Shaw, A. E., Sarmiere, P. D., Bamberg, J. R., and Letourneau, P. C. (2004). Brain-derived neurotrophic factor regulation of retinal growth cone filopodial dynamics is mediated through actin depolymerizing factor/cofilin. *The Journal of neuroscience : the official journal of the Society for Neuroscience* 24, 10741–10749. Available at: <http://www.ncbi.nlm.nih.gov/pubmed/15564592> [Accessed March 2, 2012].
- Goldberg, D. J., and Burmeister, D. W. (1986). Stages in Axon Formation : Observations of Growth of *Aplysia* Axons in Culture Using Video-enhanced Contrast-Differential Interference Contrast Microscopy. *The Journal of Cell Biology* 103, 1921–1931.
- Gomez, T. M., Robles, E., Poo, M., and Spitzer, N. C. (2001). Filopodial calcium transients promote substrate-dependent growth cone turning. *Science* 291, 1983–1987. Available at: <http://www.ncbi.nlm.nih.gov/pubmed/11239161>.
- Gonçalves-Pimentel, C., Gombos, R., Mihály, J., Sánchez-Soriano, N., and Prokop, A. (2011). Dissecting regulatory networks of filopodia formation in a *Drosophila* growth cone model. *PloS one* 6, e18340. Available at: <http://www.pubmedcentral.nih.gov/articlerender.fcgi?artid=3065487&tool=pmcentrez&rendertype=abstract> [Accessed March 15, 2012].
- Hall, A., and Lalli, G. (2010). Rho and Ras GTPases in axon growth, guidance, and branching. *Cold Spring Harbor perspectives in biology* 2, a001818. Available at: <http://www.pubmedcentral.nih.gov/articlerender.fcgi?artid=2828272&tool=pmcentrez&rendertype=abstract> [Accessed March 1, 2012].
- Hallem, E. A., Ho, M. G., Carlson, J. R., and Haven, N. (2004). The Molecular Basis of Odor Coding in the *Drosophila* Antenna. *Cell* 117, 965–979.
- Hansson, B. S., and Anton, S. (2000). Function and morphology of the antennal lobe: new developments. *Annual review of entomology* 45, 203–231. Available at: <http://www.ncbi.nlm.nih.gov/pubmed/10761576>.
- Hermann, G. J., King, E. J., and Shaw, J. M. (1997). The Yeast Gene, MDM20, Is Necessary for Mitochondrial Inheritance and Organization of the Actin Cytoskeleton. *The Journal of Cell Biology* 137, 141–153.

- Hirokawa, N., Noda, Y., and Okada, Y. (1998). Kinesin and dynein superfamily proteins in organelle transport and cell division. *Curr Opin cell biology*.
- Hirokawa, N., and Takemura, R. (2004). Kinesin superfamily proteins and their various functions and dynamics. *Experimental cell research* 301, 50–59. Available at: <http://www.ncbi.nlm.nih.gov/pubmed/15501445> [Accessed March 10, 2012].
- Holmes, K. C., Pai, E. F., Suck, D., Mannherz, H. G., and Kabsch, W. (1990). Atomic structure of the actin:DNase I complex. *Nature* 347.
- Hong, W., Mosca, T. J., and Luo, L. (2012). Teneurins instruct synaptic partner matching in an olfactory map. *Nature* 484, 201–207. Available at: <http://www.nature.com/doi/10.1038/nature10926> [Accessed March 19, 2012].
- Hu, P. (2004). A role for γ -actin in RNA polymerase III transcription. *Genes & Development* 18, 3010–3015. Available at: <http://www.genesdev.org/cgi/doi/10.1101/gad.1250804> [Accessed May 3, 2012].
- Huber, F., Käs, J., and Stuhrmann, B. (2008). Growing actin networks form lamellipodium and lamellum by self-assembly. *Biophysical journal* 95, 5508–5523. Available at: <http://www.pubmedcentral.nih.gov/articlerender.fcgi?artid=2599839&tool=pmcentrez&rendertype=abstract> [Accessed June 11, 2011].
- Hummel, T., Vasconcelos, M. L., Clemens, J. C., Fishilevich, Y., Vosshall, L. B., and Zipursky, S. L. (2003). Axonal targeting of olfactory receptor neurons in *Drosophila* is controlled by Dscam. *Neuron* 37, 221–231. Available at: <http://www.ncbi.nlm.nih.gov/pubmed/12546818>.
- Hummel, T., and Zipursky, S. L. (2004). Afferent induction of olfactory glomeruli requires N-cadherin. *Neuron* 42, 77–88. Available at: http://www.ncbi.nlm.nih.gov/entrez/query.fcgi?cmd=Retrieve&db=PubMed&dopt=Citation&list_uids=15066266.
- Hung, R. J., Yazdani, U., Yoon, J., Wu, H., Yang, T., Gupta, N., Huang, Z., van Berkel, W. J., and Terman, J. R. (2010). Mical links semaphorins to F-actin disassembly. *Nature* 463, 823–827. Available at: http://www.ncbi.nlm.nih.gov/entrez/query.fcgi?cmd=Retrieve&db=PubMed&dopt=Citation&list_uids=20148037.
- Hung, R.-J., Pak, C. W., and Terman, J. R. (2011). Direct redox regulation of F-actin assembly and disassembly by Mical. *Science (New York, N.Y.)* 334, 1710–1713. Available at: <http://www.ncbi.nlm.nih.gov/pubmed/22116028> [Accessed March 9, 2012].
- Jefferis, G. S., Marin, E. C., Watts, R. J., and Liquid, L. (2002). Development of neuronal connectivity in *Drosophila* antennal lobes and mushroom bodies. *Development*, 80–86.

- Jefferis, G. S. X. E., and Hummel, T. (2006). Wiring specificity in the olfactory system. *Seminars in cell & developmental biology* 17, 50–65. Available at: <http://www.ncbi.nlm.nih.gov/pubmed/16439169> [Accessed March 19, 2012].
- Jefferis, G. S. X. E., Marin, E. C., Stocker, R. F., and Luo, L. (2001). Target neuron prespecification in the olfactory map of *Drosophila*. *Nature* 414, 204–208.
- Jefferis, G. S. X. E., Vyas, R. M., Berdnik, D., Ramaekers, A., Stocker, R. F., Tanaka, N. K., Ito, K., and Luo, L. (2004). Developmental origin of wiring specificity in the olfactory system of *Drosophila*. *Development (Cambridge, England)* 131, 117–130. Available at: <http://www.ncbi.nlm.nih.gov/pubmed/14645123> [Accessed March 1, 2012].
- Jhaveri, D., and Rodrigues, V. (2002). Sensory neurons of the Atonal lineage pioneer the formation of glomeruli within the adult *Drosophila* olfactory lobe. *Development (Cambridge, England)* 129, 1251–1260. Available at: <http://www.ncbi.nlm.nih.gov/pubmed/11874920>.
- Jhaveri, D., Saharan, S., Sen, A., and Rodrigues, V. (2004). Positioning sensory terminals in the olfactory lobe of *Drosophila* by Robo signaling. *Development (Cambridge, England)* 131, 1903–1912. Available at: <http://www.ncbi.nlm.nih.gov/pubmed/15056612>.
- Kasai, M. K. I., Asakura, S. H. O., and Oosawa, F. (1962). The cooperative nature of G-F tranformation of actin. *Biochimica et Biophysica Acta* 57.
- Katada, S., Hirokawa, T., Oka, Y., Suwa, M., and Touhara, K. (2005). Structural basis for a broad but selective ligand spectrum of a mouse olfactory receptor: mapping the odorant-binding site. *The Journal of neuroscience : the official journal of the Society for Neuroscience* 25, 1806–1815. Available at: <http://www.ncbi.nlm.nih.gov/pubmed/15716417> [Accessed March 2, 2012].
- Kim, J. H., Cho, A., Yin, H., Schafer, D. A., Mouneimne, G., Simpson, K. J., Nguyen, K.-V., Brugge, J. S., and Montell, D. J. (2011). Psidin, a conserved protein that regulates protrusion dynamics and cell migration. *Genes & development* 25, 730–741. Available at: <http://genesdev.cshlp.org/cgi/content/abstract/25/7/730> [Accessed April 6, 2011].
- Koestler, S. a, Rottner, K., Lai, F., Block, J., Vinzenz, M., and Small, J. V. (2009a). F- and G-actin concentrations in lamellipodia of moving cells. *PloS one* 4, e4810. Available at: <http://www.pubmedcentral.nih.gov/articlerender.fcgi?artid=2652108&tool=pmcentrez&rendertype=abstract> [Accessed March 5, 2012].
- Koestler, S. a, Rottner, K., Lai, F., Block, J., Vinzenz, M., and Small, J. V. (2009b). F- and G-actin concentrations in lamellipodia of moving cells. *PloS one* 4, e4810. Available at: <http://www.pubmedcentral.nih.gov/articlerender.fcgi?artid=2652108&tool=pmcentrez&rendertype=abstract> [Accessed March 5, 2012].

- Komiyama, T., Carlson, J. R., and Luo, L. (2004a). Olfactory receptor neuron axon targeting: intrinsic transcriptional control and hierarchical interactions. *Nat Neurosci* 7, 819–825. Available at: <http://www.ncbi.nlm.nih.gov/pubmed/15247920> [Accessed March 19, 2012].
- Komiyama, T., Carlson, J. R., and Luo, L. (2004b). Olfactory receptor neuron axon targeting: intrinsic transcriptional control and hierarchical interactions. *Nat Neurosci* 7, 819–825. Available at: http://www.ncbi.nlm.nih.gov/entrez/query.fcgi?cmd=Retrieve&db=PubMed&dopt=Citation&list_uids=15247920.
- Komiyama, T., and Luo, L. (2006). Development of wiring specificity in the olfactory system. *Current opinion in neurobiology* 16, 67–73. Available at: <http://www.ncbi.nlm.nih.gov/pubmed/16377177>.
- Larsson, M. C., Domingos, A. I., Jones, W. D., Chiappe, M. E., Amrein, H., and Vosshall, L. B. (2004). Or83b Encodes a Broadly Expressed Odorant Receptor Essential for Drosophila Olfaction. *Neuron* 43, 703–714.
- Lattemann, M., Zierau, A., Schulte, C., Seidl, S., Kuhlmann, B., and Hummel, T. (2007). Semaphorin-1a controls receptor neuron-specific axonal convergence in the primary olfactory center of Drosophila. *Neuron* 53, 169–184. Available at: http://www.ncbi.nlm.nih.gov/entrez/query.fcgi?cmd=Retrieve&db=PubMed&dopt=Citation&list_uids=17224401.
- Lee, T., and Luo, L. (1999). Mosaic Analysis with a Repressible Neurotechnique Cell Marker for Studies of Gene Function in Neuronal Morphogenesis. *Neuron* 22, 451–461.
- Lieber, T., Kidd, S., and Struhl, G. (2011). DSL-Notch signaling in the Drosophila brain in response to olfactory stimulation. *Neuron* 69, 468–481. Available at: <http://www.pubmedcentral.nih.gov/articlerender.fcgi?artid=3216490&tool=pmcentrez&rendertype=abstract> [Accessed March 7, 2012].
- Lin, C. H., Espreafico, E. M., Mooseker, M. S., and Forscher, P. (1997). Myosin drives retrograde F-actin flow in neuronal growth cones. *The Biological bulletin* 192, 183–185. Available at: <http://www.ncbi.nlm.nih.gov/pubmed/9057289>.
- Lin, S., Lai, S.-L., Yu, H.-H., Chihara, T., Luo, L., and Lee, T. (2010). Lineage-specific effects of Notch/Numb signaling in post-embryonic development of the Drosophila brain. *Development (Cambridge, England)* 137, 43–51. Available at: <http://www.pubmedcentral.nih.gov/articlerender.fcgi?artid=2796933&tool=pmcentrez&rendertype=abstract> [Accessed March 19, 2012].
- Lowery, L. A., and Van Vactor, D. (2009). The trip of the tip: understanding the growth cone machinery. *Nature reviews. Molecular cell biology* 10, 332–343. Available at: <http://www.ncbi.nlm.nih.gov/pubmed/19373241>.

- Lucanic, M., and Cheng, H.-J. (2008). A RAC/CDC-42-independent GIT/PIX/PAK signaling pathway mediates cell migration in *C. elegans*. *PLoS genetics* 4, e1000269. Available at: <http://www.pubmedcentral.nih.gov/articlerender.fcgi?artid=2581894&tool=pmcentrez&rendertype=abstract> [Accessed July 10, 2012].
- Maciver, S. K., Pope, B. J., Whytock, S., and Weeds, a G. (1998). The effect of two actin depolymerizing factors (ADF/cofilins) on actin filament turnover: pH sensitivity of F-actin binding by human ADF, but not of *Acanthamoeba* actophorin. *European journal of biochemistry / FEBS* 256, 388–397. Available at: <http://www.ncbi.nlm.nih.gov/pubmed/9760179>.
- Mallavarapu, a, and Mitchison, T. (1999). Regulated actin cytoskeleton assembly at filopodium tips controls their extension and retraction. *The Journal of cell biology* 146, 1097–1106. Available at: <http://www.pubmedcentral.nih.gov/articlerender.fcgi?artid=2169471&tool=pmcentrez&rendertype=abstract>.
- Malnic, B., Hirono, J., Sato, T., and Buck, L. B. (1999). Combinatorial receptor codes for odors. *Cell* 96, 713–723. Available at: <http://www.ncbi.nlm.nih.gov/pubmed/10089886>.
- Marsick, B. M., Flynn, K. C., Santiago-Medina, M., Bamburg, J. R., and Letourneau, P. C. (2010). Activation of ADF/cofilin mediates attractive growth cone turning toward nerve growth factor and netrin-1. *Developmental neurobiology* 70, 565–588. Available at: <http://www.pubmedcentral.nih.gov/articlerender.fcgi?artid=2908028&tool=pmcentrez&rendertype=abstract> [Accessed May 30, 2012].
- Matusek, T., Gombos, R., Szécsényi, A., Sánchez-Soriano, N., Czibula, A., Pataki, C., Gedai, A., Prokop, A., Raskó, I., and Mihály, J. (2008). Formin proteins of the DAAM subfamily play a role during axon growth. *The Journal of neuroscience : the official journal of the Society for Neuroscience* 28, 13310–13319. Available at: <http://www.ncbi.nlm.nih.gov/pubmed/19052223> [Accessed March 15, 2012].
- Medalia, O., Beck, M., Ecke, M., Weber, I., Neujahr, R., Baumeister, W., and Gerisch, G. (2007). Organization of Actin Networks in Intact Filopodia. *Current Biology* 17, 79–84. Available at: <http://linkinghub.elsevier.com/retrieve/pii/S0960982206025012> [Accessed May 7, 2012].
- Moriyama, K., Iida, K., and Yahara, I. (1996). Phosphorylation of Ser-3 of cofilin regulates its essential function on actin. *Genes to cells : devoted to molecular & cellular mechanisms* 1, 73–86. Available at: <http://www.ncbi.nlm.nih.gov/pubmed/9078368>.
- Mullins, R. D., Heuser, J. a, and Pollard, T. D. (1998). The interaction of Arp2/3 complex with actin: nucleation, high affinity pointed end capping, and formation of branching networks of filaments. *Proceedings of the National Academy of Sciences of the United States of America* 95, 6181–6186. Available at: <http://www.pubmedcentral.nih.gov/articlerender.fcgi?artid=27619&tool=pmcentrez&rendertype=abstract>.

- Muqit, M. M. K., and Feany, M. B. (2002). Modelling neurodegenerative diseases in. *Nature reviews. Neuroscience* 3.
- Murray, M. J., and Whittington, P. M. (1999). Effects of roundabout on growth cone dynamics, filopodial length, and growth cone morphology at the midline and throughout the neuropile. *The Journal of neuroscience : the official journal of the Society for Neuroscience* 19, 7901–7912. Available at: <http://www.ncbi.nlm.nih.gov/pubmed/10479692>.
- Newsome, T. P., Åsling, B., and Dickson, B. J. (2000). Analysis of *Drosophila* photoreceptor axon guidance in eye-specific mosaics. *Development* 860, 851–860.
- Ng, J., and Luo, L. (2004). Rho GTPases regulate axon growth through convergent and divergent signaling pathways. *Neuron* 44, 779–793. Available at: <http://www.ncbi.nlm.nih.gov/pubmed/15572110>.
- Ng, J., Nardine, T., Harms, M., Tzu, J., Goldstein, A., Sun, Y., Dietzl, G., Dickson, B. J., and Luo, L. (2002a). Rac GTPases control axon growth, guidance and branching. *Nature* 416, 442–447. Available at: <http://www.ncbi.nlm.nih.gov/pubmed/11919635>.
- Ng, M., Roorda, R. D., Lima, S. Q., Zemelman, B. V., Morcillo, P., and Miesenböck, G. (2002b). Transmission of olfactory information between three populations of neurons in the antennal lobe of the fly. *Neuron* 36, 463–474. Available at: <http://www.ncbi.nlm.nih.gov/pubmed/12408848>.
- Ohashi, K., Hosoya, T., Takahashi, K., Hing, H., and Mizuno, K. (2000). A *Drosophila* homolog of LIM-kinase phosphorylates cofilin and induces actin cytoskeletal reorganization. *Biochemical and biophysical research communications* 276, 1178–1185. Available at: <http://www.ncbi.nlm.nih.gov/pubmed/11027607> [Accessed August 9, 2011].
- Ohyama, K., Yasuda, K., Onga, K., Kakizuka, A., and Mori, N. (2011). Spatio-temporal expression pattern of the NatB complex, Nat5/Mdm20 in the developing mouse brain: Implications for co-operative versus non-co-operative actions of Mdm20 and Nat5. *Gene expression patterns : GEP*. Available at: <http://www.ncbi.nlm.nih.gov/pubmed/22101279> [Accessed November 28, 2011].
- Oland, L. A., Biebelhausen, J. P., and Tolbert, L. P. (2008). Glial investment of the adult and developing antennal lobe of *Drosophila*. *J Comp Neurol* 509, 526–550. Available at: http://www.ncbi.nlm.nih.gov/entrez/query.fcgi?cmd=Retrieve&db=PubMed&dopt=Citation&list_uids=18537134.
- Piper, M., Anderson, R., Dwivedy, A., Weinl, C., van Horck, F., Leung, K. M., Cogill, E., and Holt, C. (2006). Signaling mechanisms underlying Slit2-induced collapse of *Xenopus* retinal growth cones. *Neuron* 49, 215–228. Available at: <http://www.ncbi.nlm.nih.gov/pubmed/16423696>.

- Polevoda, B., Cardillo, T. S., Doyle, T. C., Bedi, G. S., and Sherman, F. (2003). Nat3p and Mdm20p are required for function of yeast NatB Nalpha-terminal acetyltransferase and of actin and tropomyosin. *The Journal of biological chemistry* 278, 30686–30697. Available at: <http://www.ncbi.nlm.nih.gov/pubmed/12783868> [Accessed January 4, 2011].
- Polevoda, B., and Sherman, F. (2003a). Composition and function of the eukaryotic N-terminal acetyltransferase subunits. *Biochemical and Biophysical Research Communications* 308, 1–11. Available at: <http://linkinghub.elsevier.com/retrieve/pii/S0006291X03013160> [Accessed August 4, 2010].
- Polevoda, B., and Sherman, F. (2003b). N-terminal acetyltransferases and sequence requirements for N-terminal acetylation of eukaryotic proteins. *J Mol Biol* 325, 595–622. Available at: http://www.ncbi.nlm.nih.gov/entrez/query.fcgi?cmd=Retrieve&db=PubMed&dopt=Citation&list_uids=12507466.
- Pollard, T. D. (1986). Rate constants for the reactions of ATP- and ADP-actin with the ends of actin filaments. *The Journal of cell biology* 103, 2747–2754. Available at: <http://www.pubmedcentral.nih.gov/articlerender.fcgi?artid=2114620&tool=pmcentrez&rendertype=abstract>.
- Pollard, T. D., Blanchoin, L., and Mullins, R. D. (2000). Molecular mechanisms controlling actin filament dynamics in non muscle cells. *Annual review of biophysics*.
- Pollard, T. D., and Weeds, a G. (1984). The rate constant for ATP hydrolysis by polymerized actin. *FEBS letters* 170, 94–98. Available at: <http://www.ncbi.nlm.nih.gov/pubmed/6427006>.
- Rose, D., and Chiba, a (1999). A single growth cone is capable of integrating simultaneously presented and functionally distinct molecular cues during target recognition. *The Journal of neuroscience : the official journal of the Society for Neuroscience* 19, 4899–4906. Available at: <http://www.ncbi.nlm.nih.gov/pubmed/10366624>.
- Sabo, S. L., and McAllister, a K. (2003). Mobility and cycling of synaptic protein-containing vesicles in axonal growth cone filopodia. *Nature neuroscience* 6, 1264–1269. Available at: <http://www.ncbi.nlm.nih.gov/pubmed/14608359> [Accessed April 27, 2012].
- Sahin, M., Greer, P. L., Lin, M. Z., Poucher, H., Eberhart, J., Schmidt, S., Wright, T. M., Shamah, S. M., O'connell, S., Cowan, C. W., et al. (2005). Eph-dependent tyrosine phosphorylation of ephexin1 modulates growth cone collapse. *Neuron* 46, 191–204. Available at: <http://www.ncbi.nlm.nih.gov/pubmed/15848799> [Accessed March 15, 2012].
- Sarmiere, P. D., and Bamburg, J. R. (2004). Regulation of the neuronal actin cytoskeleton by ADF/cofilin. *Journal of neurobiology* 58, 103–117. Available at: <http://www.ncbi.nlm.nih.gov/pubmed/14598374>.

- Sato, K., Pellegrino, M., Nakagawa, T., Nakagawa, T., Vosshall, L. B., and Touhara, K. (2008). Insect olfactory receptors are heteromeric ligand-gated ion channels. *Nature* 452, 1002–1006. Available at: <http://www.ncbi.nlm.nih.gov/pubmed/18408712> [Accessed March 9, 2012].
- Schaefer, A. W., Kabir, N., and Forscher, P. (2002). Filopodia and actin arcs guide the assembly and transport of two populations of microtubules with unique dynamic parameters in neuronal growth cones. *The Journal of cell biology* 158, 139–152. Available at: <http://www.pubmedcentral.nih.gov/articlerender.fcgi?artid=2173029&tool=pmcentrez&rendertype=abstract> [Accessed March 5, 2012].
- Schlieff, M. L., and Wilson, R. I. (2010). Olfactory Processing and Behavior Downstream from Highly Selective Receptor Neurons. *Nat Genet* 10, 623–630.
- Schmidt, A., and Hall, A. (2002). Guanine nucleotide exchange factors for Rho GTPases: turning on the switch. *Genes & development* 16, 1587–1609. Available at: <http://www.ncbi.nlm.nih.gov/pubmed/12101119> [Accessed March 12, 2012].
- Schneider, B. I. (1972). Cell lines derived from late embryonic stages of *Drosophila melanogaster*. *J. Embryol. exp. Morph.* 27, 353–365.
- Schneider, I. (1964). Differentiation of larval *drosophila* eye-antennal Discs in Vitro. *Journal of Experimental Zoology*.
- Sekino, Y., Kojima, N., and Shirao, T. (2007). Role of actin cytoskeleton in dendritic spine morphogenesis. *Neurochemistry international* 51, 92–104. Available at: <http://www.ncbi.nlm.nih.gov/pubmed/17590478> [Accessed March 12, 2012].
- Singer, J. M., and Shaw, J. M. (2003). Mdm20 protein functions with Nat3 protein to acetylate Tpm1 protein and regulate tropomyosin-actin interactions in budding yeast. *Proc Natl Acad Sci U S A* 100, 7644–7649. Available at: http://www.ncbi.nlm.nih.gov/entrez/query.fcgi?cmd=Retrieve&db=PubMed&dopt=Citation&list_uids=12808144.
- Singh, N., and Nayak, S. (1985). Fine Structure And Primary Sensory Projections Of Sensilla On The Maxillary Palp Of *Drosophila melanogaster* Meigen (Diptera: Drosophilidae). *Int. J. Insect Morphol. & Embryol.* 14, 291–306.
- Small, J. V., Isenberg, G., and Celis, J. E. (1977). Polarity of actin at the leading edge of cultured cells. *Nature* 272.
- Spletter, M. L., Liu, J., Liu, J., Su, H., Giniger, E., Komiyama, T., Quake, S., and Luo, L. (2007). Lola regulates *Drosophila* olfactory projection neuron identity and targeting specificity. *Neural development* 2, 14. Available at: <http://www.pubmedcentral.nih.gov/articlerender.fcgi?artid=1947980&tool=pmcentrez&rendertype=abstract> [Accessed March 19, 2012].

- Starheim, K. K., Arnesen, T., Gromyko, D., Rynningen, A., Varhaug, J. E., and Lillehaug, J. R. (2008). Identification of the human N(alpha)-acetyltransferase complex B (hNatB): a complex important for cell-cycle progression. *The Biochemical journal* *415*, 325–331. Available at: <http://www.ncbi.nlm.nih.gov/pubmed/18570629> [Accessed August 4, 2010].
- Stocker, R. F. (2001). *Drosophila* as a focus in olfactory research: mapping of olfactory sensilla by fine structure, odor specificity, odorant receptor expression, and central connectivity. *Microsc Res Tech* *55*, 284–296. Available at: <http://www.ncbi.nlm.nih.gov/pubmed/11754508> [Accessed March 27, 2012].
- Stocker, R. F., Lienhard, M. C., Borst, A., and Fischbach, K. (1990). Neuronal architecture of the antennal lobe in *Drosophila melanogaster*. *Cell and Tissue Research*.
- Stocker, R. F., Singh, R. N., Schorderet, M., and Siddiqi, O. (1983). Projection patterns of different types of antennal sensilla in the antennal glomeruli of *Drosophila melanogaster*. *Cell and tissue research* *232*, 237–248. Available at: <http://www.ncbi.nlm.nih.gov/pubmed/6411344>.
- Strasser, G. a, Rahim, N. A., VanderWaal, K. E., Gertler, F. B., and Lanier, L. M. (2004). Arp2/3 is a negative regulator of growth cone translocation. *Neuron* *43*, 81–94. Available at: <http://www.ncbi.nlm.nih.gov/pubmed/15233919>.
- Suter, D. M., and Forscher, P. (2001). Transmission of growth cone traction force through apCAM-cytoskeletal linkages is regulated by Src family tyrosine kinase activity. *The Journal of cell biology* *155*, 427–438. Available at: <http://www.pubmedcentral.nih.gov/articlerender.fcgi?artid=2150837&tool=pmcentrez&rendertype=abstract> [Accessed May 21, 2012].
- Sweeney, L. B., Couto, A., Chou, Y.-H. H., Berdnik, D., Dickson, B. J., Luo, L., and Komiyama, T. (2007). Temporal target restriction of olfactory receptor neurons by Semaphorin-1a/PlexinA-mediated axon-axon interactions. *Neuron* *53*, 185–200. Available at: <http://www.ncbi.nlm.nih.gov/pubmed/17224402>.
- Sánchez-Soriano, N., Gonçalves-Pimentel, C., Beaven, R., Haessler, U., Ofner-Ziegenfuss, L., Ballestrem, C., and Prokop, A. (2010). *Drosophila* growth cones: a genetically tractable platform for the analysis of axonal growth dynamics. *Developmental neurobiology* *70*, 58–71. Available at: <http://www.ncbi.nlm.nih.gov/pubmed/19937774> [Accessed August 24, 2011].
- Sánchez-Soriano, N., Tear, G., Whittington, P., and Prokop, A. (2007). *Drosophila* as a genetic and cellular model for studies on axonal growth. *Neural development* *2*, 9. Available at: <http://www.pubmedcentral.nih.gov/articlerender.fcgi?artid=1876224&tool=pmcentrez&rendertype=abstract> [Accessed November 30, 2010].

- Takahashi, H., Mizui, T., and Shirao, T. (2006). Down-regulation of drebrin A expression suppresses synaptic targeting of NMDA receptors in developing hippocampal neurones. *Journal of neurochemistry* 97 *Suppl 1*, 110–115. Available at: <http://www.ncbi.nlm.nih.gov/pubmed/16635259> [Accessed July 10, 2012].
- Tanaka, E., Ho, T., and Kirschner, M. W. (1995). The role of microtubule dynamics in growth cone motility and axonal growth. *The Journal of cell biology* 128, 139–155. Available at: <http://www.pubmedcentral.nih.gov/articlerender.fcgi?artid=2120332&tool=pmcentrez&rendertype=abstract>.
- Tea, J. S., Chihara, T., and Luo, L. (2010). Histone deacetylase Rpd3 regulates olfactory projection neuron dendrite targeting via the transcription factor Prospero. *The Journal of neuroscience : the official journal of the Society for Neuroscience* 30, 9939–9946. Available at: <http://www.pubmedcentral.nih.gov/articlerender.fcgi?artid=2924735&tool=pmcentrez&rendertype=abstract> [Accessed March 19, 2012].
- Technau, G. M. (2008). Chapter 6 - Development of the Drosophila Olfactory System. In *Brain Development in Drosophila melanogaster*.
- Tobacman, L. S., and Korn, E. D. (1983). The kinetics of actin nucleation and polymerization. *The Journal of biological chemistry* 258, 3207–3214. Available at: <http://www.ncbi.nlm.nih.gov/pubmed/6826559>.
- Tobin, S. L., and Zulauf, E. (1980). Multiple Actin-Related Sequences melanogaster Genome in the Drosophila. *Cell* 19, 121–131.
- Trost, M., English, L., Lemieux, S., Courcelles, M., Desjardins, M., and Thibault, P. (2009). The phagosomal proteome in interferon-gamma-activated macrophages. *Immunity* 30, 143–154. Available at: <http://www.ncbi.nlm.nih.gov/pubmed/19144319> [Accessed March 15, 2011].
- Vosshall, L. B. (2000). Olfaction in Drosophila. *Curr Opin Neurobiol* 10, 498–503. Available at: http://www.ncbi.nlm.nih.gov/entrez/query.fcgi?cmd=Retrieve&db=PubMed&dopt=Citation&list_uids=10981620.
- Vosshall, L. B., Amrein, H., Morozov, P. S., Rzhetsky, a, and Axel, R. (1999). A spatial map of olfactory receptor expression in the Drosophila antenna. *Cell* 96, 725–736. Available at: <http://www.ncbi.nlm.nih.gov/pubmed/10089887>.
- Wicher, D., Schäfer, R., Bauernfeind, R., Stensmyr, M. C., Heller, R., Heinemann, S. H., and Hansson, B. S. (2008). Drosophila odorant receptors are both ligand-gated and cyclic-nucleotide-activated cation channels. *Nature* 452, 1007–1011. Available at: <http://www.ncbi.nlm.nih.gov/pubmed/18408711> [Accessed March 20, 2012].

- Wilson, S. I. (2010). Target practice: Zic2 hits the bullseye! *The EMBO journal* 29, 3037–3038. Available at: <http://www.pubmedcentral.nih.gov/articlerender.fcgi?artid=2944073&tool=pmcentrez&rendertype=abstract> [Accessed July 10, 2012].
- Zheng, J. Q., Wan, J. J., and Poo, M. M. (1996). Essential role of filopodia in chemotropic turning of nerve growth cone induced by a glutamate gradient. *The Journal of neuroscience : the official journal of the Society for Neuroscience* 16, 1140–1149. Available at: <http://www.ncbi.nlm.nih.gov/pubmed/8558243>.
- Zhu, H., and Luo, L. (2004). Diverse functions of N-cadherin in dendritic and axonal terminal arborization of olfactory projection neurons. *Neuron* 42, 63–75. Available at: http://www.ncbi.nlm.nih.gov/entrez/query.fcgi?cmd=Retrieve&db=PubMed&dopt=Citation&list_uids=15066265.

